Hydrogen sulfide (H_2S) production by mycobacteria

TAFARA T.R. KUNOTA

2020

Submitted in fulfilment of the requirements for the degree of Doctor of Philosophy in the discipline of Medical Microbiology in the School of Laboratory Medicine and Medical Sciences, College of Health Science, University of KwaZulu-Natal, South Africa

PREFACE

"If anything kills 10 million people in the coming decades, it probably won't be a missile – it will be a Microbe" - ***William Henry Gates III, "Bill Gates"***

The study described in this thesis was carried out at the Africa Health Research Institute (AHRI), Nelson R. Mandela School of Medicine, University of KwaZulu-Natal in Durban in South Africa between April 2017, and September 2020 under the supervision of Prof. Adrie J.C. Steyn. The materials and methods section, most of the results, figures, general discussion, and conclusions arrived at in this study and most sections presented in this thesis have been synthesized into a manuscript and submitted to *Nature Communications* (currently in review, Manuscript number: NCOMMS-20-45815-T). These sections include the materials and methods, most of the results, figures, general discussion, and conclusions. Attached in the appendix section is proof of submission of the draft manuscript. This manuscript was submitted at the time of writing this thesis.

We are excited to share our findings that conclusively demonstrate for the first time that *M. tuberculosis* (*Mtb*) is an avid producer of the gasotransmitter hydrogen sulfide (H_2S). We show that H_2S modulates respiration, central metabolism, oxidative stress, and susceptibility to the anti-TB drug, clofazimine.

As for the findings presented in this thesis; not only have we demonstrated that *Mtb* produces H_2S, but we have also identified a protein responsible for H_2S production and its corresponding gene. Further, we disrupted this gene and complemented the corresponding knockout *Mtb* strain. How endogenous H_2S modulates *Mtb* respiration is consistent with recent studies in our research group, showing that exogenous H_2S modulates *Mtb* respiration (*Nat Commun* 11:557, 2020, doi.org/10.1038/s41467-019-14132-y) and that either bacterial or host H_2S suppresses host glycolysis upon infection to exacerbate disease (*PNAS*, 2020, doi.org/10.1073/pnas.1919211117). Importantly, since both *Mtb* and the host contribute to supraphysiological levels of H_2S at the site of infection and because of H_2S's potent pro- and anti-inflammatory effects, these disproportionately high levels of H_2S represent a new paradigm whereby *Mtb* contributes to disease.

Overall, our findings represent a significant conceptual advance that will broadly impact the TB field as H_2S is a previously overlooked confounding factor in all experiments. Therefore, we are of the view that our findings will be of immediate interest to the wide scientific audience, especially those with interests in *Mtb* physiology, bioenergetics, gasotransmitters, anti-TB drug studies, and bacterial pathogenesis. Hence, the findings in this thesis represent a paradigm for how *Mtb* H_2S metabolism promotes disease and is expected to make a vital contribution to our understanding of *Mtb* physiology. Once these mechanisms are known, we strongly anticipate that targeted pharmacological manipulation or new diagnostics will be developed and will result in novel approaches to TB treatment.

`

DECLARATION

I, Mr **TAFARA TAKUNDA REMIGIO KUNOTA**, declare as follows:

1. That the work described in this thesis has not been submitted to UKZN or any other tertiary institution for purposes of obtaining an academic qualification, whether by myself or any other party.
2. That my contribution to the project was as follows:
   - Performed all the H_2S measurement experiments using lead acetate assay and bismuth (III) chloride assays and Unisense amperometric sensor on liquid cultures.
   - Prepared the mycobacterial lysates and performed all the H_2S measurement experiments using bismuth (III) chloride assays, most of the in-gel non-denaturing native PAGE analysis. Some of these in-gel assays were then used for LC-MS/MS protein identification.
   - Performed most of the carbon tracing experiment using [U-^{13}C]-Cysteine and [U-^{13}C]-glucose for LC-MS/ MS targeted metabolomics analysis.
   - Performed all CFU-based assays.
   - Analyzed all the results of the above-mentioned experiments.
3. That the contributions of others to the project were as follows:
   - Dr. Aejaz Rahman, (*Post-Doctoral fellow within the Steyn Research Group at AHRI*) performed and analyzed the results of all flow cytometry assays to quantify reactive oxygen intermediates (ROI).
   - Barry Truebody, (*Laboratory Technician within the Steyn Research Group at AHRI*) constructed all the recombinant strains of *Mtb* and *Msm*.
   - Dr. Jared S. Mackenzie, (*Post-Doctoral fellow within the Steyn Research Group at AHRI*) performed all the extracellular metabolic flux analysis (using the extracellular flux analyzer XFe96).
   - Dr Michael Berney, (*Project Collaborator, from the Department of Microbiology and Immunology, Albert Einstein College of Medicine, NY, USA*) constructed the recombinant strains of *Mtb*Δ*rv1077*.

Signed:…… [redacted] …….

On this ……**03rd** ……day of……**DECEMBER**……..2020.

I hereby certify that this statement is correct

[redacted] ……..

Prof. Adrie J.C. Steyn (Supervisor)

`

DEDICATIONS

Special dedication of this work goes out to my beloved wife, Precious, my true joy and pillar of support in life. From the commencement of this journey to the end, she was there. She has and will always provide unwavering support and encouragement in all endeavours in life, for that I am grateful and blessed. I would also like to dedicate this work to my daughter, Christine, for her patience as her father wrote this thesis and subsequent manuscripts.

I also dedicate this work to Mrs S.R. Kunota, Tinotenda R. Kunota, Abigirl Chifamba and to my Late Father, Mr Marko R. Kunota for their faith and unwavering support in my academic journey.

"Now faith is the substance of things hoped for, the evidence of things not seen."

- Hebrews 11:1

`

ACKNOWLEDGEMENTS

This doctoral thesis is the conclusion of the strenuous journey towards my Ph.D. that I have undertaken over the past four and half years. Despite losing one year of my PhD studies on another project with different research group, the sense of fulfilment of this milestone, is all because of the contributory efforts of colleagues, friends, and family members.

I am greatly indebted to my research guide and supervisor, Prof. Adrie J.C. Steyn, who accepted me as his Ph.D. student and offered me his mentorship, nurturing my research interests, and developing my research skills and communication in microbiology. With his enthusiasm and constructive criticism, he has inspired me to see through the completion of this rather big project. His insightful comments, and need to develop rigorous, reproducible, and scientifically accurate results have been the primary resource for getting my research focus on the right track. Thank you!

My overwhelming gratitude and acknowledgement is extended to Dr. Aejaz Rahman (*Post-Doctoral fellow within the Steyn Research Group at AHRI*), for providing invaluable advice on academic matters regarding this project. His valuable experience and advice on experimental planning and execution, microbiology techniques and teaching moments on the standard operating procedures in microbiology were instrumental in the successful completion of this project. His valuable time assisting in big CFU based assays is greatly acknowledged. With his invaluable experience, he managed to assist and teach me how to interpret data and present it graphically. His invaluable experience and mentoring helped navigate the technical challenges experienced with regards to H_2S measurement on lysates using the Unisense amperometric sensor. His prior knowledge and experience with commonly used H_2S producing enzyme inhibitors, amino-oxyacetate (AOAA) and DL-Propargylglycine (PAG), the same inhibitors he had worked with in his published study, also helped address the technical difficulty experienced when performing in-gel non-denaturing native PAGE analysis using AOAA. I am also thankful to him for performing the flow cytometry assays to quantify reactive oxygen intermediates (ROI). He was also instrumental in aiding the identification of the H_2S generating enzyme from peptide fragments contained in the LC-MS/MS report. Special acknowledgement is given for providing fresh perspective on data analysis and performing confirmatory data analysis and some of the data presentation in the manuscript drafts. He was very approachable and addressed even the smallest hurdle I presented to him. Thank you!

I would also like to thank the energetic team of researchers in the Steyn Research group at AHRI, with special acknowledgment to Barry Truebody (*Laboratory Technician within the Steyn Research Group at AHRI*), for all his phenomenal and exemplary genetic and biochemistry work in constructing the recombinant strains of *Mtb* and assistance in the CFU based assays. He also performed the growth assays of *Mtb* and *Msm* strains in cysteine, performed one of the carbon tracing experiment using [U-

`

^{13}C]-Cysteine and [U-^{13}C]-glucose for LC-MS/MS targeted metabolomics analysis when I could not due to "Republic of South Africa's COVID-19 national lockdown regulations", and also measured activity of the H_2S degrading enzyme. THANK YOU! it was a pleasure working with you. I will cherish the long journey, "1 year", of recombinant strain development; what a learning experience that was for both of us, THANK YOU again!

To Dr. Jared S. Mackenzie (*Post-Doctoral fellow within the Steyn Research Group at AHRI*), the Steyn Research group resident mycobacterial extracellular metabolic flux analysis expert, THANK YOU for performing all the extracellular metabolic flux analysis (using the extracellular flux analyzer XFe96).

I take this opportunity to Steyn Research group at UAB, with specially acknowledgement to Dr. Ritesh R. Sevalkar for the purification of our protein of interest, and the H_2S degrading enzyme; to Hayden Pacl for assisting me with R studio package software. To the rest of Steyn Research group members, THANK YOU for brilliant suggestions they gave during our laboratory meetings, presentations and during our daily interactions which ultimately led to my growth as a research scientist and as a team player.

No research is possible without infrastructure, requisite materials, and financial support. Thank you to AHRI for continuous support of all kinds, including financial, and the incredible services from the clinical core and pharmacology (especially for all the LC-MS/MS analysis).

I would also like to thank Dr Michael Berney, (Albert Einstein College of Medicine, NY, USA) for constructing the recombinant strains of *Mtb*Δ*rv1077*, Dr Michelle Larson (Albert Einstein College of Medicine, NY, USA) for providing the specialized transducing phage for *rv3684* and Dr Alessandro Giuffrè (CNR Institute of Molecular Biology and Pathology, Rome, Italy) for providing the OASS expressing plasmid.

This study was supported by the South Africa's Council for Scientific and Industrial Research (CSIR) under CSIR DST - Interbursary Support (IBS) for the years 2017, 2018 and 2019 awarded to Tafara T.R. Kunota and NIH grants R01AI134810, R01AI137043, R33AI138280, a Bill and Melinda Gates Foundation Award (OPP1130017), South Africa MRC, NRF BRICS Program awarded to Prof. Adrie J.C. Steyn. This work would be simply impossible without these research grants.

My sincerest thanks go to all those people whom I have failed to mention here for their contribution to this project.

I am also deeply thankful to the Almighty God for His everlasting love, mercy and kindness that guides my steps in the quest for knowledge.

`

LIST OF PUBLICATIONS

The publications (published, in print and/or submitted) that constitute this thesis and the contribution I made to each of the manuscripts are presented here.

- Tafara T.R. Kunota, Md. Aejazur Rahman, Barry E. Truebody, Jared S. Mackenzie, Vikram Saini, Dirk A. Lamprecht, John H. Adamson, Ritesh R. Sevalkar, Jack R. Lancaster Jr., Michael Berney, Joel N. Glasgow and Adrie J.C. Steyn. ***Mycobacterium tuberculosis* H_2S functions as a sink to modulate central metabolism, bioenergetics, and drug susceptibility.** *Nature Communications*. Manuscript number: NCOMMS-20-45815-T), (Submitted 18 November 2020, Under Peer Review)

  Authors contributions

  I and my supervisor (Prof. Adrie J.C. Steyn) and Dr Md. Aejazur Rahman conceptualized the paper. I participated in experimental design, conducted most of the experiments and data analysis. I did the literature search for the introduction and I drafted the paper which all other co-authors later critically reviewed and edited. In addition to critically reviewing and editing the draft manuscript, other co-authors also performed specialized experiments within the experimental design.

- Saini V, Chinta KC, Reddy VP, Glasgow JN, Stein A, Lamprecht DA, Rahman MA, Mackenzie JS, Truebody BE, Adamson JH, Kunota TTR, Bailey SM, Moellering DR, Lancaster JR Jr, Steyn AJC. **Hydrogen sulfide stimulates *Mycobacterium tuberculosis* respiration, growth and pathogenesis.** *Nat Commun*. 2020 Jan 28;11(1):557. doi: 10.1038/s41467-019-14132-y. PMID: 31992699; PMCID: PMC6987094.

  My contributions

  I performed the in-vitro stress assay demonstrating the direct effect of the inhibitor AOAA on *Mtb* viability.

`

Table of Contents

`

`

LIST OF FIGURES

`

LIST OF TABLES

`

LIST OF ACRONYMS

AIDS	Acquired Immune Deficiency Syndrome
AOAA	Amino-oxyacetate
CBS	Cystathionine-β-synthase
CSE	Cystathionine-γ-lyase
CFZ	Clofazamine
COMP	Compliment
CYS	L-Cysteine
DNA	Deoxyribonucleic Acid
HIV	Human Immunodeficiency Virus
HPLC	High Pressure Liquid Chromatography
LC-MS	Liquid Chromatography–Mass Spectrometry
MTBC	Mycobacterium Tuberculosis Complex
MDR-TB	Multidrug Resistant Tuberculosis
Mtb	*Mycobacterium tuberculosis*
PAG	DL-Propargylglycine
PCR	Polymerase Chain Reaction
POC	Point-Of-Care
RIF	Rifampicin
RNS	Reactive Nitrogen Species
ROI	Reactive Oxygen Intermediates
TB	Tuberculosis
WHO	World Health Organization
WT	Wild type
XDR-TB	Extensively Drug Resistant Tuberculosis

`

ABSTRACT

The gasotransmitter hydrogen sulfide (H_2S) has been recognized as a physiological mediator with a variety of functions across all domains of life. Many prokaryotic bacterial species endogenously generate H_2S in their natural environments. However, to date, it is not known whether *Mycobacterium tuberculosis* (*Mtb*) is an endogenous producer of H_2S. In this study, we tested the hypothesis that *Mtb* endogenously produces H_2S to modulate respiration, central metabolism, oxidative stress, and drug susceptibility. We demonstrated that fast-growing non-pathogenic, slow-growing pathogenic mycobacterial species, as well as drug resistant clinical strains of *Mtb* species produce H_2S. Here we demonstrate that fast-growing non-pathogenic *M. smegmatis* produces barely detectable quantities of H_2S, whereas MDR *Mtb* produces large quantities of H_2S. We have also developed a native PAGE-based assay for the rapid screening of H_2S producing enzymes in the lysates of mycobacterial species. Using LC-MS/MS, we identified the protein, Rv3684 as an H_2S-producing enzyme *in Mtb*. Disruption of *rv3684*, demonstrated using the genetic knock out of *rv3684*, reduces, but does not eliminate, H_2S production, suggesting the involvement of multiple genes in H_2S production. Whole *Mtb* cell-based and lysate assays showed reduced levels of H_2S production in the *Mtb* knockout strain compared to the wild-type strain. Noticeably, we demonstrated that the *Mtb* mutant is resistant to oxidative stress and the anti-TB drugs clofazimine and rifampicin. We also found that endogenous H_2S is an effector molecule that maintains bioenergetic homeostasis by regulating *Mtb* respiration, and that H_2S also plays a key role in central metabolism by modulating the balance between oxidative phosphorylation (OXPHOS) and glycolysis. In summary, our findings reveal previously unknown concepts of *Mtb* physiology with respect to *Mtb*-derived H_2S and energy metabolism which has significant implication for routine laboratory culturing, understanding susceptibility and TB disease.

CHAPTER 1: INTRODUCTION

1.1 Tuberculosis

In this introduction subsection, we aim to provide an overview of the historical background, epidemiology, transmission, and infection of tuberculosis. We will also provide an overview of the host's immune response to infection, diagnostics, and anti-TB drugs available for the treatment of TB patients.

Tuberculosis (TB) is one of the most ancient diseases of humankind and the primary cause of morbidity and mortality in underdeveloped and developing countries [1]. The World Health Organization (WHO) has ranked TB in the top ten causes of death amongst infectious diseases worldwide [2]. TB is an infectious disease caused by a group of bacterial species termed *Mycobacterium tuberculosis* complex (*MTBC*) [3]. *MTBC's* include *Mycobacterium tuberculosis (Mtb)* and *Mycobacterium africanum,* the causative agents of TB in humans [4], where *Mycobacterium africanum* was found to cause human TB only in certain African regions [5]. In addition, *MTBC's* also include causative agents of TB in mammal such as *Mycobacterium bovis, Mycobacterium caprae* and *Mycobacterium pinnipedii.* s; *Mycobacterium microti* is the only known causative agent of TB in voles [4].

TB has a long history with humankind [6]; the oldest cases are traced back to the Neolithic settlement in the Eastern Mediterranean (3200-2300 BC) [7], with evidence of TB also being found in antique Egyptian mummies (2000-3000 B.C.) [8]. Throughout history, TB has been described using many names , including "white plague", "phthisis", "wasting away", "consumption", "Pott's disease", "Gibbus deformity", and "scrofula" [9]. In 1680, the Franciscus Sylvius carried out anatomic-pathological studies in pulmonary nodules from TB patients, which he named as "tubercula" (small knots), observing their evolution to lung ulcers (cavities) [9]. The first credible speculation of the infectious nature of TB was performed by the British Doctor Benjamin Marten, who proposed in 1722 that TB could be transmitted through the "breath" of a sick person, which is then inhaled by a healthy one, leading to illness [9]. It was not until the late 19th century when Robert Koch managed to isolate and culture the causative agent of TB in humans from crushed tubercles - *Mycobacterium tuberculosis (Mtb)* [10].

Person-to-person transmission of *Mtb* occurs by aerosolized particles [11]. Tuberculosis spread rapidly during the industrial revolution in Europe, fuelled by the change in environmental conditions [12]. With no treatment options available, it spread uncontrollably across Europe between 1908-1940, eventually reaching sub-Saharan Africa [12]. It is believed that in the early and mid-19th century, mortality rates due to TB began to decline slowly and continued to decline due to many factors that include access to antibiotics and improved living conditions [6]. However, the advent of the human immunodeficiency

`

virus (HIV) epidemic in the 1980s, and the widespread emergence of drug-resistant strains of *Mtb,* was a deadly combination, leading to the World Health Organization (WHO) declaring TB a global emergency in 1993 [13].

Globally, an estimated 10 million (range, 9.0–11.1 million) people fell ill with TB in 2018 [2]. African countries in particular have been hard hit by the TB epidemic, with South Africa presenting with one of the highest TB incident rates in the world (Figure A). The high TB burden in South Africa is partly attributed to conditions of poverty that favour transmission of the disease, with many of the more impoverished communities within the country residing in informal settlements whilst also making use of public transportation in the form of taxis and buses [14]. These are often poorly ventilated and encourage TB transmission as passengers are forced to sit close to each other with suboptimal airflow, particularly in the winter months [14]. In 2006, a province in South Africa, KwaZulu Natal, reported a well-documented outbreak of multidrug-resistant (MDR) and extensively drug-resistant (XDR) tuberculosis [15, 16].

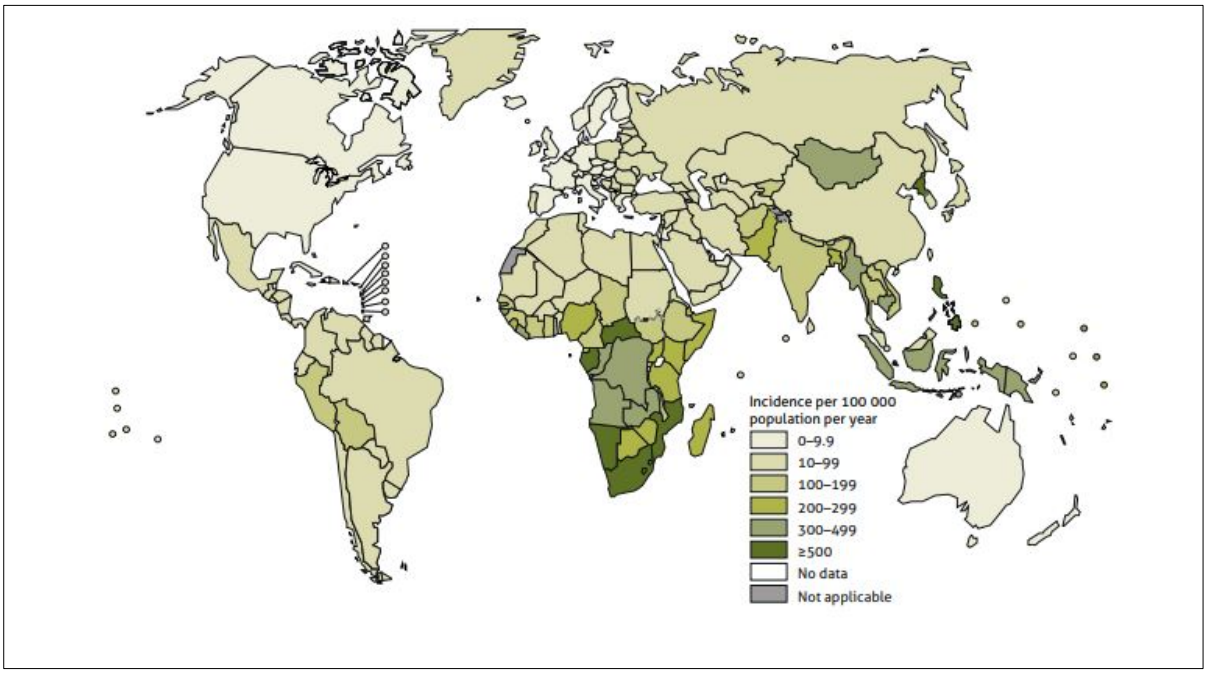

Figure A: Estimated TB incidence rates in 2018 [2]. The Southern African region has some of the highest incidence rates of TB.

`

Tuberculosis – The disease

Tuberculosis disease can be divided into latent and active disease states. Latently infected patients are infected with *Mtb,* but do not have TB disease, present with symptoms, and are unable to spread the disease [17]. This type of infection can only be detected through a tuberculin skin test, or a blood test [17]. Patients with latent infection are the largest reservoir for potential transmission [17]. Most people latently infected with TB do not die because of the disease, however the highest risk for a latently infected person is when reactivation (*i.e.*, transition from latent to active disease state) occurs and it silently spreads to close contacts [17]. Active TB occurs when *Mtb* bacilli overcome the immune system and multiply, characterized by fever, weight loss and a bloody cough [11]. Persons who have active TB disease are usually infectious and may spread the bacteria to others.

A person is infected with TB when they inhale aerosolized particles containing *Mtb* bacilli via the nose and mouth, the particles then travel along trachea, bronchus, bronchioles and eventually to the alveoli in the lung. TB is mainly a lung infection; however, it can spread to other organs and tissues. When the bacilli are detected by the immune system, the immune system responds, leading to the formation of a cluster of immune cells called granulomas at the site of infection [18, 19]. *Mtb* can infect several cell types, including neutrophils, macrophages and endothelial cells [19-21]. When the cell is infected by *Mtb*, the bacilli reside in different cellular compartments such as phagosomes [22], autophagosomes [23] and the cytosol [24, 25]. Several cellular and immunological mechanisms are initiated by the host in order to control the infection [26-28]. However, *Mtb* also employs several evasion and virulence strategies.

Tuberculosis diagnostics

It is believed that insufficient diagnostics impede the control of TB. It has previously been reported that there is an average loss of 30-90 days from a patient's first visit at a health care facility, to diagnosis [29, 30]. Most conventional TB diagnostics include sputum smear microscopy, culture, tuberculin skin test and chest radiography. These tests provide a diagnosis; however, they fall short due to the need for point-of-care (POC) testing required in resource limited settings [31]. It has been reported that some of these tests are insufficient to help control TB in HIV ravaged regions [32]. For example, chest X-rays are one of the most widely used TB diagnostics, providing a radiological evaluation of suspected or proven pulmonary TB [31]. However, it has been reported to be insufficient for the diagnosis of pulmonary TB [31]. For pulmonary TB, sputum smear microscopy is the preferred test in countries with a high burden of disease [33]. Sputum smear microscopy is relatively inexpensive and rapid [33-35]. In resource limited settings, the most common and reliable diagnostic test is the culture based growth detection assay; which offers high sensitivity and phenotypic drug susceptibility profiles (i.e. provides insight into which *Mtb* strains are drug-sensitive or drug-resistant) [31]. The main disadvantage of culture-based assays is the need for laboratory infrastructure and trained personnel. In addition to these limitations, the test to result turnaround time is equivalent to 2-6 weeks, which is not

`

ideal for POC testing. For POC testing, diagnostic tests such as humoral immune response tests [36, 37], cellular immune response tests [38], tuberculin skin tests [39, 40] and antigen detection tests [41] are used since they are rapid and relatively inexpensive, without the need for specially trained personnel. However, some of these tests; such as the antibody detection test, are not WHO recommended for clinical use due to reduced sensitivity [34]. A few years ago, nucleic acid amplification tests were introduced as a test that offers high specificity and accuracy, rapid turnaround times and minimal health care personnel training [42, 43]. The Xpert MTB/RIF system for MDR-TB screening is the most commonly used nucleic acid amplification test available in high TB burden areas [44]. The Xpert MTB/RIF assay simultaneously detects *Mtb* and rifampicin resistance by polymerase chain reaction (PCR) amplification [45]. In addition to detecting *Mtb* RIF resistance, the Xpert MTB/RIF offers accurate results and is seen as having potential to be used in POC settings since it requires minimally trained health personnel [46, 47].

Tuberculosis treatment

Standard tuberculosis treatment takes 6 to 9 months to achieve complete killing and to ensure that there is no reoccurrence of infection [48]. The first line of treatment for TB disease consists of treatment regimens comprising of isoniazid (INH), rifampicin (RIF), pyrazinamide (PZA), and ethambutol (EMB) [49]. This regimen for treating TB disease has a treatment stage of 2 months (intensive treatment with INH, RIF, PZA and EMB), followed by a continuation stage of either 4 or 7 months (treatment with INH, RIF); the whole regimen treatment totals 6-9 months [50]. Drug-resistant TB is caused by TB bacteria that are resistant to at least one first-line anti-TB drug. Multidrug-resistant TB (MDR TB) is resistant to more than one anti-TB drug and at least INH and RIF [50]. To treat MDR TB, a combination of second-line drugs including the injectables streptomycin, amikacin, kanamycin, capreomycin and the oral drugs ethionamide, prothionamide, cycloserine, terizidone, para-aminosalicylic acid, thioacetazone, are used [49, 51, 52]. Treatment with second line drugs is longer and has more side effects than the first line drugs [53]. Extensively drug-resistant TB (XDR TB) is a rare type of MDR TB that is resistant to isoniazid and rifampicin, plus any fluoroquinolones (levofloxacin, ofloxacin or moxifloxacin) and at least one of three injectable second-line drugs (*i.e.*, amikacin, kanamycin, or capreomycin) [54-56]. XDR TB is resistant to the most potent TB drugs, as a result, patients are left with treatment options that are much less effective [56]. XDR TB is of special concern for people with HIV infection or other conditions that can weaken the immune system [56]. These people are more likely to develop TB disease once they are infected, and also have a higher risk of death once they develop active TB [56, 57]. Recently, WHO consolidated the guidelines regarding the treatment of MDR TB and RIF mono-resistant tuberculosis (RR TB) [58]. WHO has ranked the MDR TB drug regimens based on their estimated efficacy profiles such that the regimens have been re-classified into groups A, B and C [58]. The group A drugs include fluoroquinolones, levofloxacin or moxifloxacin; bedaquiline and linezolid; group B includes clofazimine and cycloserine or terizidone, and group C

`

contains ethambutol, delamanid, pyrazinamide, imipenem-cilastatin or meropenem, amikacin or streptomycin, ethionamide or prothionamide, and *p*-aminosalicylic acid [58, 59]. This new MDR TB drug regimen re-classification, comprising of second line drugs, is a guideline for designing individualized MDR-TB treatment [59].

In addition to the global anti-TB drug crisis, the lack of effective *Mtb* vaccines and affordable diagnostics make it essential to better understand the mechanisms whereby *Mtb* causes disease. Progress has been made in defining the biological basis of *Mtb* pathogenesis; however, there is still a critical gap in our knowledge of precisely how *Mtb* causes disease, and novel virulence paradigms are desperately needed to fill this gap. One of these gaps concerns the effect of gasotransmitters in *Mtb* pathogenesis.

1.2 Gasotransmitters

Hydrogen sulfide (H_2S) is a toxic gas which has been recognized as the third gasotransmitter [60]. H_2S, along with nitric oxide (NO) and carbon monoxide (CO), constitute a group of endogenously produced gaseous signalling molecules known as 'gasotransmitters' that have a wide range of physiological functions [60-65]. NO has been shown to play an important role as part of the host defence mechanism against pulmonary infections, whereas *Mtb* has been shown to be able to withstand high concentrations of CO and may even be able to utilize it as an alternative carbon source in nutrient limited conditions [66-68]. We discuss these gaseous signalling molecules, 'gasotransmitters' further below.

1.2.1 Nitric oxide (NO)

Since its recognition as 'molecule of the year' in 1992 by Science magazine [69], NO, previously characterized as an important vasodilator [64], has been found to regulate a vast array of physiological functions, such as its role in the immune response, as well as the cardiovascular and nervous systems [70]. NO has also been implicated in cellular signalling, and maintenance of redox haemostasis [71, 72]. The enzyme family, nitric oxide synthase (NOS), is responsible for the endogenous production of NO via NADPH- and O_2-dependent oxidation of L-arginine to L-citrulluine [73, 74]. This oxidation of L-arginine to NO and L-citrulluine occurs in the presence of five co-factors (heme, tetrahydrobiopterin (BH4), flavin mononucleotide (FAD), flavin adenine dinucleotide (FMN) and Ca -calmodulin) [75]. In the absence of L-arginine, NOS is a superoxide generator [76]. Three mammalian isoforms exist and are classified by their localisation and expression patterns, and these are neuronal NOS1 (nNOS) and endothelial NOS3 (eNOS), and the inducible NOS2 (iNOS) [64]. eNOS is found in cells and tissues other than the endothelium, whereas nNOS is found in cells other than neurons, with iNOS expressed predominantly in cells of the myeloid lineage, including macrophages and neutrophils [64, 73]. iNOS is generally induced by redox stress, exposure to microbial pathogens or bacterial endotoxins, and pro-inflammatory cytokines such as IL-1, IFN-γ and TNFα [73].

`

NO is a major reactive nitrogen species (RNS) and reacts with atmospheric O_2, superoxide anions ($O_2^{\cdot-}$), heme/non-heme iron and thiol groups (-SH) of proteins [73]. Host production of NO in humans is confirmed by the presence of iNOS and nitrotyrosine in macrophages at the site of infection [77, 78]. Studies have shown that, even though *Mtb* has evolved to escape immune mechanisms and survive within macrophages [79, 80], iNOS/NO is essential for host defence against *Mtb* infection [81-83]. Within the phagosome, *Mtb* experiences oxidative and nitrosative stress, and to survive, it inhibits iNOS translocation to the phagosome [84]. In addition, low levels of NO have been shown to inhibit *Mtb* respiration and growth, as well as induce the dormancy regulon genes [73, 85]. Induction of these genes enable *Mtb* to enter dormancy, and upon detecting immune suppression in the host, *Mtb* is capable of reactivating from dormancy and start replicating to cause disease [80]. In *Mtb*, the DosS/T/R three component heme sensor system is responsible for activating the state of dormancy *in vitro* [73, 86, 87]. In summary, upon *Mtb* infection, NO displays bi-functionality; firstly, NO helps the host's defence against *Mtb* infection and secondly, low quantities of NO can utilised by *Mtb* to survive the host's immune response by enabling *Mtb* to enter the state of dormancy.

1.2.2 Carbon monoxide (CO)

Carbon monoxide (CO), a colourless and odourless gas, has long been considered as a potent respiratory poison [88]. CO has also been widely regarded as a classical respiratory inhibitor and is capable of exerting vasodilatory, anti-inflammatory, and antiapoptotic effects [89]. In competition with oxygen, CO primarily binds to ferrous oxygen-reactive heme proteins [64]. Most of the CO produced in mammals and microbes is endogenously produced by the enzyme heme oxygenase (HO) [88, 90]. Two major HO enzymes have been characterized in mammals and have been shown to have roles in the oxidation of heme and production of CO and biliverdin. These enzymes are known as the inducible HO, HO-1, and the constitutive HO, HO-2 [90]. The biological function of the third HO isoform, HO-3, is still unclear [90, 91]. Expression of HO-1 at low levels is found in almost all cell types, and this expression is highly induced by cellular redox stress, hypoxia, bacterial lipopolysaccharides and pathogenic challenges including mycobacterial species, while the brain solely expresses HO-2 [73, 90].

The role of CO, via a carbon monoxide-releasing molecule (CO-RM), as an antibacterial agent, was previously demonstrated in *Escherichia coli*, *Pseudomonas aeruginosa* and *Staphylococcus aureus* [92, 93]. Similarly, a mouse model demonstrated the role of CO in the host response to bacterial infections. In this study, they observed that addition of CO-RM results in enhanced bacterial clearance in HO-1 deficient mice when exposed to a model of abdominal sepsis [94]. In this same study, they also found that mice overexpressing HO-1 in the intestinal ilieum were able to clear the bacterial load aided by the presence of circulating phagocytic/inflammatory leukocytes [95]. This study demonstrated the importance of endogenous HO-1 expression in protecting against the lethal effects of polymicrobial sepsis. Similar to NO, CO is capable of inducing the dormancy regulon genes, allowing *Mtb* to persist during a latent infection [68, 96]. Upon infection with *Mtb*, HO-1 is induced in infected macrophages

`

both *ex vivo* and *in vivo*, with the gaseous product, CO, activating expression of the dormancy regulon in *Mtb* [68]. In the same study, HO-1 gene-deficient infected macrophages lead to a reduction in the expression of the Dos dormancy regulon. In bacteria, HO-1–generated CO enhances the immune response and leads to bacterial clearance, while for *Mtb,* HO-1–generated CO contributes to *Mtb*'s survival [97]. In humans, HO-1 has been shown to be essential for controlling myeloid cell inflammation and associated oxidative and nitrosative stress, thereby protecting the host against TB immunopathology [98]. Thus, *Mtb* is able to tolerate both moderate and high concentrations of CO to adapt to the host environment [68].

In summary, exposure, of *Mtb* to HO-1 derived CO, and iNOS derived NO, induces the dormancy regulon genes, allowing the bacillus to survive during infection.

1.2.3 Hydrogen Sulfide (H_2S)

Since its discovery in 1777 by Carl Wilhelm Scheele [99], hydrogen sulfide (H_2S) has been shown to be five-fold more toxic than CO [100], have a distinctive smell of rotten eggs [101, 102], and was first ascribed to having a physiological function by Abe and Kimura [103]. This study demonstrated that H_2S could serve as an endogenous neuromodulator [103]. Since then, H_2S has been discovered to be synthesized enzymatically in mammalian and human tissues [101, 104], transforming the known 'toxic gas' status of H_2S into a promising therapeutic compound. Several important physiological functions have been shown to be regulated by H_2S, such as a vasorelaxation [105] and immunomodulation [106, 107]. In addition, there is compelling evidence that H_2S is a pharmacological effector molecule involved in preventing ischemia-reperfusion injury [108, 109] and in inducing a "suspended animation-like" state in animals [110]. Human and clinical studies have accumulated large sets of contradictory data with respect to H_2S levels in human blood, where reports have suggested a wide range of sulfide levels from 13 µM to 300 µM. With such a wide range of reported H_2S levels in the blood, its possible the H_2S levels are in the nanomolar range. This contradictory data has been extensively reviewed by Wedmann *et al*. (2014) [108], Kimura *et al*. (2012) [111] and Li *et al*. (2013) [112].

1.2.3.1 H_2S Chemistry

H_2S is a sulfur analogue of water and, due to its weak intermolecular force, exists in a gaseous form that is colourless, but has a rotten egg odour and is both flammable and poisonous at high concentrations [112, 113]. H_2S is soluble in water, with its solubility reported to be about 80 mM at 37 °C, 100 mM at 25 °C, and 122 mM at 20 °C [112]. It also has a high lipid solubility, which allows it to easily diffuse through cell membranes without the need for a specific transporter [114]. H_2S is a weak acid in aqueous solution, whereby it's volatility dissociates immediately and equilibrates with its anions, hydrosulfide anions (HS^-) and sulfide (S^{2-}) as described in **Equation 1** [112]. Hydrogen sulfide's properties of gas–aqueous distribution, including Henry's Law coefficient, have also been well characterized [112].

`

Equation 1: $H_2S_{(g)} \leftrightharpoons H_2S_{(aq)} \leftrightharpoons HS^- + H^+ \leftrightharpoons S^{2-} + 2H^+$

According to a detailed review by Li and Lanchester [112] in which they surveyed various research reports on the pKa values of H_2S, they settled on the assumption that the values of $pKa_1 \sim 7$ (at 25 °C) and $pKa_2 \sim 12.20 – 17.3$ (varies between room temperature and 25 °C) where pKa is the negative log of the acid dissociation constant (Ka) value. They calculated that 28% of the total hydrogen sulfide in a pH 7.4 solution exists as H_2S, whereas 72% is in the form of HS^-, and because of the high pKa_2 values, S^{2-} was taken as negligible in the solution. Li and Lanchester [112] did report that a precise pKa values need to be used under the exact experimental conditions for the calculation of H_2S concentration since it was shown by Hughes *et al*. (2009) [115] that at physiological pH, the concentration of $H_2S_{(aq)}$ at 20 °C (pKa_1 6.98) can be twice as much as that at 37 °C (pKa_1 6.76). This complex nature of H_2S in solution, coupled with its volatility, make it a technically challenging gas to work with. How H_2S is enzymatically and non-enzymatically produced is discussed below.

1.2.3.2 Endogenous production of H_2S

Both eukaryotic and prokaryotic cells endogenously produce H_2S via both enzymatic and non-enzymatic pathways [114, 116]. The most characterized enzymes involved in the production of H_2S, are cystathionine-β-synthase (CBS), cystathionine-γ-lyase (CSE) and 3-mercaptopyruvate sulfurtransferase (3MST) [60, 114, 117-120]. CBS and CSE are pyridoxal 5′-phosphate (PLP)-dependent enzymes and are located in the cytosol, whereas PLP-independent 3-mercaptopyruvate sulfurtransferase (3MST) mainly resides and generates H_2S within mitochondria [114, 121, 122]. CBS and CSE are generally acknowledged as the main sources of physiological mammalian H_2S [123].

Bacterial production of H_2S was discovered in the late 19th century [102]. Since then, a host of bacteria have been reported to endogenously produce H_2S, including *Escherichia coli* (*E. coli*), [124], *Staphylococcus aureus*, *Bacillus anthracis*, *Pseudomonas aeruginosa Salmonella* spp., *Shigella* spp. [125, 126] and oral bacteria like *Fusobacterium* spp., *Treponema denticola,* and *Prevotella tannerae* [127, 128]. Some of the earliest reports of the role of cysteine in H_2S production by multiple bacterial species was performed by Patricia Clark in the 1950s [126]. This includes partial characterization of H_2S producing enzymes [102]. To date, some of these bacterial species have been shown to possess orthologs of the transsulfuration pathway enzymes, CBS, CSE and 3MST [125]. However, reports of the role of cysteine in *Mtb* H_2S production and the enzymes involved are lacking.

Since the early work by Patricia Clarke, the addition of cysteine to bacterial cultures has been shown to stimulate H_2S production [126, 129, 130]. In both bacteria and mammalian cells, CBS and CSE can synthesize H_2S from L-cysteine (Cys) [61, 122, 131], whereas, the peroxisomal enzyme d-amino oxidase (DAO) can only synthesize H_2S from D-cysteine [132]. H_2S is produced by CBS via a β-replacement reaction with cysteine, also via β-replacement of cysteine by homocysteine to produce H_2S [133, 134], shown in Figure B. CSE produces H_2S by the α, β-elimination reaction with cysteine and

`

in the presence of high concentrations of homocysteine, H_2S is produced by the γ-replacement reaction between two molecules of homocysteine [134], shown in Figure B. 3MST produces H_2S from 3-mercaptopyruvate (3MP), which is produced by cysteine aminotransferase (CAT) from cysteine and α-ketoglutarate [122, 135]. A summary of the reactions catalyzed by these enzymes is shown in Table 1 [136]. Cysteine has been assumed to be the primary source of H_2S biosynthesis; however, nonenzymatic production of H_2S can occur through glucose, glutathione, inorganic and organic polysulfides and elemental sulfur [137]. H_2S is also produced through direct reduction of glutathione and elemental sulfur via sulfite reductases, where elemental sulfur is reduced through reducing equivalents of the glucose oxidation pathway like NADH, or NADPH [137-139]. Glucose reacts with methionine, homocysteine, and cysteine to produce gaseous sulfur compounds such as methanethiol and H_2S [137]. H_2S formation from thiosulfate results from a reductive reaction involving pyruvate, which acts as a hydrogen donor [137]. It has been proposed that rhodanese metabolizes thiosulfate to produce H_2S and sulfite [135, 140]. The use of H_2S in biomedical experiments is made difficult because of its chemical properties. Because of its chemical complexity, H_2S releasing agents are often used. These H_2S releasing agents are discussed in the subsequent section.

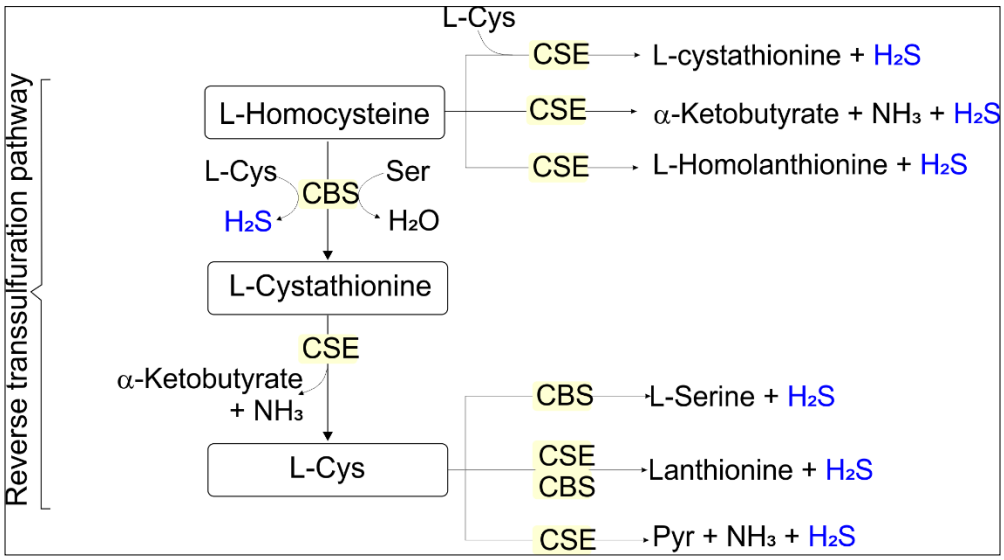

Figure B: Schematic showing the various possible H_2S generating enzymes and the reactions they catalyse in the reverse transsulfuration pathway.

`

Table 1: A summary of the H_2S generating reactions catalyzed by CBS, CSE and 3MST.

Reactions catalyzed by CBS	Serine + Homocysteine → Cystathionine + H_2O Cysteine + Homocysteine → Cystathionine + **H_2S** Cysteine + Cysteine → Lanthionine + **H_2S** Cysteine + H_2O → Serine + **H_2S**
Reactions catalyzed by CSE	Cystathionine → Cysteine + α-ketoglutarate + NH_3 Cysteine + Homocysteine → Cystathionine + **H_2S** Cysteine + Cysteine → Lanthionine + **H_2S** Cysteine → Pyruvate + NH_3 + **H_2S** Homocysteine + Homocysteine → Homolanthionine + **H_2S** Homocysteine → α-ketoglutarate + NH_3 + **H_2S**
Reactions catalyzed by CAT then 3MST	Cysteine + α-ketoglutarate → 3-mercaptopyruvate + Glutamate (This the initial transamination reaction involving CAT) 3-mercaptopyruvate → pyruvate + **H_2S**

1.2.3.3 Commonly used exogenous sources of H_2S

Inorganic sulfide salts such as sodium sulfide (Na_2S) and sodium hydrogen sulfide (NaHS) are commonly used as H_2S releasing agents. These sodium salts have disadvantages, such as their rapid release of H_2S levels and short half-life when dissolved, or injected [141]. To study the biological effects of H_2S in many cells, tissues, and animals it is unlikely there will be any H_2S present in the medium or sample type within a short time of adding either NaHS or Na_2S. H_2S donors with a regulated release have been developed, such as GYY4137 (morpholin-4-ium 4 methoxyphenyl(morpholino) phosphinodithioate or morpholin-4-ium 4 methoxyphenyl(morpholino) phosphinodithioate). GYY4137, a water-soluble derivative of Lawesson's reagent, can also release H_2S upon hydrolysis [142, 143]. Contrary to the efficacy of the inorganic sulfide salts, GYY4137 releases H_2S slowly both in aqueous media and when administered to animals over a period of hours to days [144], it is for this reason GYY4137 is the most preferred slow donor of H_2S. In addition, GYY4137 has been shown to have vasodilatory and antihypertensive activity [143]. The common methods for H_2S measurement below are discussed below.

1.2.3.4 Methods of H_2S measurement

The concentration of H_2S in solution is greatly affected by its volatility since it is a gas. This is especially problematic since most laboratory experiments are performed in vials that contain a headspace. The most commonly employed methods for measuring H_2S concentration in blood or plasma are the methylene blue method (MB), bismuth (III) chloride (BC) assay, sulfite-sensitive ion selective electrodes (ISE), monobromobimane (MBB), HPLC or GC analysis of headspace gas, and amperometric electrodes/sensors [141]. Alternatively, lead acetate [$Pb(Ac)_2$] strips, one of the oldest methods of H_2S measurement in the headspace of *in-vitro* experiments can be used. This method is

`

based on the specific reactivity of lead acetate with H_2S, resulting in the formation of a brown lead sulfide stain on the strip [145]. Some of these methods are best suited for H_2S measurement in water and buffers and are less reliable in blood and tissue; also, they can be performed under anoxic or hypoxic conditions since these factors affect the balance between H_2S production and oxidative metabolism [141].

Methylene blue is one of the most commonly used colorimetric assays, where methylene blue is generated by the reaction of H_2S with *N*,*N*-dimethyl-*p*-phenylenediamine sulfate (NDPA) and iron (III) chloride ($FeCl_3$) [141, 146]. Methylene blue is light-absorbing and is quantifiable spectrophotometrically. For H_2S measurement, ISE measure the sulfide anion (S^{2-}) specifically and a strong alkali is mixed in to drive the H_2S equilibria, Equation 1, in favour of the formation of S^{2-} while preventing its oxidation thereof. The BC method is a microplate-based assay that measures H_2S produced when bismuth (III) sulfide is generated by the reaction of a bismuth (III) salt with H_2S. This assay is quantifiable spectrophotometrically [128]. The MBB assay measures H_2S via derivatizing it with two (2) molecules of monobromobimane to form the fluorescent sulfide dibimane, which is then assayed by High Performance Liquid Chromatography (HPLC) with fluorescent detection [141]. H_2S amperometric sensors measure dissolved H_2S gas in real-time under both normoxic and hypoxic conditions [141, 147].

1.3 Knowledge gap – the role of H_2S in *Mtb* physiology

Bacterial production of H_2S was initially considered to be a by-product of sulfur metabolism with an unclear physiological role; however, there are studies that have shown that the disruption of H_2S-producing genes in multiple bacterial species increases antibiotic susceptibility [124, 125]. For example, in *E. coli*, 3MST produces the majority of cellular H_2S from Cys [124]. When 3MST is disrupted, a reduction in H_2S generation is observed, leading to increased sensitivity to oxidative stress-inducing compounds, in particular, hydrogen peroxide [124]. This implicates 3MST-derived H_2S in the maintenance of redox homeostasis. The findings in these studies have impacted our understanding of H_2S in bacterial drug resistance. In *Mtb*, genes encoding the enzymes to produce H_2S have been identified in the genome, however, to date, there is no clear evidence that conclusively demonstrates that *Mtb* produces H_2S.

One of the most studied interactions of H_2S is with the metalloprotein cytochrome c oxidase, which is classified as a hemoprotein. H_2S reversibly inhibits cytochrome c oxidase (Complex IV) at high concentrations, and at low concentrations, stimulates mitochondrial respiration [148-151]. At high concentrations of H_2S, it competitively binds to Complex IV, resulting in the inhibition of O_2 binding. H_2S interacts with Complex IV through the O_2-binding copper (Cu_B)/heme (a_3) iron binuclear site in oxidized state (Cu^{2+}/Fe^{3+}) and reduces the enzyme [152]. A recent study has shown that H_2S targets the

`

Mtb electron transport chain to increase respiration and ATP levels leading to increased growth [153]. Upon *Mtb* infection of macrophages, host-generated H_2S exacerbates disease by suppressing host central metabolism and induces the Dos dormancy regulon [153, 154]. Further, CSE and 3MST are substantially upregulated in human lung tissue infected with Mtb, and it has been proposed that Mtb triggers supraphysiological levels of host-generated H_2S at the site of infection to suppress host immunity, thereby exacerbating disease [154]. Further, recent studies have shown that *Mtb* senses host-generated H_2S during infection to reprogram its metabolism accordingly [153]. Again, studies formally demonstrating H_2S production by *Mtb* are lacking.

H_2S has been reported to interact with inorganic metals via oxidation/reduction and ligation [112]. With respect to oxidation/reduction, complete electron transfer occurs between H_2S and the metal. As for ligation, coordinate complexes are formed when H_2S binds with metals. In both oxidation/reduction and ligation, the interactions of H_2S and metals is predicated on the basis of H_2S acting as a nucleophile [112]. In a biological setup, H_2S is known to covalently modify ferryl/peroxo heme within hemoglobin and myoglobin resulting in the formation of green colored sulfhemoglobin and sulfmyoglobin species, both of which are indicators of H_2S poisoning [112, 152, 155]. Additionally, H_2S can react with nonheme iron present in iron-sulfur (Fe-S) cluster containing proteins to generate insoluble precipitates (65). H_2S is also known for directly scavenging free radical species [156]. Because of its dissociation properties in aqueous solution – Equation 1, at 37°C and pH 7.4, the physiological temperature and pH of fluids in *in vitro* studies; 80 % of the total H_2S in solution exists as HS^-. HS^- is a one-electron chemical reductant, which through hydrogen atom transfer, or single electron transfer is able quench free radicals, Reactive Oxygen Species (ROS), Reactive Nitrogen Species (RNS), peroxynitrite ($ONOOH/ONOO^-$), and hypochlorite ($HOCL/^-OCL$) [61, 112, 152, 156-158]. HS^- and H_2S react with molecular oxygen (O_2) differently. HS^- reacts rapidly with O_2 in the presence of divalent metal cations such as $Fe^{2+}$and Cu^{2+} [156]. H_2S's reaction with O_2, referred to as autoxidation, can be catalyzed by metalloproteins like ferritin [112] to generate free radicals [159]. Because of the lack of studies formally demonstrating H_2S production by *Mtb*, the effect of *Mtb*'s contribution to the H_2S pool *in vivo* brings forth questions on the role of H_2S in *in-vivo* studies. For example, does the H_2S pool (*Mtb*'s H_2S + host's H_2S) maintain its cytoprotectant nature in scavenging ROS and RNS?

H_2S has been shown to signal through protein sulfhydration. H_2S fulfills its signaling function by inducing post-translational modification (PTM) of protein cysteine residues to create an S-sulfhydryl/thiol (R-SH) or hydropersulfide (R-SSH), in a process called S-sulfhydration or persulfidation [160]. Persulfidation is when R-SSH is formed by the oxidation of thiols (from −2 to −1 oxidation state) [152, 161]. Persulfidation is of interest because it can alter protein activity and influence diverse biological processes [160]. It is generally accepted that H_2S is the signalling molecule, however, H_2S itself cannot react with cysteine thiolates since in aqeous solution it exist as H_2S/HS^- and

`

either can only act as reductant, therefore H_2S's direct participation in oxidation reactions of–SH groups to R-SSH groups is unfeasible [160, 161]. This implies that R-SSH groups cannot be formed in a direct reaction of H_2S with R–SH groups. Hence, the persulfidation can occur only when one of the reagents (–SH group or H_2S) is in the oxidized form [161]. This represents a gap in our knowledge of how proteins are modified by H_2S and more important it brings forth a question on how *Mtb*-derived H_2S modifies *Mtb's* proteins and the host's proteins upon infection of macrophages by *Mtb*.

As H_2S signalling demonstrates diverse roles in both prokaryotic and eukaryotic biology and disease, the clear demonstration of H_2S production in *Mtb* will significantly advance our understanding of the role of H_2S in signalling, *Mtb* physiology and infection. This gap in the evidence of *Mtb* H_2S production forms the basis of the aims of our study (Section 1.4).

`

1.4 Aims of the Thesis

Bacteria producing H_2S are identified through the smell of the characteristic "rotten egg" odour generated by their cultures. However, smell cannot be used for *Mtb* due to its aerosolized mode of transmission and infection. Thus, clear evidence of H_2S production in *Mtb* is needed to direct further studies investigating the role of H_2S in *Mtb* physiology and infection. The aims of this thesis are:

i. To determine if mycobacteria produce H_2S.
ii. To determine the role of H_2S in mycobacterial energy metabolism and drug susceptibility.

The aims of this thesis are based on the premise discussed below.

1.4.1 Scientific Premise

Since the discovery of *Mtb* by Robert Koch in 1882, the capacity of *Mtb* to produce H_2S has been overlooked. One likely reason is that *Mtb* is highly contagious and spread through inhalation of aerosols; thus, the typical '*sniff*' test for the rotten egg odour cannot be performed without significant health risk. Furthermore, working with H_2S is non-trivial [141] as H_2S can be produced non-enzymatically from cysteine [162]. However, it has been reported that in *M. smegmatis,* H_2S production and media acidification were detected when oxygen was limited in the presence of 0.1% elemental sulfur [163], while in *Mtb*, pH-dependent H_2S generation was detected [164]. Then again, the inference by these reports that *Mtb* produces H_2S should be viewed with caution as H_2S can be spontaneously generated from media components [162]. Furthermore, Shatalin *et al.* (2011) demonstrated that genetic disruption of H_2S-producing (CBS, CSE and 3MST) genes increased the susceptibility of bacteria (*E. coli*, *Staphylococcus aureus*, *Bacillus anthracis*, and *Pseudomonas aeruginosa*) to numerous antibiotics [125]. These reports and the identification of *Mtb* homologues of H_2S-producing genes in literature and KEGG pathways (https://www.genome.jp/kegg/), **Table 2**, suggest that *Mtb* can produce H_2S, which may confer antibiotic resistance due to alterations in *Mtb* physiology.

`

Table 2: Summary of identified putative *Mtb* H37Rv enzymes involved in sulfur metabolism, sulfur amino acid biosynthesis and H_2S production.

	Enzymes capable of Sulfide reactions	***Mtb* Locus**	**Gene Product**	**Annotated Pathway/Function**	**Catalytic Activity**	**Ref.**
1	Probable cystathionine gamma synthase/O-succinylhomoserine sulfhydrylase	Rv0391	*MetZ*	Methionine Biosynthesis/Probable Cystathionine γ-synthase	*O*-succinylhomoserine -> homocysteine	[165]
2	Cysteine synthase	Rv0848	*CysK2*	Cysteine Biosynthesis	(1) *O*-phospho-L-serine -> *S*-sulfocysteine (**2**) *O*-phospho-L-serine + H_2S -> L-cysteine + phosphate	[166]
3	Cystathionine beta synthase	Rv1077	*Previously CysM2*	Cysteine Biosynthesis/Serine sulfhydrase/Transulfuration Pathway	(1) homocysteine + serine -> cystathionine (**2**) cysteine + homocysteine -> cystathionine + H_2S	[167]
4	Cystathionine gamma synthase/cystathionine gamma lyase	Rv1079	*MetB*	Methionine Biosynthesis/Probable Cystathionine γ-synthase/Transulfuration Pathway	(1) *O*-succinyl-L-homoserine + L-cysteine -> cystathionine + succinate (**2**) cystathionine -> α-ketobutyrate +NH_3	[165]
5	Cysteine synthase	Rv1336	*CysM*	Cysteine Biosynthesis	*O*-phospho-L-serine + CysO-SH -> CysO-Cys + PO_4^{3-}	[166]
6	Cysteine synthase	Rv2334	*CysK1*	Cysteine Biosynthesis	*O*-acetyl-L-serine + H_2S -> L-cysteine + acetate	[166]
7	Ferredoxin-dependent sulfite reductase	Rv2391	*SirA*	Sulfate Assimilation	SO_3^{2-} -> S^{2-}	[168]
8	Methionine synthase	Rv3340	*MetC*	Methionine Biosynthesis/Probable O-acetylhomoserine sulfhydrylase	(1) O-acetyl-L-homoserine + methanethiol -> L-methionine + acetate (**2**) *O*-acetyl-L-homoserine + H_2S <-> L-homocysteine + acetate	[169]

`

1.4.2 Hypotheses

This thesis has two hypotheses:

1. *Mtb* produces H_2S.

We will test this hypothesis by firstly measuring the production of H_2S by *Mtb* and other mycobacterial strains using $PbAc_2$ strips and the BC assay. H_2S endogenously produced by *Mtb* will be quantified using a highly sensitive sulfide gas amperometric microsensor. Secondly, we will identify H_2S producing enzymes in *Mtb* using non-denaturing native polyacrylamide gel electrophoresis (PAGE) of mycobacterial cell lysates.

2. H_2S modulates *Mtb* physiology and drug susceptibility.

We will test this hypothesis by generating an *Mtb* genetic knock-out mutant deficient in H_2S production and examine how the physiology and drug susceptibility of this mutant differs from that of the wild-type. Firstly, we will use an innovative, non-invasive technology, termed real-time extracellular flux analysis, to study the respiration of both the wild-type and the mutant. Secondly, we will use stable isotope mass spectrometry (using LC-MS/MS) analysis to examine the levels and flux of metabolites in glycolysis, pentose phosphate pathway, and the TCA cycle of both the wild type and the mutant. Thirdly, we will assess the drug susceptibility of the wild type and mutant by counting the colony forming units of the mycobacteria cultured with anti-TB drugs in the presence or absence of exogenously added H_2S. Fourthly, we will examine how H_2S alters *Mtb* redox homeostasis using flow cytometry. An oxidative stress experiment involving the incubation of the wild-type and mutant with cumene hydroperoxide will provide insights into how H_2S alters *Mtb* redox homeostasis.

1.4.3 Rationale

The rationale for this research is:

1. Successful demonstration of H_2S production by *Mtb* will impact the TB field because H_2S is a previously overlooked gasotransmitter in *Mtb*.
2. Successful generation of a genetic knockout mutant in deficient in H_2S production will identify genes that contribute to H_2S production and enhance our understanding of mechanisms linking H_2S production to sulfur and central energy metabolism. In addition, the mutant deficient in H_2S production will enable further studies into the role of H_2S in *Mtb* physiology.
3. Successful completion of our studies investigating how the bioenergetics and redox status of the mutant deficient in H_2S production differ to that of the wild type will advance our understanding of *Mtb* physiology. This new knowledge may lead to the identification of new targets for the development of novel pharmacological interventions and innovative anti-mycobacterial strategies.

4. Since H_2S has been used as a valuable diagnostic feature in bacterial classification and bacterial diagnosis [170-175], establishing that *Mtb* produces H_2S may lead to the development of a range of rapid H_2S-based diagnostic assays where H_2S is used as a diagnostic and/or prognostic biomarker.

`

CHAPTER 2: METHODOLOGY

2.1 General

All mycobacteria strains were cultured in Middlebrook 7H9 media (Difco) supplemented with 0.01 % tyloxapol (Sigma), 0.2 % glycerol (Sigma) and 10% (oleic acid, bovine albumin fraction V, dextrose, and catalase (OADC), unless stated otherwise. Cultures were placed in a shaking incubator (100 rpm) at 37°C. Strains examined included *Mb* H37Rv, *Mtb* CDC1551, *Mycobacterium bovis* (supplemented media with 100 µM sodium pyruvate), *Mycobacterium bovis* BCG, *M. smegmatis*, two drug susceptible *Mtb* strains (TKK-01-0027 and TKK-01-0047) and two multi-drug resistant *Mtb* strains (TKK-01-0035 and TKK-01-0001). The drug MIC_{50} values used during this study were as follows: Clofazimine (CFZ), 211 nM; Rifampicin (RIF), 486 nM; Isoniazid (INH) 240 nM. Where required, the following antibiotics were used; hygromycin B (100 µg/ml for *E. coli*, 50 µg/ml for mycobacteria) and kanamycin (50 µg/ml for *E. coli*, 25 µg/ml for mycobacteria). Dihydroethidium (DHE) were purchased from ThermoFisher Scientific (Cat. # D11347). Restriction enzymes were obtained from Thermo Scientific (Germany). KOD Xtreme Hotstart DNA polymerase kit was obtained from Merck (Darmstadt, Germany). T4 DNA ligase was obtained from New England Biolabs (NEB). *E. coli* DH5α, used for cloning and DNA manipulation, was routinely cultured in Luria-Bertani liquid media at 37 °C. Oligonucleotides were synthesized by Thermo (USA). All other reagents were purchased from Merck or Sigma-Aldrich.

Table 3*:* Bacterial strains used in this study

Strain	Description	Source
M. tuberculosis H37Rv	Wild type (wt)	ATCC
M. bovis BCG Pasteur	Vaccine strain	ATCC
M. bovis	Wild type	ATCC
M. tuberculosis TKK-01-0027	Clinical drug susceptible *Mtb* strain (DS27)	Alex Pym, AHRI
M. tuberculosis TKK-01-0047	Clinical drug susceptible *Mtb* strain (DS47)	Alex Pym, AHRI
M. tuberculosis TKK-01-0035	Clinical multi-drug resistant *Mtb* strain (MDR35)	Alex Pym, AHRI
M. tuberculosis TKK-01-0001	Clinical multi-drug resistant *Mtb* strain (MDR01)	Alex Pym, AHRI
M. tuberculosis Δ*rv3684*	*rv3684* deletion mutant (Δ*rv3684*) in H37Rv; Hyg^R	This study
M. tuberculosis Δrv3684::hsp$_{60}$-rv3684	*rv3684* complement (*comp*) of Δ*rv3684*; Hyg^R and Kan^R	This study
M. tuberculosis CDC1551	Wild type (wt)	ATCC
M. tuberculosis Tn::rv3682	*rv3682* transposon mutant in CDC1551; Kan^R	John Hopkins University, School of Medicine, TARGET
M. tuberculosis Tn::rv3683	*rv3683* transposon mutant in CDC1551; Kan^R	John Hopkins University, School of Medicine, TARGET
M. smegmatis mc^2155	Wild type (wt)	ATCC
M. smegmatis wt$_p$-rv3684	*rv3682-rv3683-rv3684* complemented strain under control of the *Mtb* native promoter (*wt$_p$*) in mc^2155	This study
M. smegmatis hsp$_{60}$-rv3684	*rv3682-rv3683-rv3684* complemented strain under control of *hsp$_{60}$* promoter in mc^2155	This study

`

2.2 Preparation of mycobacterial lysates

All cultures were grown to an OD_{600} of ~0.8. The cells were then harvested from 30 ml of culture and centrifuged at 4,000 x g for 5 min. The supernatant was discarded, and the pellet was resuspended in 1-2 ml of lysis buffer (50 mM Tris-HCl, pH 8.0; 150 mM NaCl; protease inhibitor [Roche]), depending on the size of the cell pellet. Cells were lysed in the Magnalyser (Roche) at 7000 rpm for 1 min and then placed on ice for 4 min. This was repeated 3-4 times. The lysates were then centrifuged at 15,000 x g for 10 min. The supernatant was collected and passed through a 0.22 µm filter. Protein determination was performed using the Micro BCA Protein Assay Kit (ThermoFisher Scientific) and the absorbance at 562 nm was measured using a Biotek Synergy H4 Hybrid plate reader. Lysates were stored at -80°C until use.

2.3 H_2S measurement using the lead acetate assay

Mycobacterial cultures were harvested at an OD_{600} of 0.8-1, and centrifuged at 3,500 x g for 5 min. The bacterial pellet was resuspended in an equal volume of 7H9 media containing 0.01% tyloxapol, 0.2% glycerol and 10% OADC. 10 ml of diluted culture at an OD_{600} of 0.1 was then transferred to a 30 ml culture bottle. Lead acetate strips (Thermo Fisher Scientific) were affixed to the inner wall of the culture bottles. The strips were monitored for the formation of dark colored lead sulfide precipitate and scanned after 48 h. The intensity of the dark lead sulfide stain is proportional to the amount of H_2S present. The lead sulfide stain was then scanned and quantified by measuring the grayscale values for a specific area of each strip and normalized to OD_{600} using ImageJ software version 1.53a (Java 1.8.8_12 (64 bit) [176].

2.4 H_2S measurement using the bismuth (III) chloride ($BiCl_3$) assay

The $BiCl_3$ (BC) assay is used to measure H_2S based on the reaction of H_2S with a bismuth (III) salt to form bismuth (III) sulfide (Bi_2S_3), which appears as a brown-to-black precipitate [128]. The BC assay was performed in 96-well plates using intact H37Rv bacteria and lysates as described by Basic *et al.* (2015) [127]. Once the OD_{600} of cultures reached ~0.8-1, the cultures were centrifuged at 3500 x g for 5 min. The supernatant was discarded, and the culture pellet was resuspended in the initial volume of media before centrifugation. The BC assay solution (2x) contained 0.4 M triethanolamine-HCl/Tris-HCl (Sigma), pH 8.0; 1 mM $BiCl_3$ (Sigma); 20 µM pyridoxal 5-phosphate monohydrate (PLP) (Sigma), 20 mM EDTA (Sigma) and 40 mM L-cysteine (Cys) (Sigma). 100 µl of the mycobacteria cell (OD_{600} = 1.0) suspension or lysate (5 µg), with or without the inhibitors amino-oxyacetate (AOAA) and DL-propargylglycine (PAG) were mixed with 100 µl of freshly prepared 2x bismuth solution in clear flat-bottomed 96-well microtiter plates (Costar). Cell suspensions of the various strains were normalized to the same OD_{600} ~1, while for lysates, normalized to the protein concentration. Bi_2S_3 formation was determined by measuring the absorbance at 405 nm. The kinetics for mycobacterial cells was measured every 30 min for 15-20 h at 37 °C with shaking, using a Hidex Sense Plate reader. Enzymatic kinetics

`

using lysates was measured every 5 min for 5-20 h, with shaking at room temperature (~20–22 °C) using a Biotek Synergy H4 Hybrid Reader.

2.5 H_2S measurement using the Unisense amperometric microsensor

H_2S released by cell cultures and lysates was measured at room temperature, with a sensitive sulfide gas amperometric microsensor, H_2S-500 (Unisense, A/S, Denmark) connected to a microsensor multimeter (Unisense, A/S, Denmark) as an amplifier for data acquisition. The signal for H_2S was collected in mV and converted to µM using the NaHS (freshly prepared) standard curve generated from a concentration range of 0 to 100 µM (prepared in an anaerobic glovebox). The H_2S microsensor was calibrated in accordance with the manufacturer's instructions. Bacteria at an OD_{600} of 0.2 were cultured in media with or without 1 mM Cys. After 72 h, H_2S concentration measured using microsensor in the cell culture and the cell-free culture supernatants (referred to as 'cleared supernatants').

For real-time H_2S measurement in lysates, the microsensor was placed in a 2 ml tube containing 1 ml assay buffer (0.4 M triethanolamine-HCl, pH 8.0; 20 µM PLP, 10 mM EDTA) with or without 20 mM Cys. The signal was allowed to stabilize for 2-5 min after which 40 µg *Mtb* lysate was added to the reaction. When appropriate, Cys (0.1 to 4 mM) were added subsequently to the tube at different intervals. To confirm AOAA inhibition, *Mtb* lysate preincubated with AOAA (4 mM) was added to the assay buffer containing 20 mM Cys. OASS activity was measured as follow. The microsensor was placed in 1 ml PBS solution. A 10 µl aliquot of 25 mM NaHS was added to the reaction tube twice. After the signal stabilized, 30 ng of OASS was added to the reaction. After 2 min, OAS substrate was added to the reaction to a final concentration of 10 mM and the H_2S signal monitored in real time.

2.6 Native PAGE analysis and in-gel BC assay

Equal amounts (15-25 µg per lane) of mycobacterial lysates were resolved on 10% PAGE gels (Bio-Rad) under non-denaturing conditions using running buffer containing 25 mM Tris-base and 190 mM glycine. To detect the presence of H_2S-producing protein bands, gels were incubated in 20-50 ml of BC solution and incubated at room temperature with shaking. Gels were monitored every 20-60 mins for the appearance of dark-colored Bi_2S_3. For gels exposed to AOAA, gels were incubated in 20 ml of 2 mM AOAA in 50 mM Tris-HCl pH 8.0 with shaking at room temperature for 5 mins, followed by BC solution containing 2 mM AOAA for overnight.

`

2.7 Extracellular Flux analysis

The oxygen consumption rate (OCR) of *Mtb* strains were measured using a Seahorse XF96e Extracellular Flux Analyzer (Agilent). *Mtb* bacilli were adhered to the bottom of a Cell-Tak-coated XF cell culture microplate at $2x10^6$ bacilli per well. Cell-Tak has no effect on *Mtb* basal respiration [177]. Assays were carried out in unbuffered 7H9 media (pH 7.35) with no carbon source. *Mtb* bacilli were grown in this unbuffered 7H9 media, containing only 0.01 % Tyloxapol, for 24 h before being seeded into the XF cell culture microplate and the start of the experiment. In general, basal OCR was measured for ~25 min before automatic sequential injection of the compounds through the drug ports of the sensor cartridge. The duration of OCR measurements after compound addition and the concentration used, varied by experiment. OASS modulation of *Mtb* OCR in the presence of Cys was performed by the simultaneous addition of Cys, OASS and substrate OAS (final concentration of 4 mM, 0.03 µg/ml and 4 mM, respectively). All OCR data figures indicate the time of each addition as dotted lines. OCR data points are representative of the average OCR during 4 min of continuous measurement in the transient microchamber, with the error being calculated from the OCR measurements taken from at least three replicate wells by the Wave Desktop 2.2 software (Seahorse Biosciences). The transient microchamber is automatically re-equilibrated between measurements through the up and down mixing of the probes of the XF96 sensor cartridge in the wells of the XF cell culture microplate.

2.8 CFU-based assays

Mid-log phase mycobacterial cultures were diluted to an OD_{600} of 0.01 in catalase-free 7H9 media. For survival studies in the presence of NaHS, bacterial cultures (7H9 with 10 % OAD) were untreated or treated with anti-TB drugs and NaHS at indicated concentrations. For survival studies in the presence of antioxidants, bacterial cultures(7H9 with 10 % OAD) were treated with or without 0.25 mM cumene hydroperoxide (CHP) for 16 h. For survival studies in the presence of CFZ, bacterial cultures were treated with or without clofazimine of MIC 60x, 100x and 300x for 8 days. For all studies, samples were taken at indicated time points, serially diluted in PBS containing 0.01 % tyloxapol and plated onto 7H11 OADC agar plates. Plates were incubated at 37 °C for 4 weeks to determine CFU counts.

2.9 ROI assay

ROI production in *Mtb* strains (OD_{600} ~1.0) was measured using the dihydroethidium ROI sensing dye (DHE - Excitation/Emission at 500/605 nm). *Mtb* strains were cultured in Middlebrook 7H9 media supplemented with 0.2 % glycerol and 0.01 % tyloxapol at 37ºC with either 10 % OAD (oleic acid, albumin, dextrose) with/without 0.25 mM cumene hydroperoxide (CHP) or 10 % OADC (oleic acid, albumin, dextrose and catalase) with/without 60x MIC of CFZ for 16 h in 4 replicates. After treatment, *Mtb* cultures were washed by centrifugation (3000 x g) and resuspended in 1x PBS (pH 7.4) containing 10 µM DHE, incubated further for 20 min at 37ºC followed by two washes with PBS to remove residual

`

extracellular dye. The fluorescence of DHE-stained cells was acquired with a FACS Aria III cell sorter using the 500 nm laser excitation, and BP 610/20 nm for emission acquisition. The cells were acquired at a constant flow rate of setting 4 and a threshold rate of approximately 1,000-2,000 events per second and 100,000 total events were recorded per sample. For result analysis, the bacterial population was identified according to the forward and side scattering property of the population (FSC versus SSC). Bacterial aggregation removed from the data analysis using doublet discrimination from the plot of FCS-width Vs FSC-height. Data analysis in percentage DHE+ cells and mean fluorescent intensity was calculated with the FlowJoTM v10.4.2 (Tree Star, Ashland, OR).

2.10 Identification of proteins by LC-MS/MS

The entire Bi_2S_3 stained protein band was excised from the gel, rinsed with water and cut into approximately 1 mm x 4mm pieces using a sterile scalpel. The gel slices were then rinsed with 100 mM ammonium bicarbonate solution and collectively transferred into a sterile Eppendorf® LoBind 1.5 ml microcentrifuge tube. 500 µl of acetonitrile (ACN) was added and the sample was incubated on ice for 10 min. The sample was then briefly centrifuged, the acetonitrile removed and 100 µl of 10 mM dithiothreitol (DTT) solution was added to rehydrate the gel pieces and reduce the proteins. The sample was incubated in 10 mM DTT solution at 56 °C for 30 min, removed, cooled to room temperature and then 500 µl of ACN was added and the sample was incubated on ice for 10 min. The sample was then centrifuged, and the supernatant was removed, 100 µl of 55 mM iodoacetamide solution was added and the sample was incubated at room temperature for 30 min in the dark to facilitate protein alkylation. Following alkylation, 500 µl of ACN was added and the sample was incubated on ice for 10 min. All solution was then removed and 200 µl of trypsin (Promega, sequence grade) solution at a concentration of 13 ng/ml was added to the gel slices, the sample was mixed gently and incubated at 4 °C for 2 h to allow the gel slices to re-hydrate and slow diffusion of trypsin into the polyacrylamide gel matrix. The samples were incubated in the trypsin solution at 37 °C, overnight (18-24 h) for optimum in-gel protein digestion. The resulting peptides were extracted by adding 400 µl of 5 % formic acid/acetonitrile (1:2, v/v) solution to the sample followed by 15 min incubation at 37 °C on a shaking heating block set at 450 rpm. The sample was briefly centrifuged, the solution transferred to a sterile Eppendorf® LoBind microcentrifuge tube, and the sample dried using a SpeedVac concentrator (Labconco, USA) set at 40°C. The dried, extracted peptides were then reconstituted in 50 µl of 5 % formic acid solution, transferred to a glass vial and 1 µl of sample was injected for nano-LC-MS/MS analysis.

The peptide digests were analyzed using a Thermo Q Exactive Orbitrap mass spectrometer coupled to a Dionex UltiMate 3000 UPLC system. The tryptic peptides were maintained at 6°C in the autosampler and were separated on a 15 cm nano capillary column (ID 75 µM) packed in the laboratory with Supelco 3.5 µM C18 stationary phase. A 45 min gradient from 1% acetonitrile, 99 % water/0.1 % formic acid, to 50 % acetonitrile/water, 0.1 % formic acid, flow rate 300 nl/min, was used for the analysis. Peptide

`

fragment mass spectra were acquired using a full MS, data dependent MS2 Top 10 method. The MS RAW files were processed using Thermo Scientific™ Proteome Discoverer™ 2.2 software and SEQUEST™ peak-finding search engine application to compare the mass spectra to the *Mtb* FASTA database to identify relevant proteins and peptides. The method was set to consider carbamidomethyl modifications and methionine oxidation. The protein candidates were then screened for high confidence, possible lyase candidates demonstrating pyridoxal phosphate binding domains. A targeted method was constructed using the 5 strongest peptide fragment ions for the most likely candidate, Rv3684/Cds1, and the samples re-analyzed using this method to confirm the presence of the enzyme.

2.11 Preparation of mycobacterial genomic DNA

Genomic DNA was isolated from *Mtb* H37Rv as follows: *Mtb* H37Rv was grown to late log phase (OD_{600} = 1.0) in 50 ml 7H9 liquid media. Cells were harvested (2,000 x g, 20 min) supernatant was discarded and 6 ml of a freshly prepared solution of 3 parts chloroform to 1-part methanol added. Tubes were then vortexed for 1 min. Tris-buffered phenol (6 ml) was then added and the tube vortexed for a further 30 sec. Finally, 9 ml of 4 mM guanidine thiocyanate solution were added, and the tubes inverted several times. After centrifuging at 2000 x g for 15 min the upper phase was removed, and an equal volume of isopropanol added to precipitate genomic DNA. The DNA was collected by centrifugation and washed with 70% ethanol before being air dried and suspended in 100 µl Tris-EDTA, pH 7.5.

Table 4: Plasmids used in this study

Vector/construct	Relevant genotype and properties	Source
pMV261	*E. coli*- Mycobacterium *shuttle vector, $hsp_{60,}$ ColE1/pAL500 oriM,* Kan^R	William R. Jacobs Jr. (Albert Einstein College of Medicine)
rv3684 phasmid	*rv3684::res–hyg–res*	Michelle Larsen (Albert Einstein College of Medicine)
cbs phasmid	*cbs::res–hyg–res*	This study
pMV261::*hsp_{60}-rv3684*	The *rv3684* open reading frame cloned under the control of the *hsp60* promoter subcloned into pMV261	This study
pMV261::*wt_p-rv3684*	The *rv3682-rv3683-rv3684* open reading frames containing the native promoter (*wt_p)* promoter subcloned into pMV261	This study
pET15b	*amp^r, E. coli* vector used for production of his-tag fused proteins	Novagen
pET15b-*rv3684*	*Mtb rv3684* ORF subcloned into pET15b	This study
pET28b-OASS	Construct encoding N-terminally 6xHis-tagged EhOASS (O-acetylserine sulfhydrylase from *Entamoeba histolytica*	Alessandro Giuffrè (CNR Institute of Molecular Biology and Pathology, Rome, Italy)

`

Table 5: Oligonucleotides used in this study

Oligonucleotide	Sequence (5' → 3')	Description
Rv3684F	TATGGATCCTATGAGCGGCGGGGCCTGTATC	*rv3684* forward primer for pMV261 subcloning, *Bam* HI
Rv3684R	GTTATCGATTAGGCTGCGGACCGCGATAC	*rv3684* reverse primer for pMV261 subcloning, *Cla* I
ponABCF	TAAGGATCCAAGGTAGTCCGACCACGAAAC	*rv3682*, *rv3683* and *rv3684* forward primer, *Bam* HI
ponABCR	ATAATCGATCTACCAAGCTGCGCCACAC	*rv3682*, *rv3683* and *rv3684* reverse primer, *Cla* I
Rv3684CF	GAACCCAATGAACTATCTGAC	Forward primer for Δ*rv3684* confirmation
Rv3684CR	GCATAGCGCATAGAGGAA	Reverse primer for Δ*rv3684* confirmation
UUT	GATGTCTCACTGAGGTCTCT	"Universal uptag" primer for Δ*rv3684* confirmation
Rv3684CEF	AATAATCATATGTTGAGCGGCGGGGCCT	*rv3684* forward primer for pET15b subcloning, *Nde* I
Rv3684CER	AATAATGGATCCTCACGTCCATCGACAG	*rv3684* reverse primer for pET15b subcloning, *Bam* HI
Rv1077CF	GGTCGACTATCGGTTGATT	Forward primer for Δ*rv1077* confirmation
Rv1077CR	ACATTGCGTTTATCCTCACT	Reverse primer for Δ*rv1077* confirmation

2.12 Construction of *Δrv3684* and *Δrv1077* mycobacterial strains

The *rv1077* (*cbs*) and *rv3684* knockout *Mtb* strains were generated by homologous recombination using specialized phage transduction according to Badarov *et al*. (2002) [178]. The *rv3684* allelic exchange substrate (AES) phasmid was a kind gift from Michelle Larsson (Albert Einstein College of Medicine). The AES contains *rv3684* disrupted by the hygromycin resistance gene. Briefly, the AES phasmid was amplified in *E. coli* DH5α and purified using a DNA plasmid Mini-prep kit (Thermo). *M. smegmatis* was then transduced with the AES and a high titer phage lysate prepared. *Mtb* H37Rv was grown to an OD_{600} of ~0.8 and washed twice with buffer (50 mM Tris-HCl, pH 7.6, 150 mM NaCl, 10 mM $MgCl_2$, 2 mM $CaCl_2$) then mixed with the high titer phage lysate in a 1:1 ratio and incubated at 37 °C overnight. After centrifugation (16,000 x g, 10 mins, 4 °C) the pellet was resuspended in 0.2 ml 7H9 media and plated on hygromycin selective 7H10 agar. After 3 weeks at 37 °C, 5 individual colonies were inoculated in 7H9 media supplemented with 50 µg/ml hygromycin. Genomic DNA of each colony was extracted, and gene deletion confirmed using PCR with primers Rv3684CF, Rv3684CR (*rv3684*) or Rv1077CF, Rv1077CR (*rv1077*) and UUT.

2.13 Mycobacterial complementation

The *rv3684* ORF was PCR amplified from genomic *Mtb* DNA using KOD Xtreme HotStart DNA polymerase (Roche) according to manufacturer's protocol and primers (Rv3684F and Rv3684R). The PCR product and pMV261 vector were digested with *Bam*HI and *Cla*I (Thermo), isolated using agarose

`

purification, and ligated using T4 DNA ligase (NEB) to produce pMV261::*hsp*$_{60}$-*rv3684*. A second complementation vector was constructed. The ORF of *rv3682*, *rv3683* and *rv3684*, with an additional 500 bp upstream region, was PCR amplified using primers ponABCF and ponABCR. The amplicon was digested using *Bam* HI and *Cla* I and ligated into the pMV261 vector. Complementation vectors expressing *rv3684* under the control of either the *hsp*$_{60}$ or native promoter were electroporated (Gene Pulser Xcell, Biorad) into the *Mtb* Δ*rv3684* strain and transformants selected on 7H10 agar plates containing hygromycin (50 µg/ml) and kanamycin (25 µg/ml). The vectors were similarly electroporated into *M. smegmatis*. Complemented strains were grown in 7H9 media containing 25 µg/ml kanamycin.

2.14 Purification of recombinant proteins

The *rv3684* 1041 bp open reading frame was PCR amplified using *Mtb* genomic DNA and primers Rv3684CEF and Rv3684CER (see Supplementary Table 4). The PCR product was digested with *Nde* I and *Bam* HI and then ligated into the pET15b expression vector previously digested with *Nde* I and *Bam* HI. These restriction sites are in the pET15b MCS downstream of a 6-His coding region, resulting in addition of a 6-His tag to the N-terminus of the encoded protein. The ligated construct (pET15b-*rv3684*) was then verified by sequencing. *E. coli* BL21 (DE3) cells were transformed with pET15b-*rv3684* and grown until the OD_{600} reached 0.5-0.6. Protein expression was induced by the addition of 0.4 mM of IPTG followed by growth overnight at 18 °C. The cells were pelleted by centrifugation at 5000 rpm for 10 mins, sonicated, and the lysate used for protein purification using nickel-affinity resin (Bio-Rad) by gravity chromatography. The full description of elution conditions, storage buffer etc. is presented in the actual protocol used for the purification of Rv3684, this attached in Appendix B. OASS (pET28b-EhOASS construct encoding N-terminally 6xHis-tagged EhOASS) was overexpressed and purified from *E. coli* as describe previously [179].

2.15 Rv3684 enzyme kinetics

The rate of H_2S production by purified recombinant Cds1 was monitored via formation of Bi_2S_3, which has an absorbance maximum at 405 nm [128]. Briefly, purified Cds1 enzyme (1 µg of enzyme in 20 µl buffer) and 180 µl of BC solution were mixed in a well of a flat bottom clear 96-well plate (Costar). Bi_2S_3 formation was monitored at room temperature over 30 mins (readings taken once per minute) using a Biotek Synergy H1 hybrid plate reader. The absorbance at 405 nm was converted into product concentrations using the Beer-Lambert equation. The molar absorption coefficient for Bi_2S_3 was determined to be 3,156.9 $M^{-1}cm^{-1}$ using $Na_2S.9H_2O$ (Sigma) as a standard. Initial velocities were calculated and plotted against Cys concentrations. The K_m and V_{max} values were determined in GraphPad Prism (version 8.4.3) using the Michaelis-Menten equation. The K_{cat} values were calculated by dividing V_{max} by the nanomole of enzyme used in the reaction. Cds1 inhibition studies with AOAA

`

and PAG were performed by using 0.1 µg of purified recombinant Cds1 enzyme in 200 µl of 0.4 M triethanolamine-HCl/Tris-HCl, pH 8.0; 1 mM $BiCl_3$; 20 µM PLP, 20 mM EDTA with varying concentrations of AOAA or PAG. IC_{50} curve was plotted using values calculated from the end point absorbance values (405 nm) for Cds1 AOAA kinetic assays performed in quadruplicate.

The production of cysteine-derived pyruvate by Cds1 was performed as follows. Purified Cds1 was added to three independent tubes, respectively. 50 µl of 20 mM Cys in PBS (20 mM Na_2HPO_4, 100 mM NaCl, pH 7.5) was added and the reaction left for 15 minutes at room temperature. The reactions were stopped by heating to 80 °C for 5 minutes and the tubes centrifuged at 15,000 rpm for 5 mins. 10 µl aliquots of each reaction solution were taken from the supernatant and analysed by LC-MS/MS. Each sample was assayed in triplicate.

2.16 Identification of Rv3684 enzymatic products by LC-MS/MS

The enzymatic product of Rv3684 (with Cys as substrate) was identified using ultra high liquid chromatography coupled to high resolution/high accuracy mass spectrometry based on the analyte's exact mass and HPLC retention time compared to authentic metabolite reference standards. A reference standard mixture of important negatively charged metabolites, including pyruvate and the study samples were analysed on the Q Exactive LCMS system, as described elsewhere, using high resolution molecular ion scans. The RAW files were subjected to post-run analysis using Skyline software along with a template constructed to monitor the relevant analytes. The exact theoretical mass for ^{12}C pyruvate standard, is 87.008768 (87.0088) Da. The standard was present in the molecular ion scans with the same exact mass, in the standard mixture when subjected to analysis. The retention time for the pyruvate in standard mix on the Aminex column used is 11.0 min. In the samples, a peak was observed with the same retention time and exact mass as pyruvate standard and this was considered sufficient evidence for verification of identity.

2.17 LC-MS/MS targeted metabolomics analysis using [U-^{13}C]-Cysteine and [U-^{13}C]-Glucose

Replicate cultures (~30 ml each) inoculated at an OD_{600} of about 0.05 were grown in inkwell bottles to an OD_{600} of ~0.8 at 37 °C with shaking (150 rpm) for 7 days. Each replicate culture was pelleted by centrifuging at 3,500 x g for 10 min. The culture medium was discarded, and cells were washed three times with 30 ml of 7H9 containing 0.01 % Tyloxapol. After the last wash, the pelleted cells were resuspended in 5 ml of 7H9 media (containing 7H9 + 0.01 %Tyloxapol + 0.2 % glycerol + 10 % OAS + 0.2 % [U-^{13}C]-Glucose (Sigma-Aldrich)) or (7H9 + 0.01 % Tyloxapol + 0.2 % glycerol + 10 % OADS + 100 µM [U-^{13}C]-Cysteine (Cambridge Isotope Laboratories Inc.). After resuspension of the pellet,

`

the cultures were then incubated overnight at 37 °C on shaking (150 rpm) and harvested by centrifugation at 3,500 x g for 3 min. Cells pellets were snap frozen on dry ice for about 5 mins and then thawed and prepared for lysis using the Magnalyser (Roche) at 7000 rpm for 1 minute followed by cooling on ice for 4 min, repeated 3-4 times. The lysis was performed using a 1.8 ml solution of methanol, acetonitrile, and water in the ratio of 2:2:1). The lysate was then centrifuged at 15,000-17,000 x g for 10 min. The supernatant was collected and filtered through a 0.22 µm filter. The recovered lysate was then vacuum concentrated to dryness (Eppendorf Concentrator Plus) at 30°C for 12 h. The dried lysate pellets were then resuspended in 200 µl of purified water. 100 µl of this suspension for each replicate was submitted for LC-MS/MS targeted organic acid (metabolites) analysis and 100 µl (50 µl resuspension + 50 µl acetonitrile) was submitted for LC-MS/MS targeted amino acid analysis. LC-MS/MS was used for relative quantification of each organic acid and amino acid. The LC-MS/MS sample analysis was performed using a Thermo Scientific Dionex Ultimate 3000 UHPLC system coupled to a Thermo Scientific Q-Exactive Mass Spectrometer with a HESI source. A sample volume of 1 µl was injected onto the Waters Xbridge® BEH HILIC HPLC column (2.5 µm particles, 2.1 x 100 mm), column oven set at 40 °C and chromatographic separation was performed using gradient elution at a flow rate of 200 µl/min and total run time of 26 min. Mobile phase A contained water with 0.1 % formic acid and mobile phase B contained acetonitrile with 0.1% formic acid. Data was acquired using full scan MS (without HCD fragmentation) in positive mode, over the m/z range 50 – 750 Da at 70000 resolution. A QC sample was prepared using 21 different amino acids at a concentration of 500 ng/ml, to monitor amino acid retention time consistency and MS sensitivity. Each sample was spiked with deuterated Alanine (D4-Alanine) as an internal standard to monitor processing efficiency and data normalization. The data was processed, and peak areas calculated, using Skyline 3.7 (MacCoss Lab, University of Washington, Seattle, WA, USA).

2.18 Statistics

Unless specified in the materials and methods, all experiments were performed on 3 to 6 biological replicates and the data were expressed as mean ± SD or mean ± SEM. Statistical significance of the data was determined using GraphPad Prism software (Version 8.0), (GraphPad Software, Inc.). Specific statistical tests are noted in the figure legends and include the Student's unpaired t-test (two-tailed), and one-way or two-way ANOVA.

`

CHAPTER 3: RESULTS

Most of the results and figures arrived at in this study and presented in thesis have been synthesized into a manuscript and submitted to Nature Communications for peer-review (currently under review). Attached in the appendix section is proof of submission of the draft manuscript which was submitted at the time of writing this thesis.

3.1 Mycobacteria endogenously produce H_2S

Three independent methods were utilized to measure endogenous H_2S production by mycobacteria; 1. the widely-used lead acetate [$Pb(Ac)_2$] method, 2. the bismuth chloride ($BiCl_3$; BC) assay method [128] and 3, a highly sensitive amperometric microsensor (Unisense A/S, Denmark) [147, 180-182]. The rationale for this multifaceted approach is to compensate for potential drawbacks in each of these techniques. Hence, there is a need for careful attention to detail in each of these techniques, as well as continuous validation experiments in either the solution or the headspace. For example, despite been widely used since the 1940s, the $Pb(Ac)_2$ strip method has been shown to react non-specifically with sulfides; [183]. Additionally, since H_2S can be produced spontaneously by media components [162], results have to be carefully interpreted and validated.

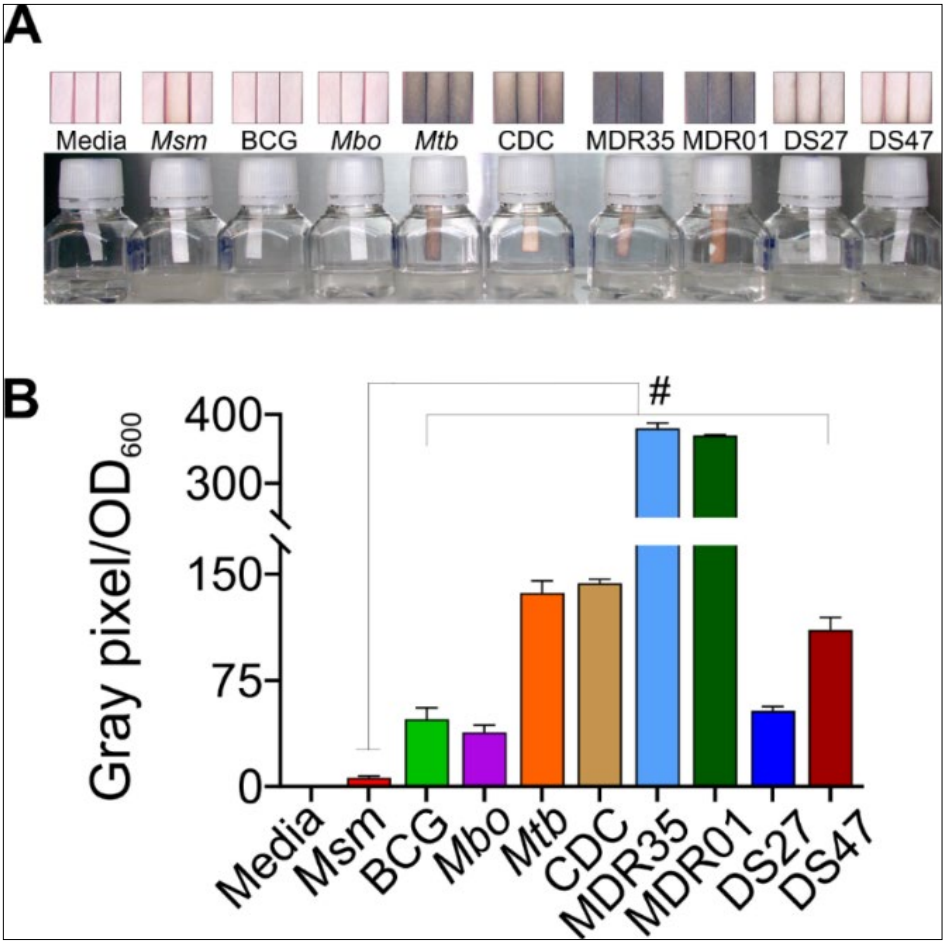

`

Figure 1: Detection of endogenously produced H_2S using lead acetate [$Pb(Ac)_2$] strips in the headspace of mycobacterial cultures. Lead acetate reacts with H_2S, resulting in the formation of a brown/black lead sulfide (PbS) stain on the strip. (A) H_2S detection in cultures of mycobacterial species using lead acetate strips. *Msm* – *M. smegmatis*, BCG – *M. bovis* BCG, *Mbo* – *M. bovis*, *Mtb* – *Mtb* H37Rv, CDC – *Mtb* CDC1551, MDR – multi-drug resistant and DS – drug sensitive clinical strains of *Mtb*. Note: Strips shown, (Figure 1A top insert) were scanned after 48 h of incubation. The inkwell bottles shown are representative of an earlier independent experiment after 72 h of incubation. (B) Estimation of H_2S production by quantifying lead sulfide formed on the strips (Figure 1A top insert) using ImageJ and data normalized to culture OD_{600}. Data shown is representative of two independent experiments, with mean ±SD from 3 lead acetate strips of the 3 cultures of each mycobacteria. All *P* values are relative to *Msm*. Statistical analysis was performed using GraphPad Prism 7.02. One-way ANOVA with Dunnett's multiple comparisons test was used for statistical significance; $\#P < 0.0001$.

Firstly, lead acetate [$Pb(Ac)_2$] strips were used to detect H_2S in the headspace of mycobacterial cultures (Figure 1A). This method is based on the reactivity of lead acetate with H_2S, resulting in the formation of a brown/black lead sulfide (PbS) stain on the strip [145]. Here, we show that H_2S is endogenously produced by slow-growing *Mtb* laboratory strains [*Mtb* H37Rv, *Mtb* CDC1551 (CDC)], *Mtb* clinical strains [(drug-sensitive (DS) and multi-drug resistant (MDR)], *M. bovis* BCG (BCG), *M. bovis (Mbo)* as well as the fast-growing *M. smegmatis (Msm)*, inoculated to the same optical density (Figure 1A). Since H_2S production may be growth-phase dependent, in a second independent experiment (Figure 1B), we quantified PbS formation on lead acetate strips and normalized the measured values to culture density as previously described [162, 176, 184]. Notably, BCG, *Mbo*, and the DS clinical *Mtb* strains produced significantly less H_2S compared to the laboratory strains *Mtb* H37Rv and CDC. Intriguingly, the slow-growing pathogenic *Mtb* strains, particularly multidrug-resistant (MDR) strains, produced the highest levels of H_2S, whereas *Msm* produced virtually undetectable amounts of H_2S (Figure 1B).

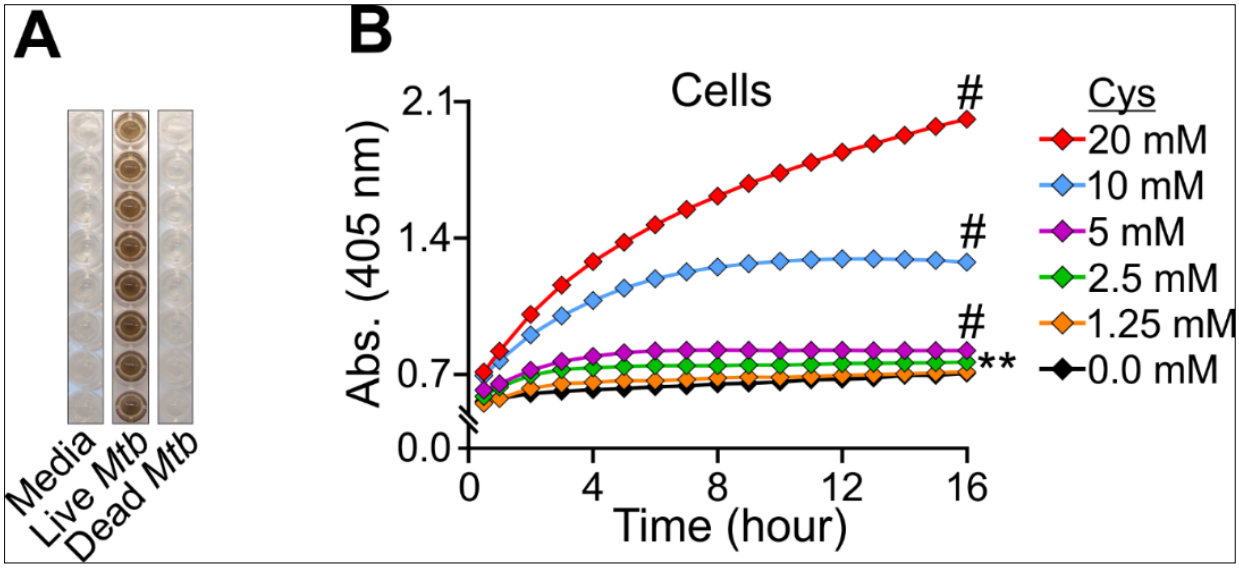

Figure 2: Detection of endogenously produced H_2S in *Mtb* culture using $BiCl_3$ (BC) microplate-based assay. Endogenously produced H_2S was measured in culture media using the microplate-based assay, $BiCl_3$ (BC), where Bi^{3+} reacts with H_2S to generate a brown/black Bi_2S_3 precipitate. (A) H_2S production by live and heat killed *Mtb*. (B) Time course measurement of H_2S production measured in *Mtb* cells with different concentrations of Cys. Data shown is representative of 2-5 independent

`

experiments, with mean ±SD from 6-8 wells. All *P* values are relative to untreated (no Cys) controls. Statistical analysis was performed using GraphPad Prism 7.02. One-way ANOVA with Dunnett's multiple comparisons test was used for statistical significance; #$P<0.0001$.

Secondly, to independently verify the results shown in Figure 1A and 1B, which measured H_2S in the headspace, endogenously produced H_2S was measured in culture media using the microplate-based assay, $BiCl_3$ (BC), which reacts with H_2S to generate a brown/black Bi_2S_3 precipitate [128]. We also used cysteine (Cys) as a substrate to induce H_2S production. We anticipated that Cys transport into *Mtb* cells would influence H_2S production [168]. Therefore, the BC assay was also used to measure H_2S in cell lysates. Importantly, the assay is not growth-based as growth inhibiting concentrations of cysteine and EDTA are used. EDTA is particularly used to prevent spontaneous generation of H_2S from Cys and iron [162]. Figure 2A, illustrates the endogenously generated H_2S generated as a product of live *Mtb* cells compared to dead *Mtb* cells and the media control, while Figure 2B and Figure 3 show that *Mtb* H_2S levels positively correlate with Cys concentration in the growth medium and cell lysates.

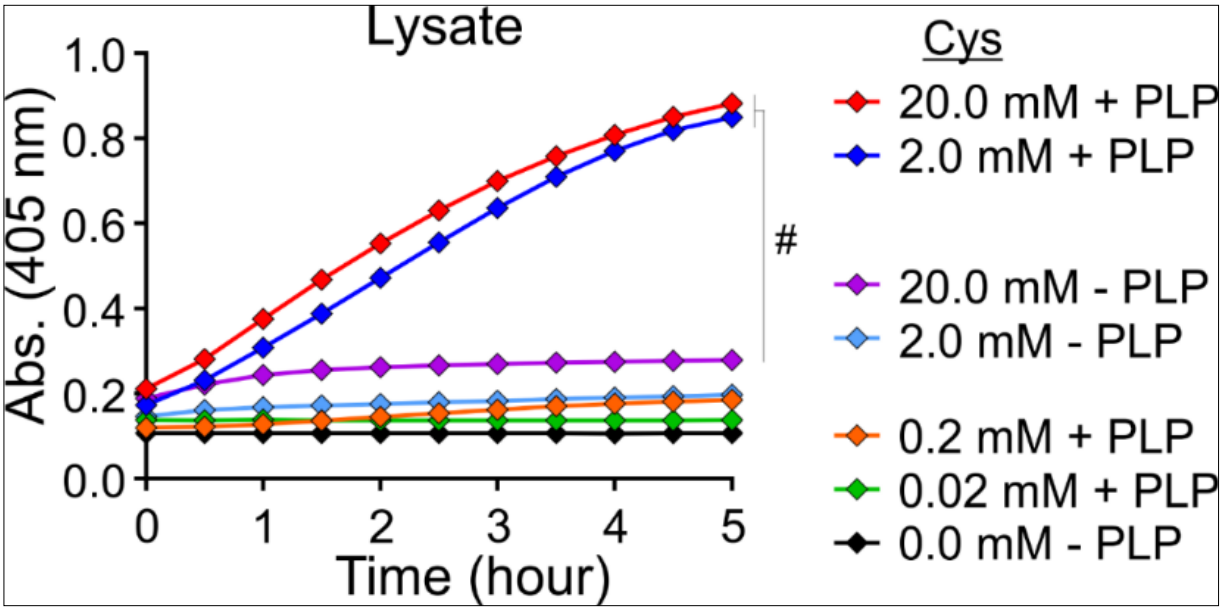

Figure 3: Detection of endogenously produced H_2S by *Mtb* lysates using a $BiCl_3$ (BC) microplate-based assay. Increased H_2S levels corresponding to increasing Cys concentrations and need for PLP as a co-factor were observed. Data shown is representative of 2-5 independent experiments, with mean ±SD from 6-8 wells. All *P* values are relative to untreated (no Cys) controls. Statistical analysis was performed using GraphPad Prism 7.02. One-way ANOVA with Dunnett's multiple comparisons test was used for statistical significance; #$P < 0.0001$.

A Cys dose response was observed for both cells (Figure 2B) and lysate-based assays (Figure 3), with increased H_2S levels corresponding to increasing Cys concentrations. As expected, we noted differences in H_2S production generated by the cell versus lysate-based assays, which we attributed to the regulation of Cys transport in live cells, but not cell lysates. Since H_2S producing activity in cell lysates requires pyridoxal 5-phosphate monohydrate (PLP) as a co-factor (Figure 3), we attempted to identify the H_2S-producing enzymes in *Mtb* by using inhibitors of two classes of possible H_2S-

`

producing enzymes. These include amino-oxyacetate (AOAA) and DL-propargylglycine (PAG). AOAA is an inhibitor of PLP-dependant enzymes and is most commonly used for blocking cystathione-β-synthase (CBS) activity [125], whereas PAG is an inhibitor of cystathione-γ-lyase (CSE) [125]. We observed an AOAA dose dependent reduction in H_2S in whole cells (Figure 4A), with the cells not being significantly affected by PAG (Figure 4B). A similar result was observed in lysates, with addition of AOAA resulting in a dose-dependent reduction (Figure 5A), while for PAG (Figure 5B), H_2S production was not significantly affected. These findings suggest that one or more PLP-dependent enzymes can produce H_2S in *Mtb*, consistent with our findings in Figure 4.

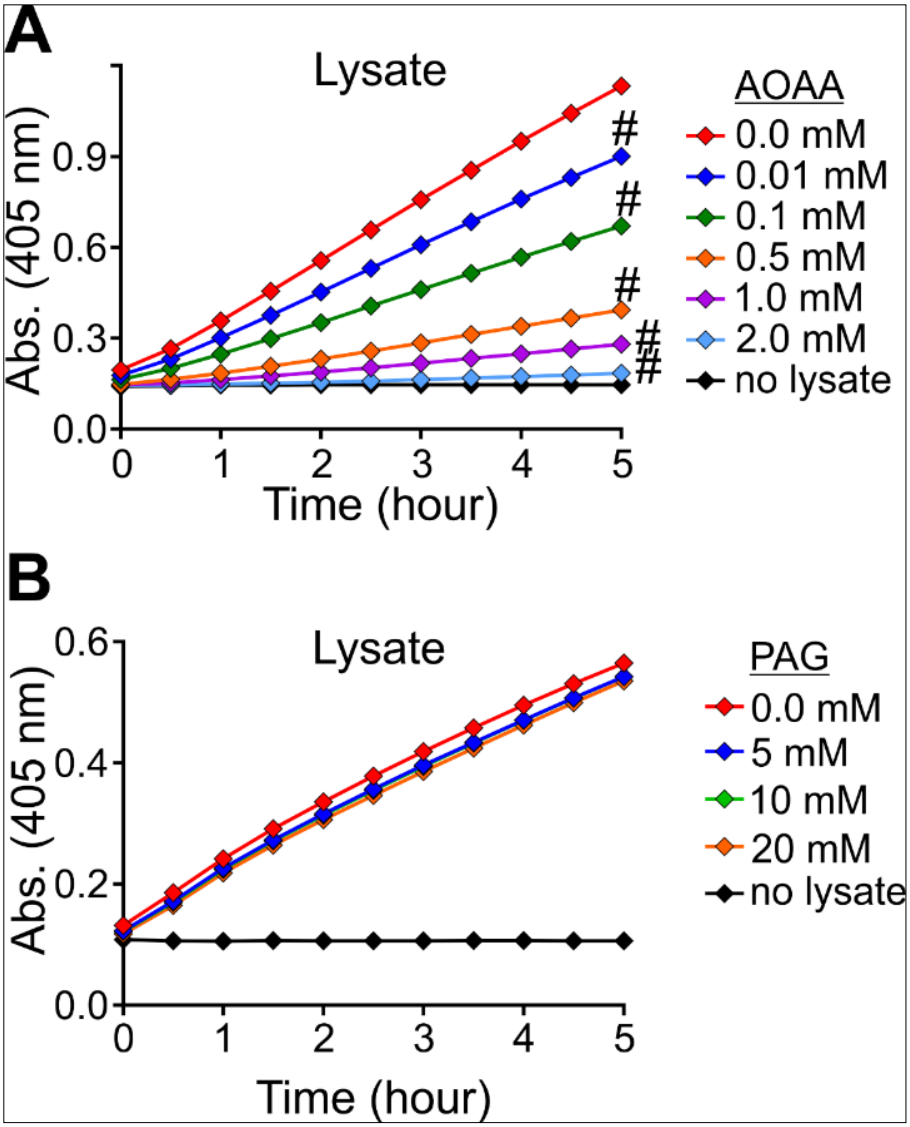

Figure 4: Detection of endogenously produced H_2S by *Mtb* cells using a $BiCl_3$ (BC) microplate-based assay with different concentrations of CBS and CSE inhibitors, AOAA and PAG respectively. (A) An AOAA dose dependent reduction in H_2S in whole cells was observed. (B) H_2S production was not significantly affected by PAG in *Mtb* cells with PAG. Data shown is representative of two independent experiments, with mean ±SD from 6-8 wells. All *P* values are relative to untreated (no inhibitor) controls. Statistical analysis was performed using GraphPad Prism 7.02. One-way ANOVA with Dunnett's multiple comparisons test was used for statistical significance; # $P < 0.0001$.

`

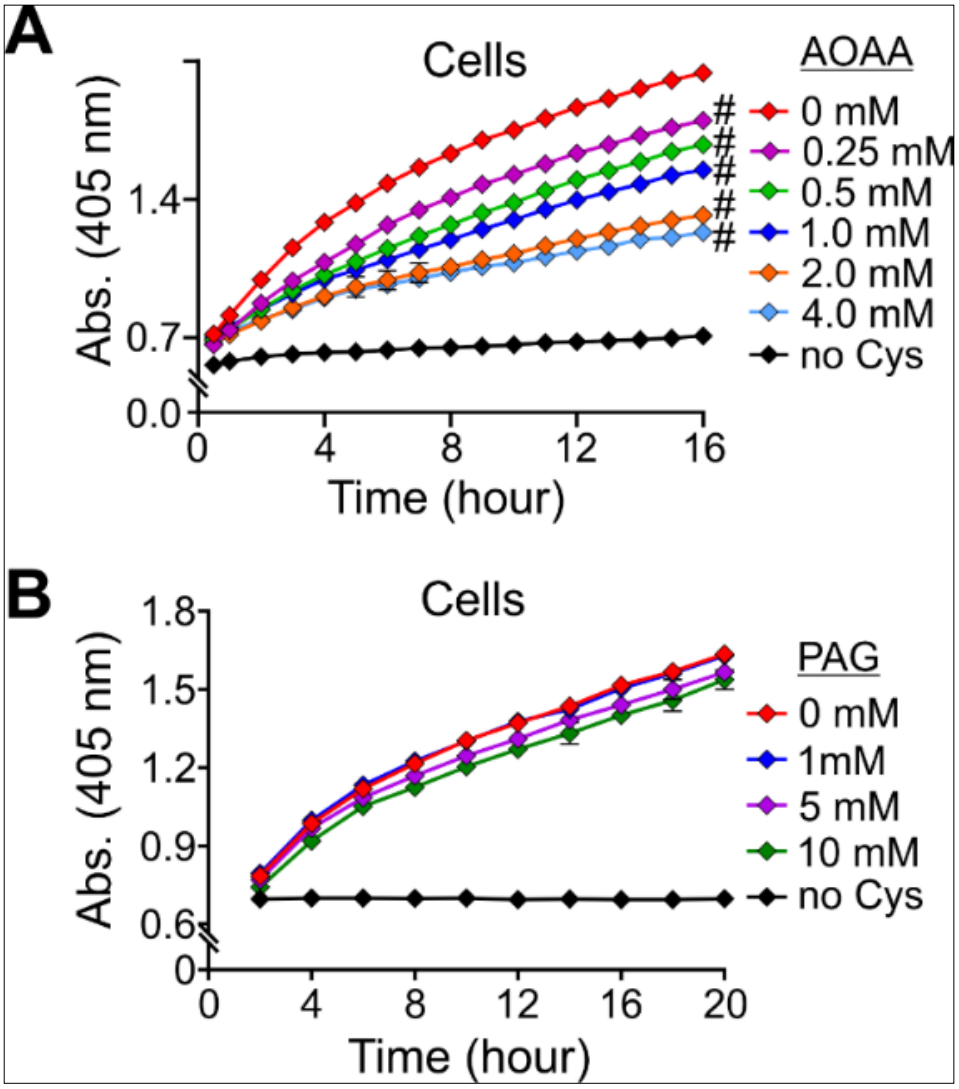

Figure 5: Detection of endogenously produced H_2S by *Mtb* lysates using $BiCl_3$ (BC) microplate-based assay with different concentrations of CBS and CSE inhibitors, AOAA and PAG respectively. (A) An AOAA dose dependent reduction in H_2S in the lysates was observed. (B) H_2S production was not significantly affected by PAG in the lysates with PAG. Data shown is representative of two independent experiments, with mean ±SD from 6-8 wells. All *P* values are relative to untreated (no inhibitor) controls. Statistical analysis was performed using GraphPad Prism 7.02. One-way ANOVA with Dunnett's multiple comparisons test was used for statistical significance; # $P < 0.0001$.

`

Thirdly, endogenous production of H_2S in *Mtb* culture media and lysates was confirmed and quantified using a highly sensitive amperometric H_2S microsensor (Unisense A/S, Sweden) that detects H_2S directly. We hypothesized that this method will support our findings obtained using the lead acetate strips and BC assays. Using the H_2S microsensor, after 72 hours of incubation, a 3-fold difference in H_2S levels was observed between *Mtb* cultures supplemented with 1 mM Cys and untreated cultures (Figure 6). Supplementation with Cys resulted in increased levels of H_2S in *Mtb* cultures and their respective cleared supernatant compared to cultures without Cys. A real-time Cys dose-dependent increase in H_2S production was observed in cell lysates using the microsensor (Figure 7), consistent with the findings shown in Figures 3. Similarly, in cell lysates, an AOAA real-time stepwise reduction in H_2S production was observed (Figure 8A). In contrast, when AOAA was pre-incubated with the lysate, no H_2S was produced upon addition of Cys (Figure 8B), indicating complete inhibition by AOAA of H_2S producing activity in the lysate. In summary, using three independent methods we provide conclusive evidence that laboratory and clinical strains of *Mtb* produce H_2S. We show that this activity is PLP-dependent, is inhibited by AOAA, and uses Cys as a sulfur source. An intriguing finding was the significant variation in H_2S levels produced by MDR and laboratory strains of *Mtb*, which may have important implications for improved diagnostics and understanding drug resistance.

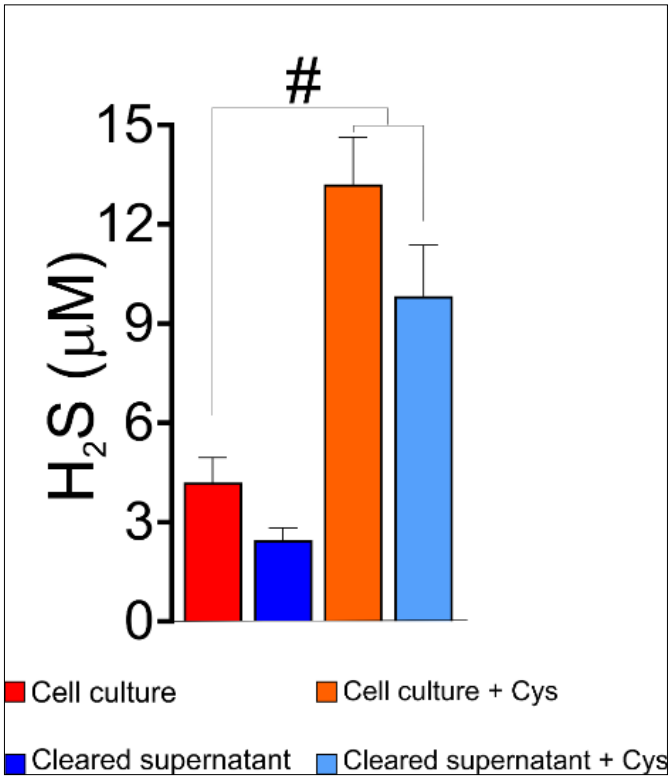

Figure 6: Detection of endogenously produced H_2S in *Mtb* culture using the Unisense A/S H_2S microsensor that detects H_2S directly. Using the H_2S microsensor, after 72 hours of incubation, a 3-fold difference in H_2S levels was observed between *Mtb* cultures supplemented with 1 mM Cys and untreated cultures. Also, supplementation with Cys resulted in increased levels of H_2S in cleared supernatants of *Mtb* cultures compared to those of cultures without Cys. Data shown is representative of two independent experiments, with mean ±SD from three cultures of each condition and strain. All *P* values are relative to untreated (no Cys) controls. Statistical analysis was performed using GraphPad Prism 7.02. One-way ANOVA with Dunnett's multiple comparisons test was used for statistical significance; #$P < 0.0001$.

`

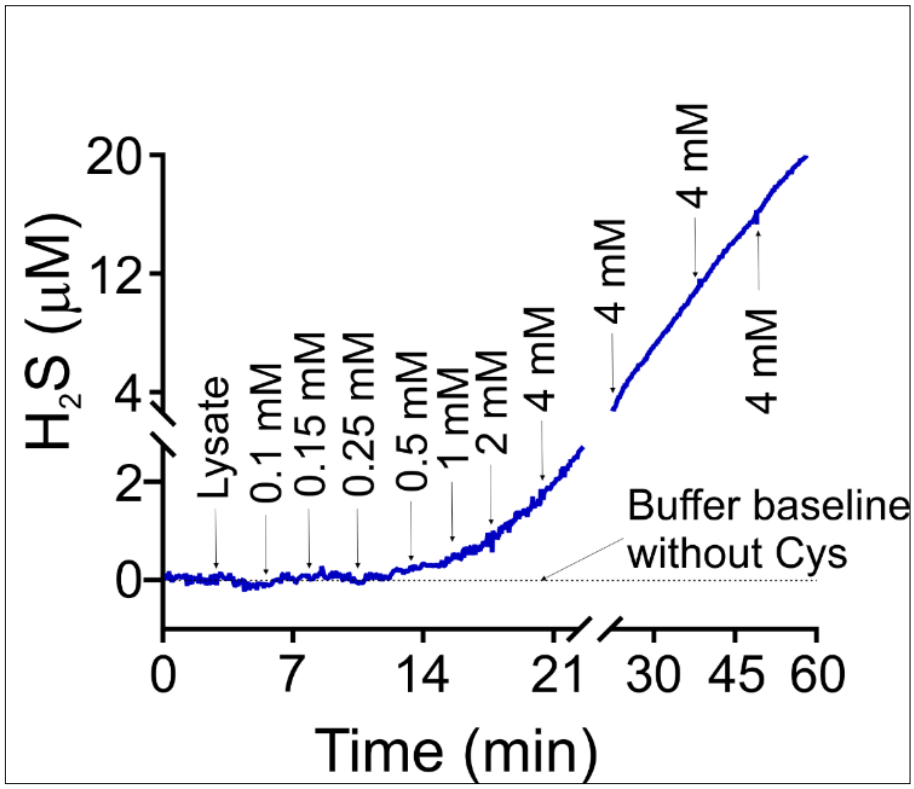

Figure 7: Detection of endogenously produced H_2S by *Mtb* lysates using the Unisense A/S H_2S microsensor that detects H_2S directly. A real-time Cys dose-dependent increase in H_2S production was observed in cell lysates using the microsensor. The Cys concentations were added in real-time (indicated by arrows). Data shown is representative of 2 independent experiments.

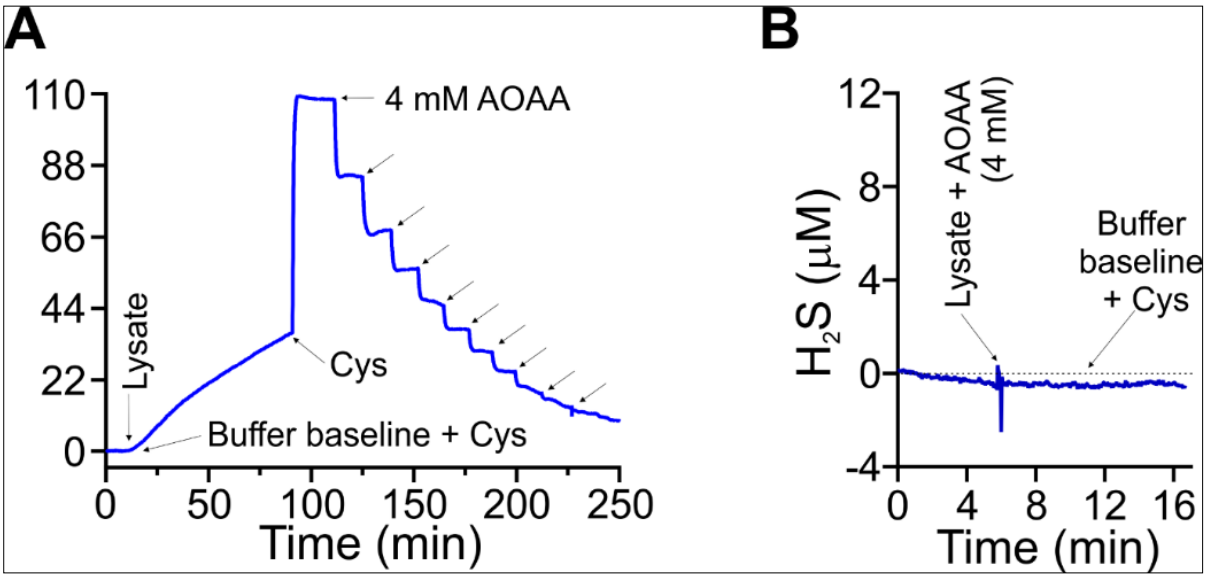

Figure 8: Detection of endogenously produced H_2S by *Mtb* lysates using the Unisense A/S H_2S microsensor that detects H_2S directly. (A) A real-time Cys dependent increase in H_2S production was observed followed by an AOAA real-time stepwise reduction in H_2S production was observed. 4 mM AOAA was added in real-time (indicated by arrows). (B) In contrast, when AOAA (4 mM) was pre-incubated with the lysate, no H_2S was produced upon addition of Cys, indicating complete inhibition by AOAA of H_2S producing activity in the lysate.

`

3.2 Identification of enzymes involved in endogenous H_2S production in *Mtb*

In an effort to identify the H_2S-producing enzymes in *Mtb*, we then pursued a biochemical approach where total lysates were resolved on non-denaturing polyacrylamide gels and enzymatic production of H_2S was detected by applying the BC assay solution directly to the gels [185].

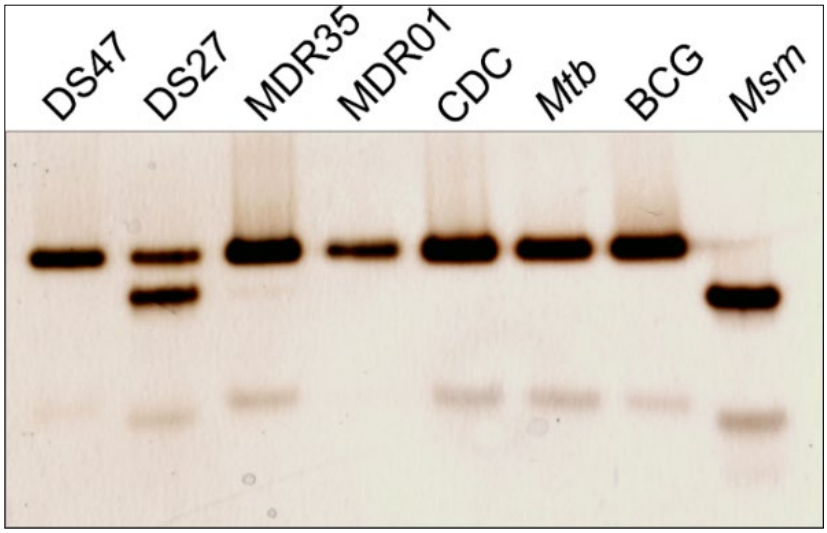

Figure 9: Detection of endogenously produced H_2S by *Mtb* lysates using non-denaturing polyacrylamide gels. Enzymatic production of H_2S was detected by applying the BC assay solution directly to the gels. Equal quantities of mycobacterial lysates separated on non-denaturing, polyacrylamide gel and assayed for H_2S production from different strains. Protein bands of various bismuth sulfide intensities (brown/black) corresponding to H_2S production are observed on the gel. Data shown is representative of 2 independent experiments performed.

Figure 9 shows equal quantities of mycobacterial lysates separated on native PAGE and assayed for H_2S-producing activity by staining the gels using the BC assay solution. Protein bands of various bismuth sulfide intensities (brown/black) corresponding to H_2S production are observed on the gel. However, upon addition of AOAA prior to BC solution, we observed a delayed emergence and reduced intensity of the H_2S producing band (Figure 10A), consistent with the reduction in H_2S kinetics observed with the dose dependent AOAA (Figures 4A and 5A). Further, the H_2S-producing activity required PLP as a co-factor (Figure 10B), suggesting that the prominent brown band is the same enzyme assayed in Figure 3, where, the absence of PLP drastically reduced the H_2S producing activity.

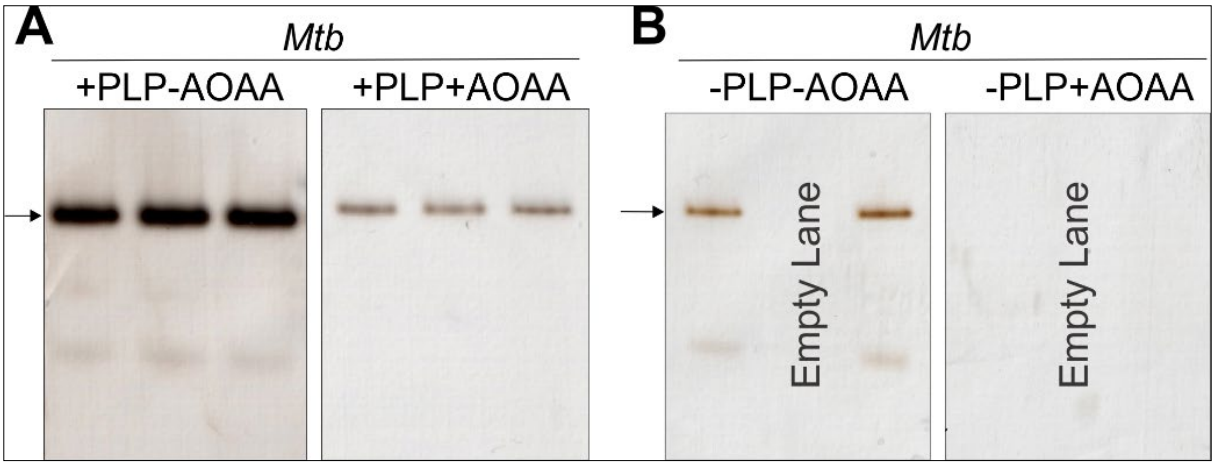

Figure 10: Detection of endogenously produced H_2S by *Mtb* lysates using non-denaturing polyacrylamide gels in the presence and absence of AOAA and PLP. (A) Upon addition of AOAA prior to BC solution, a delayed emergence and reduced intensity of the H_2S producing band. For these gels, the lysate was run in 3 lanes. (B) In the absence of PLP, the co-factor of the enzymatic activity, reduced intensity bands appeared and with the inhibitor, no bands were observed. For these gels, the lysate was run in 2 lanes sperate by an empty lane in the middle. Data shown is representative of 2 independent experiments performed.

Next, using the knowledge we had obtained in **Table 2**, regarding the presence of *Mtb* homologues of H_2S-producing genes as identified in literature and KEGG pathways (https://www.genome.jp/kegg/), we identified Rv1077 (CBS), a well-studied enzyme that produces H_2S in mammalian and bacterial cells and inhibited by AOAA but not PAG, as the starting point of our identification process. To determine the role of Rv1077 in H_2S production, we used readily available *Mtb* CDC1551 transposon mutants in the *rv1077* gene from the John Hopkins transposon mutant library available in our laboratory at AHRI. We selected 3 transposon mutants, *Tn::rv1077*, which had different insertion points for the disruptive gene. In addition to the transposon mutants, we deleted *Mtb cbs* (*rv1077*) in *Mtb* H37Rv using specialized phage transduction [178]. The transposon mutant lysates were resolved on non-denaturing polyacrylamide gel and assayed for H_2S production (Figure 11A). Our results showed that H_2S production was not reduced in these *Mtb* CDC1551 transposon mutants nor was it reduced in the *rv1077* genetic knock-out in *Mtb* H37Rv, Figure 11B.

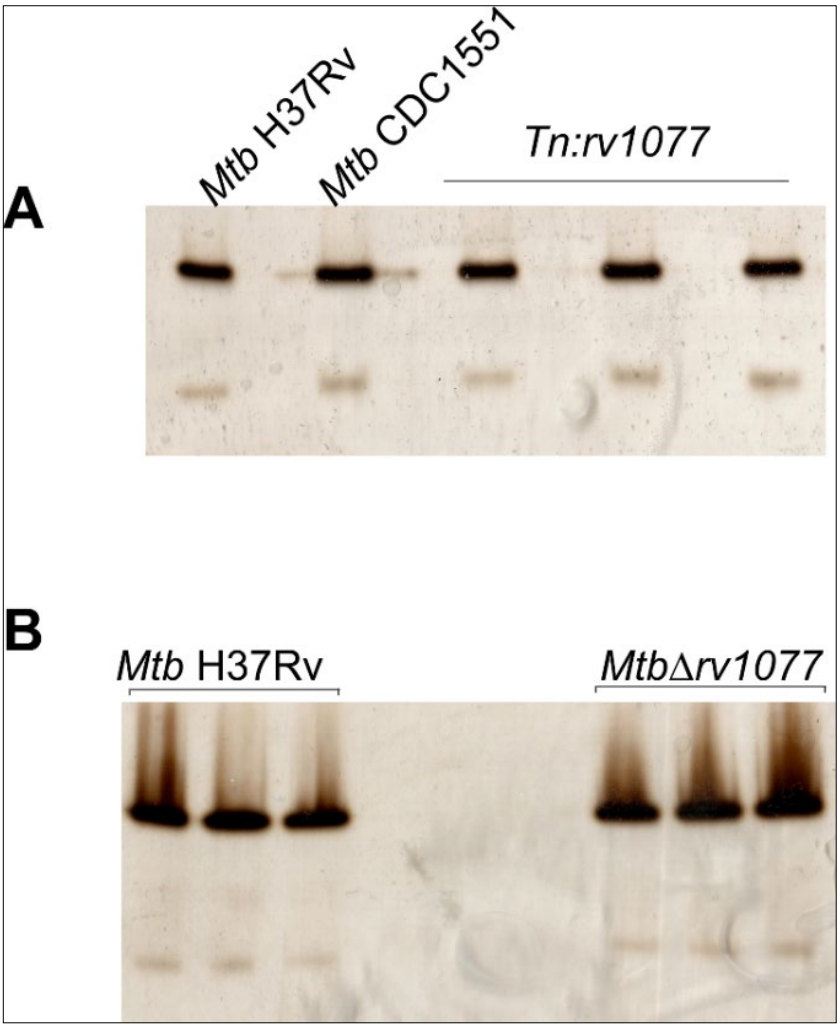

Figure 11: Role of cystathionine-β-synthase (CBS), Rv1077, in H_2S production. Detection of endogenously produced H_2S by *MtbΔrv1077* lysates using non-denaturing polyacrylamide gels. Equal quantities of *Mtb* lysates and the CBS mutant separated on native polyacrylamide gel and assayed for H_2S production. H_2S production was not reduced in (A) *Mtb* CDC1551 transposon mutants nor was it reduced in the (B) *rv1077* genetic knock-out in *Mtb* H37Rv. Data shown is representative of 2-5 independent experiments performed.

Similarly, analysis of H_2S production in *MtbΔrv1077* by BC assay of whole cells (Figure 12A) and lysates (Figure 12B) revealed that H_2S production in *MtbΔrv1077* was not reduced, but similar to that of *Mtb*.

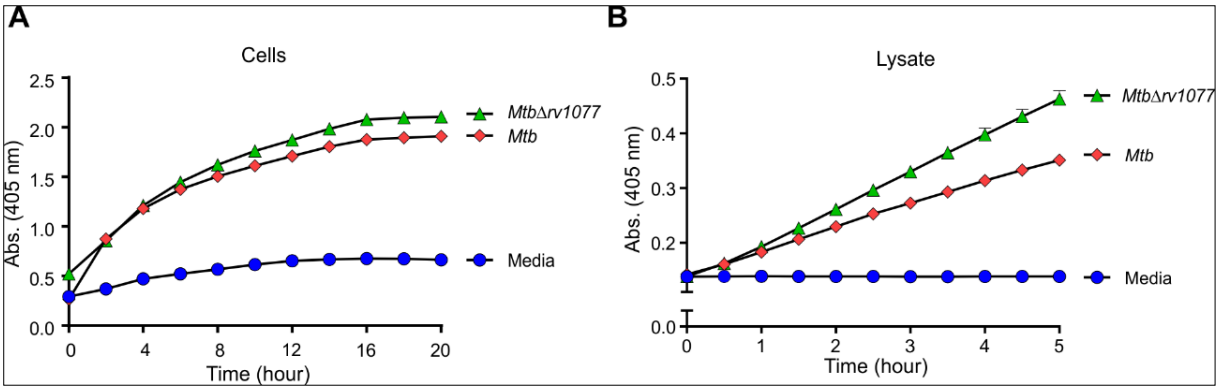

Figure 12: Role of cystathionine-β-synthase (CBS), Rv1077, in H_2S production. Detection of endogenously produced H_2S by *MtbΔrv1077* cells and lysate using $BiCl_3$ (BC) microplate-based assay. For both cells (A) and lysates (B), H_2S production in *MtbΔrv1077* was not reduced, but similar to that of *Mtb*. Data shown is representative of 2-5 independent experiments, with mean ±SD from 6-8 wells.

Next, we subjected the stained H_2S producing protein bands of *Mtb* H37Rv to in-gel tryptic digestion followed by LC-MS/MS identification (Figure 13 - insert). Several overlapping peptide fragments were identified with high confidence, leading to the identification of *rv3684* as a gene encoding a putative H_2S-producing enzyme (Figure 13).

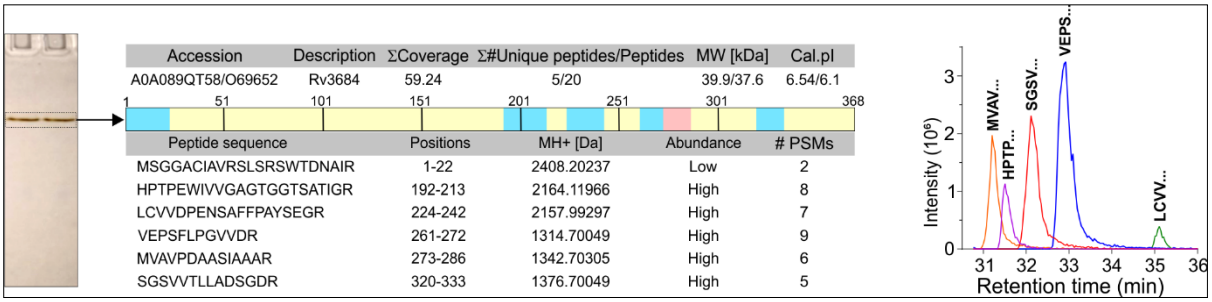

Figure 13: LC-MS/MS identification of Rv3684 fragments. Trypsin digested peptide fragments of Rv3684 identified using LC-MS/MS. The observed peptide fragments distribution (blue and pink shade over the full-length peptide map) and their amino acid sequence are shown. PSM - peptide spectrum matches; MH+ (Da) - protonated, monoisotopic mass of the peptide. Retention time of each LC-MS/MS identified peptide of Rv3684 are shown (on the right panel).

The gene, *rv3684* has been annotated as a probable lyase or Cys synthase (Mycobrowser.epfl.ch). Interestingly, on Mycobrowser.epfl.ch, we observed that there is an annotation ambiguity regarding the exact open reading frame (ORF) coding for *rv3684*. Our LC MS/MS data show that the ORF begins in *rv3683* (Figure 14). The *rv3684* ORF start codon overlaps with the stop codon of *rv3683* and both ORFs are in different coding frames (Figure 14). The ORF on Mycobrowser.epfl.ch is 22 amino acid shorter at the N-terminal. Inclusion of this N-terminal fragment aided in the identification of Rv3684, in (Mycobrowser.epfl.ch), which is annotated as belonging to the Cys synthase/cystathionine-β-synthase protein family.

`

A

N-terminal peptides detection in our study using LC MS/MS:

Sequence	# PSMs	Accessions No.	MH+ [Da]	Abundance
MSGGACIAVRSLSRSWTDNAIR	1	A0A089QT58	2408.20237	Low
SWTDNAIRLIEADAR	1	A0A089QT58	1730.86492	Low
SLSRSWTDNAIRLIEADAR	2	A0A089QT58	2174.11045	Low
SLSRSWTDNAIR	3	A0A089QT58	1405.71416	Low
SWTDNAIRLIEADARR	1	A0A089QT58	1886.99063	Low

B

Full length gene and protein sequence of Rv3684:

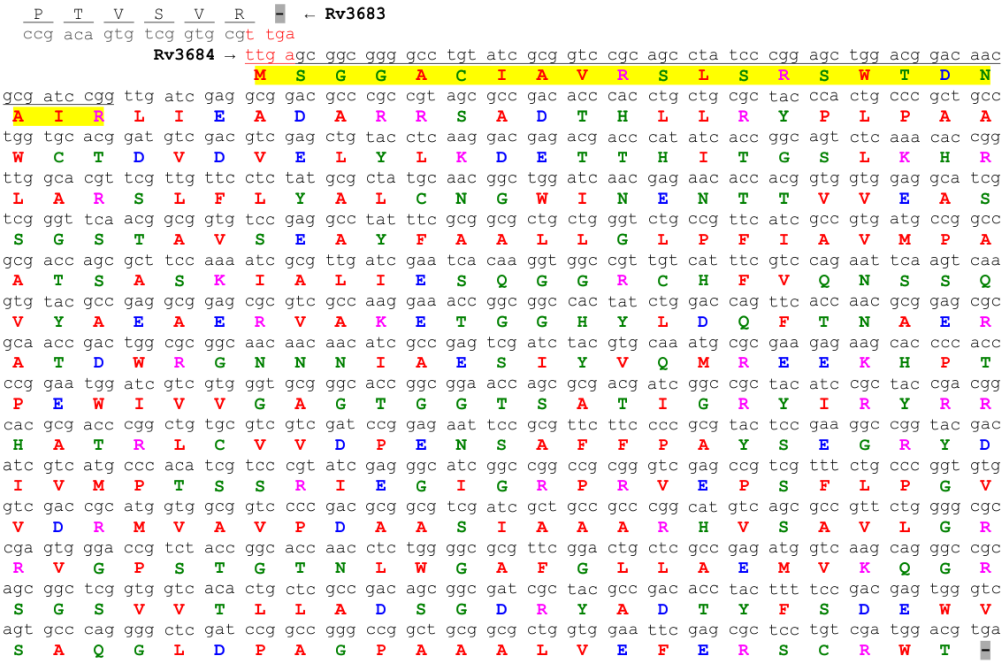

Figure 14: Full Rv3684 amino acid sequence. (A) A list of N-terminal peptide fragments of Rv3684 in *Mtb* lysate observed by LC-MS/MS. These peptide fragments correspond to the correct amino acid sequence of Rv3684. (B) The complete Rv3684 protein has 22 more amino acid residues (highlighted in yellow) at the N-terminal than as predicted in the ORF for *rv3684* by Mycobrowser.epfl.ch. The start codon of *rv3684* overlaps the stop codon of *rv3683* and both ORFs are in different coding frames. The predicted start codon (ttg) of *rv3684* in Mycobrowser.epfl.ch ummediately starts after the highlighted amino acid residues. Colour code of amino acid residues: Hydrophobic - AFILMVW (red); Polar - CGHNPQSTY (green); Basic charged - K and R (pink); Acidic charged - D and E (blue).

Since H_2S-producing enzymes can use a wide range of substrates including, but not limited to homocysteine, cystathionine and Cys to generate H_2S and other products such as serine and pyruvate (Figure 15A), we examined the substrate specificity of Rv3684. Hence, we overexpressed Rv3684 containing an N-terminal Histidine (His) tag in *E. coli* and purified by metal affinity chromatography. Using Cys as a substrate, we determined that Rv3684 produces H_2S and pyruvate, as shown by LC-

`

MS/MS analysis (Figure 15B). These results strongly suggest that Rv3684 oxidizes Cys into H_2S, pyruvate and ammonia in a α, β-elimination reaction analogous to CSE (Figure 15C) [186]. However, since Rv3684 is not inhibited by PAG (Figure 4B and 5B), our data suggest that this enzyme is functionally distinct from CSE and CBS as indicated in Figure 15C.

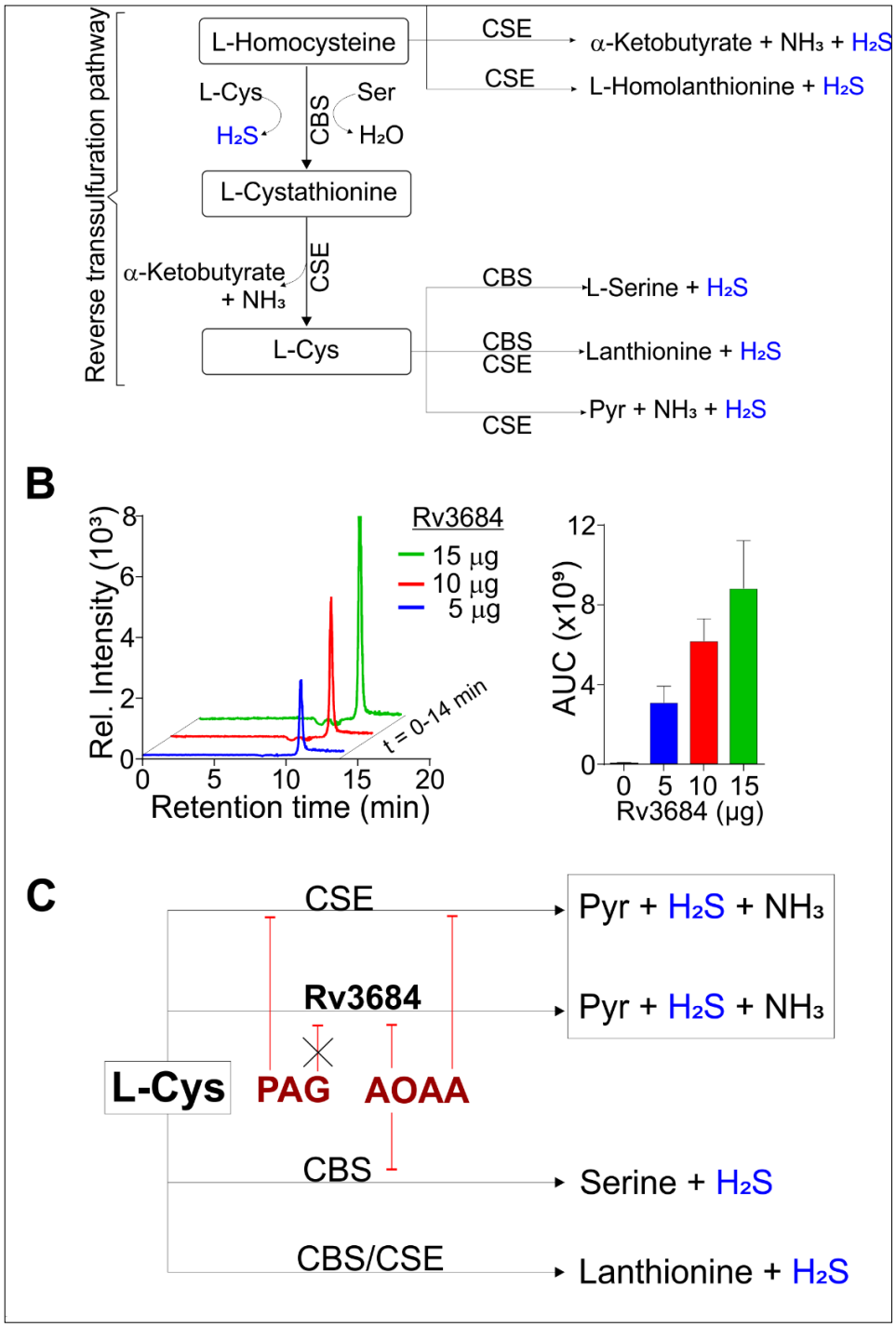

Figure 15: The catalytic activity of Rv3684. (A) Schematic showing the various possible H_2S generating enzymes and the reactions they catalyse in the reverse transsulfuration pathway. (B) LC-MS/MS identification and quantification, of pyruvate from the reaction mixture of Rv3684 and cysteine, assayed for H_2S production. (C) Proposed catalytic activity of Rv3684, using L-cysteine as a substrate.

`

In summary, using non-denaturing polyacrylamide gels stained with BC solution and the BC assay we have demonstrated the presence of H_2S-producing enzyme activity of in mycobacterial lysates, particularly in *Mtb*, which we have now identified as Rv3684. We have demonstrated that in *Mtb*, the enzymatic products of Rv3684 in the presence of Cys indicate that it is a cysteine desulfhydrase that generates H_2S and pyruvate. We thus propose the re-annotation of *rv3684* to a cysteine desulfhydrase. We also propose *rv3684* be named as encoding a cysteine desulfhydrase enzyme (*cds1*).

3.3 Genetic disruption of *rv3684* reduces endogenously produced H_2S and modulates *Mtb* growth

In this section, two lines of evidence demonstrate that we have identified Rv3684 as an H_2S producing enzyme. Firstly, genetic evidence was obtained from available *Mtb* CDC1551 transposon mutants *Tn::rv3682 (ponA2)* and *Tn::rv3683*, positioned upstream of *rv3684* (Figure 16A). Our data reveal that these mutants exhibit consecutively reduced H_2S production from equal amounts of cell lysate (Figure 16B), confirming that *rv3684* encodes an H_2S-producing enzyme and strongly suggests that *rv3682-3684* functions as an operon and is subject to a strong polar effect.

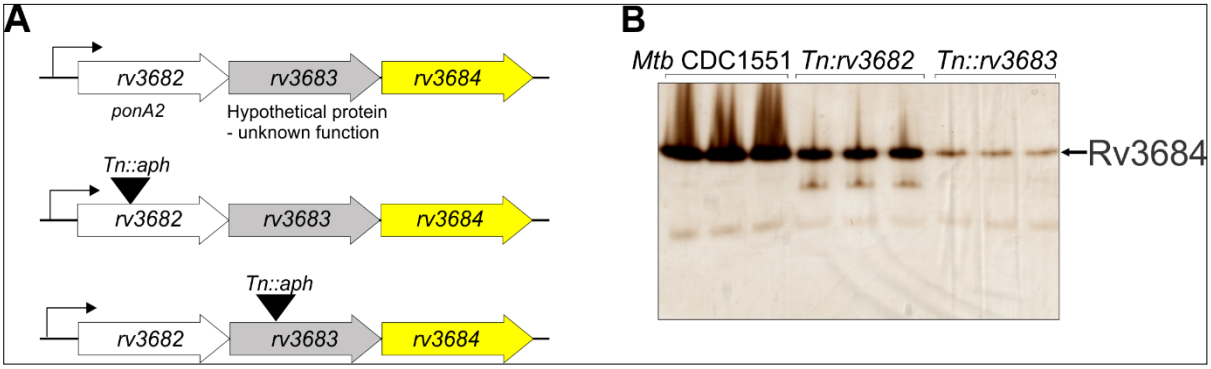

Figure 16: Genetic locus of *rv3684*. (A) The operonic location of r*v3684*. (B) The mycobacterial lysates of *Mtb* CDC1551, CDC1551 *Tn::rv3682* and CDC1551 *Tn::*rv3683 were resolved on the non-denaturing native polyacrylamide gel and assayed for H_2S production in *Mtb* CDC1551, CDC1551 *Tn::rv3682* and CDC1551 *Tn::rv3683*. Sequential reduction in H_2S production from wt *Mtb* CDC1551 to *rv3682* then to *rv3683* was observed. Data shown is representative of 2-3 independent experiments.

Next, we created *Mtb*Δ*rv3684,* an *rv3684* deletion knockout in *Mtb* H37Rv, using specialized phage transduction [178]. Using the in-gel BC assay, we observed no brown staining, indicative of H_2S production in *Mtb*Δ*rv3684* lysates (Figure 17A), and significantly reduced H_2S production in *Mtb*Δ*rv3684* cells (Figure 17B) and lysates (Figure 17C). Episomal plasmid complementation of *rv3684*, *Mtb*Δ*rv3684::rv3684* (*Mtb*Δ*rv3684comp*) restored the phenotype in both cell and lysate assays (Figure 17A-C). Notably, whereas the cell-based assay demonstrates complementation nearly identical to that of the wild type *Mtb*, the excessive enzymatic activity in the lysates of the complemented strain (Figure 17A and C) suggest a role for Cys transport in regulating H_2S production in *Mtb*. Of importance,

`

H_2S production was reduced, but not eliminated in *Mtb*Δ*rv3684* cells (Figure 17B), suggesting the presence of additional H_2S-producing enzymes in *Mtb*, consistent with the appearance of a second band in our in-gel BC assay (Figure 9). This is to be expected since several studies have shown that H_2S producing enzymes often require specific sulfur substrates, cofactors (*e.g.*, NADPH, NADH, heme) and binding thereof (*e.g.*, heme), and environmental conditions (*e.g.*, hypoxia), which may be mimicked in cell lysates.

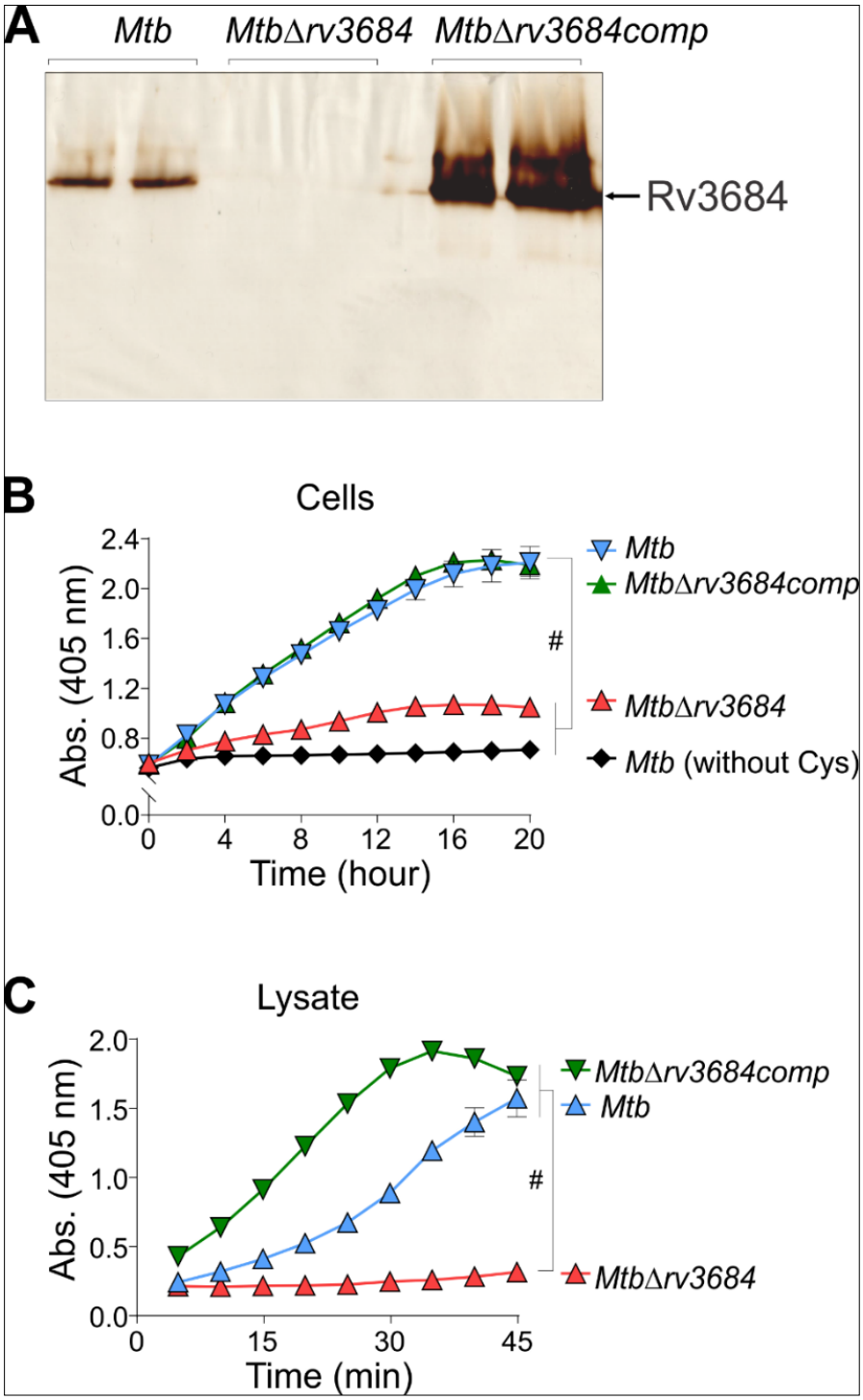

Figure 17: Deletion of *rv3684* in *Mtb* reduces H_2S production. The mycobacterial lysates of *Mtb* H37Rv, *Mtb*Δ*rv3684* and *Mtb*Δ*rv3684comp* was resolved on (A) the non-denaturing polyacrylamide gel and assayed for H_2S production. Detection of endogenously produced H_2S by (B) whole-cells and (C) lysates using $BiCl_3$ (BC) microplate-based assay. No brown staining on the native PAGE gels

`

indicative of H_2S production were observed for *Mtb*Δ*rv3684* lysates, and significantly reduced H_2S production in *Mtb*Δ*rv3684* cells and lysates was observed. Data shown is representative of 2-3 independent experiments; with mean ±SD for (B) and mean±SEM for (C) from 6-8 wells. All *P* values are relative to wt *Mtb* control. Statistical analysis was performed using GraphPad Prism 7.02. One-way ANOVA with Dunnett's multiple comparisons was used for (B) and one-way ANOVA with Tukey's multiple comparisons test was used for statistical significance for (C). # $P < 0.0001$

To obtain insight into the function of Rv3684, we examined the consequence of disrupting *rv3684* on *Mtb* grown in media containing increasing concentrations of Cys, the major source of sulfur and a substrate of Rv3684 H_2S production. Our rationale for this experiment was based on our previous observation that exogenous and host-derived H_2S supports *Mtb* bioenergetics and growth [153]. We observed a significant growth defect in *Mtb*Δ*rv3684* cells in 2 mM and 4 mM Cys compared to *Mtb* and the complemented strain (Figure 18). This suggests that Rv3684 mitigates toxic levels of Cys by

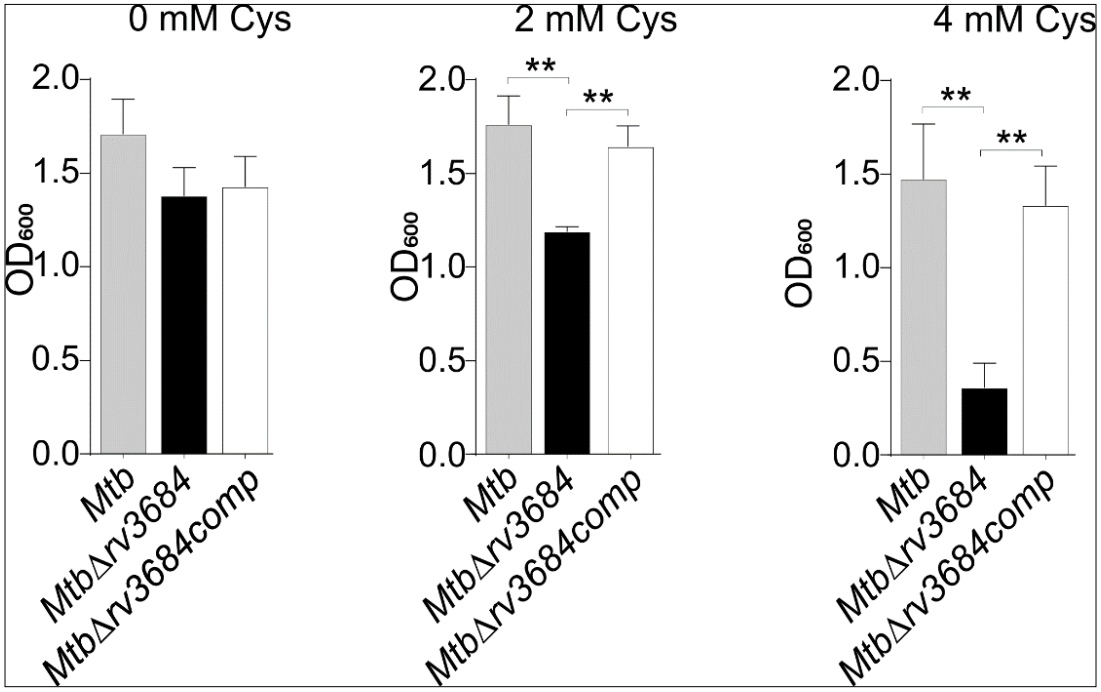

dissipating excess Cys into volatile H_2S. Overall, using biochemical and genetic approaches, we have shown that *Mtb* produces H_2S mainly through Rv3684 under the conditions tested.

Figure 18: Growth of *Mtb* H37Rv, *Mtb*Δ*rv3684* and *Mtb*Δ*rv3684*comp for 8 days in 0, 2 and 4 mM L-cysteine. A significant growth defect in *Mtb*Δ*rv3684* cells in 2 mM and 4 mM Cys compared to *Mtb* and the complemented strain. Data shown is representative of two independent experiments, with mean ±SD from 6-8 wells.. All *P* values are relative to wt *Mtb*. Statistical analysis was performed using GraphPad Prism 7.02. One-way ANOVA with Dunnett's multiple comparisons test was used for statistical significance; ** $P < 0.01$.

`

3.4 Conferring *Mtb rv3684's* H_2S-generating capacity to *M. smegmatis*

To provide further evidence of the H_2S producing activity of Rv3684, we transformed the surrogate host, *Msm,* with two complementing plasmids that express *rv3684* under control of the hsp_{60} promoter (*Msm-*hsp_{60}*-rv3684*), or *Mtb* wild-type ('operonic'; wt_p) promoter (*Msm-*wt_p*-rv3684*). The rationale for this is that *Msm* has been widely used as a surrogate host for *Mtb* in numerous genetic and secretion studies [187-190]. Since our data suggests that *Msm* produces very little H_2S, increasing the H_2S producing activity of *Msm* may provide knowledge that can potentially lead to new opportunities for studying how H_2S affects mycobacterial physiology and metabolism.

Transformation of *Msm* with these two plasmids followed by in-gel and BC assay analysis revealed increased levels of H_2S-producing activity compared to the wild-type (wt) *Msm* (Figure 19). Expression of *rv3684* in *Msm-*hsp_{60}*-rv3684* and *Msm-*wt_p*-rv3684* lead to increased H_2S production in these lysates compared to *Mtb* or WT *Msm* (Figure 19).

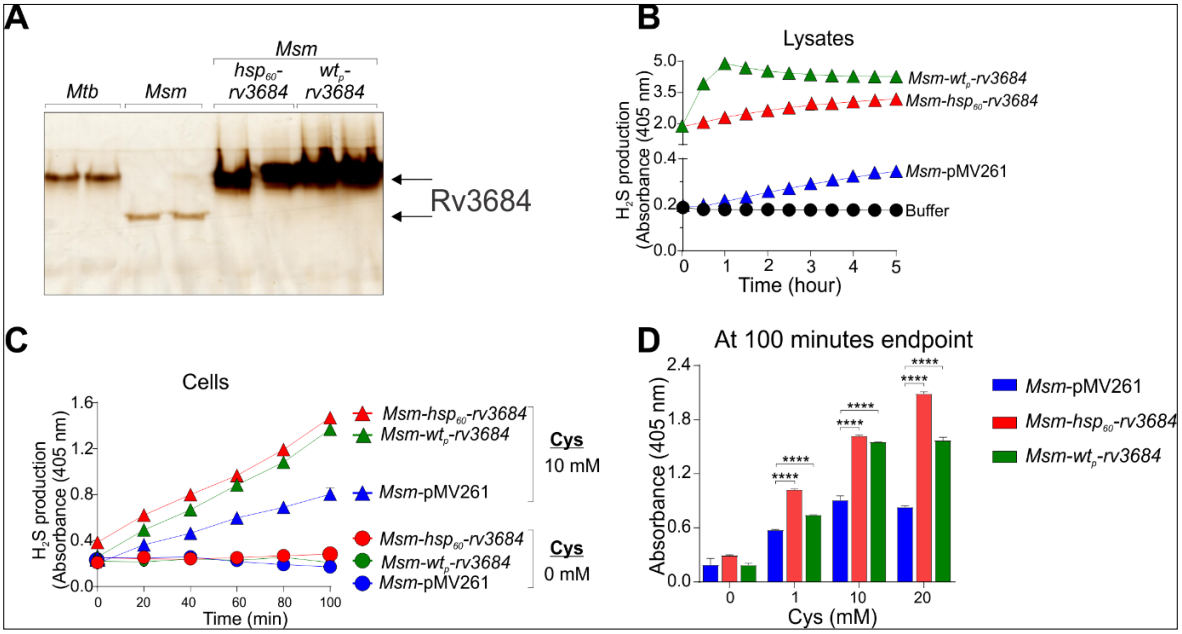

Figure 19: Conferring H_2S producing activity in *M. smegmatis*. (A) Equal quantities of mycobacterial lysates from *Mtb*, *Msm* and *Mtb* Rv3684 recombinant *Msm* were separated on a native polyacrylamide gel and assayed for H_2S production. BC assay measuring H_2S production from (B) *Msm* (with mock vector) and *Mtb* Rv3684 recombinant *Msm* lysates and (C) *Msm* (with mock vector) and *Mtb* Rv3684 recombinant *Msm* cells with/without Cys. (D) *Msm* (with mock vector) and *Mtb* Rv3684 recombinant *Msm* cells with 0, 1, 10, 20 mM Cys after 100 mins (endpoint in C). In (A) – (D), were observed that transformed *Msm* clones had increased levels of H_2S-producing activity compared to the wild-type (wt) *Msm*. Data shown is representative of two independent experiments, with mean ±SD from 6-8 wells. All *P* values are relative to wt *Msm* (with mock vector). Statistical analysis was performed using GraphPad Prism 7.02. Two-way ANOVA with Dunnett's multiple comparisons test was used for statistical significance; ****$P < 0.0001$.

Notably, transformed *Msm* clones showed intense brown H_2S producing bands that correspond to that of wild-type (wt) *Mtb* (Figure 19A). We observed that these bands migrated differently compared to

`

wt *Msm* cells transformed with a control plasmid (Figure 19A) which also show an H_2S producing band. This suggests that *Msm* also contains an enzyme with physical properties distinct from Rv3684 that produces H_2S, albeit at low levels as was evident from our results in Figure 1B. We also observed that the wt *Msm* H_2S-producing band was not seen in *Msm-hsp*$_{60}$*-rv3684* or *Msm-wt*$_p$*-rv3684*, potentially because of intracellular transcriptional or posttranscriptional regulation in the presence of overproduced Rv3684. H_2S production in the *Msm* lysate (Figure 19B) expressing Rv3684 occurred at a greater rate compared to *Msm*-pMV261(i.e. wt *Msm* transformed with the 'empty' control plasmid), indicating overproduction of H_2S in the transformed *Msm*. Figures 19C and D show that H_2S production in Rv3684 expressing *Msm* cells was less compared to the lysate (Figure 19B), although still higher compared to *Msm*-pMV261. This difference may be attributed to limitations of intracellular cysteine transportation.

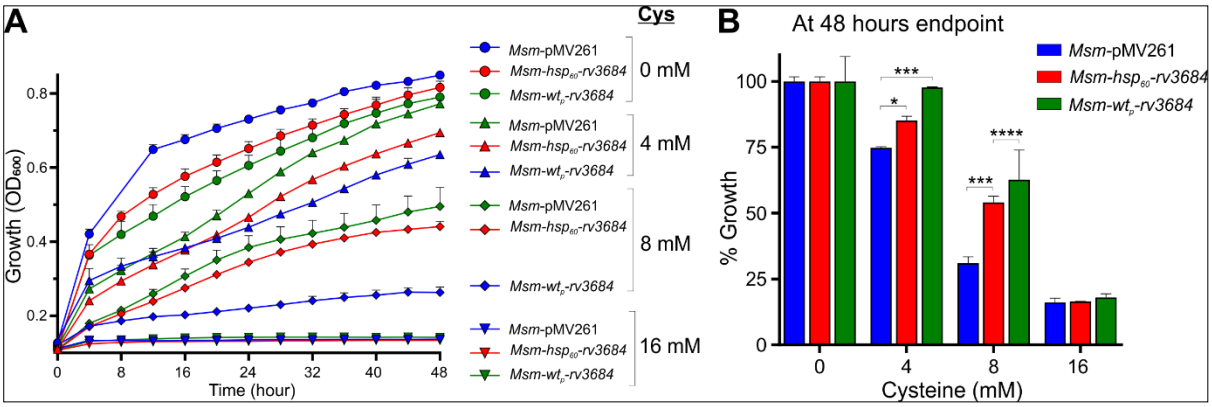

Figure 20: Rv3684 reduces Cys toxicity in transformed *Msm*. (A) Growth kinetics (OD_{600}) of *Msm* (with mock vector) and *Mtb* Rv3684 recombinant *Msm* strains in Cys supplemented media. (B) growth at 48 hours (endpoint in A) of *Mtb* Rv3684 overexpressing strains of *Msm*. A growth advantage of *Msm-hsp*$_{60}$*-rv3684* and *Msm-wt*$_p$*-rv3684* in medium containing 4 and 8 mM Cys compared to wild-type *Msm* was observed. Data shown is representative of 2 independent experiments, with mean ±SEM from 6-8 wells. All *P* values are relative to wt *Msm* (with mock vector). Statistical analysis was performed using GraphPad Prism 7.02. Two-way ANOVA with Tukey's multiple comparisons test was used for statistical significance; $*P < 0.05$, $***P < 0.001$, $****P < 0.0001$.

To examine the functional consequence of conferring increased H_2S producing activity to *Msm*, we studied the effect of *rv3684* expression on the growth of *Msm* cultured in media containing Cys concentrations of 4, 8 and 16 mM. Notably, we observed a growth advantage of *Msm-hsp*$_{60}$*-rv3684* and *Msm-wt*$_p$*-rv3684* in medium containing 4 and 8 mM Cys compared to wild-type *Msm* (Figure 20A and B). This suggests that expression of Rv3684 enables *Msm* to withstand Cys toxicity compared to wild-type *Msm*. This may occur through the degradation of excess Cys into H_2S. Hence, conferring increased H_2S producing capability to the surrogate host *Msm*, may enable a better understanding of the role played by H_2S in mycobacterial physiology.

`

3.5 Endogenous generated H_2S modulates *Mtb* respiration

Several studies have shown that depending on the concentration, H_2S can inhibit or stimulate mammalian respiration [148-151]. More recent studies have shown that exogenous H_2S significantly affects *Mtb* respiration [153], and that H_2S inhibits cytochrome *bc1*, whereas cytochrome BD is resistant to H_2S [191]. Since respiration is tightly linked to metabolism, it is important to understand the role of endogenous H_2S in the modulation of *Mtb* respiration. Hence, we hypothesized that endogenous H_2S produced by Rv3684 modulates *Mtb* respiration [154, 192]. To test this hypothesis, we used extracellular metabolic flux analysis (using the extracellular flux analyzer XFe96), a methodology developed for eukaryotic cells which we have optimized for the real-time, quantitative study of *Mtb* respiration [153, 177, 193, 194].

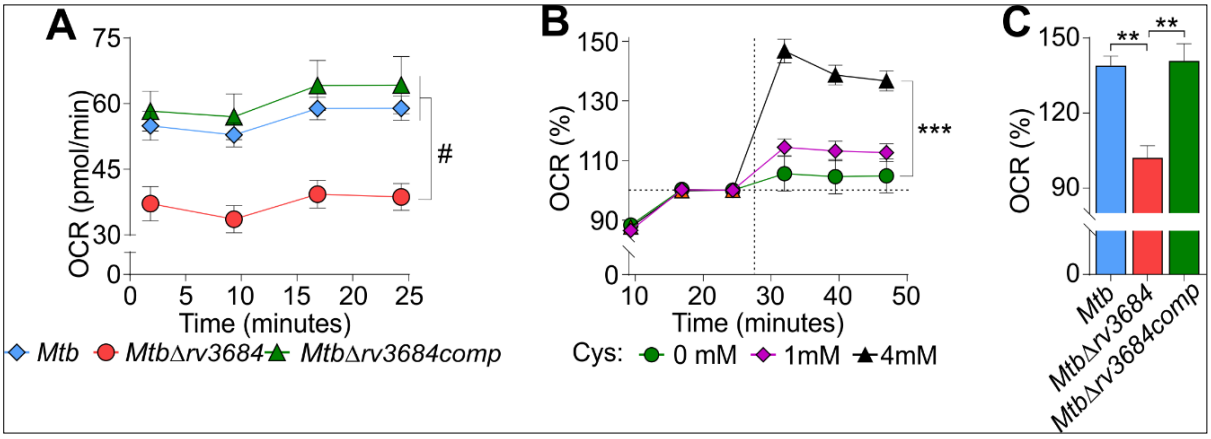

Figure 21: Endogenous H_2S stimulates respiration in *Mtb*. *Mtb* respiration was measured using an extracellular flux analyzer XFe96. The data represent an (A) oxygen consumption rate (OCR) profile showing basal respiration of *Mtb* strains. The basal oxygen consumption rate (OCR) of *Mtb*Δ*rv3684*, which was significantly lower than the basal rate in wt *Mtb* or *Mtb*Δ*rv3684comp*. (B) %OCR of *Mtb* upon addition of Cys. Increased H_2S levels via addition of Cys leads to increased respiration in a dose dependent manner. (C) %OCR of *Mtb* strains with 4 mM Cys relative to media control. Addition of Cys had no effect on *Mtb*Δ*rv3684* cells and showed significant reduction in OCR compared to wild-type and the complemented cells. Data shown is representative of 2-3 independent experiments, showing mean ±SD (for (A)) and mean±SEM (for (B)) from 6-8 wells. All *P* values are relative to untreated or wt controls. Statistical analysis was performed using GraphPad Prism 7.02. One-way ANOVA with Tukey's (for (A) and (C)) and Dunnett's (for (B)) multiple comparisons test was used for statistical significance; $^{**}P < 0.01$, $^{***}P < 0.001$, $\#P < 0.0001$.

Using the extracellular flux analyzer XFe96, we measured the basal oxygen consumption rate (OCR) of *Mtb*Δ*rv3684*, which was significantly lower compared to that of wt *Mtb* or the *Mtb*Δ*rv3684comp* strains (Figure 21A). This represents a ~40% reduction in respiration, which is highly significant in bioenergetics terms. Two lines of evidence suggest that H_2S is the effector molecule contributing to basal respiration in *Mtb*. Firstly, increased H_2S levels via addition of Cys leads to increased respiration in a dose dependent manner (Figure 21B). Secondly, addition of Cys had no effect on *Mtb*Δ*rv3684* cells and showed significant reduction in OCR compared to wild-type and the complemented cells (Figure 21C). Also, pharmacological inhibition of Rv3684 via injection of AOAA, suppressed OCR in

wt *Mtb* (Figure 22A). These data strongly suggest that the PLP binding protein Rv3684, is responsible for maintaining basal respiration, which can be increased by H_2S via addition of Cys. Likewise, addition of AOAA first, followed by Cys injection also suppressed respiration (Figure 22B), with AOAA alone having no significant effect on respiration (Figure 22C).

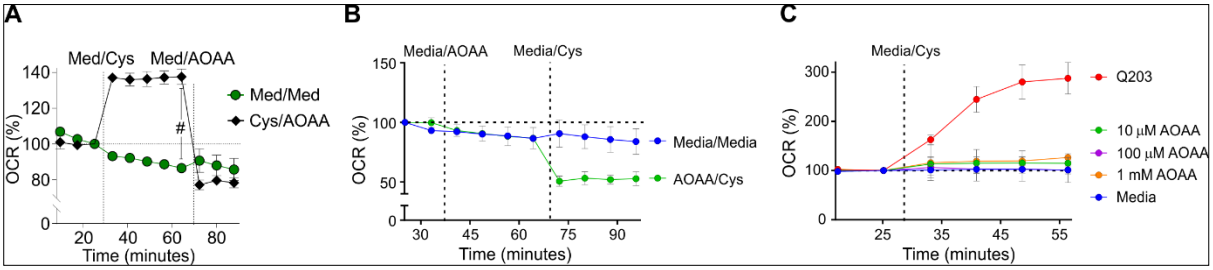

Figure 22: Pharmacological inhibition of Rv3684 via injection of AOAA. (A) %OCR of *Mtb* with sequential injection of Cys and AOAA, or media (Med) as a control, and (B) %OCR of *Mtb* with sequential injection of AOAA and Cys, or media (Med) as a control, (C) %OCR of *Mtb* for an AOAA dose response. All results indicated that inhibition of Rv3684 by AOAA suppressed OCR in wt *Mtb*. Data shown is representative of 2-3 independent experiments, showing mean ±SEM from 6-8 wells. All *P* values are relative to untreated or wt controls. Statistical analysis was performed using GraphPad Prism 7.02. An unpaired t-test was used for statistical significance; #$P < 0.0001$.

To further validate that endogenous H_2S is the effector molecule modulating basal respiration, we used an H_2S-degrading enzyme *O*-acetylserine sulfhydrylase (OASS) [179] in our bioenergetic assays. OASS assimilates H_2S by catalyzing the β-replacement of *O*-acetyl-L-serine (OAS) by sulfide to form Cys and acetate. Enzymatic activity of OASS was confirmed in an H_2S probed based assay, showing that sequential addition of NaHS increases H_2S levels, followed by mixing of OASS (causing a small decrease in H_2S), whereas, a rapid decrease in H_2S was observed after the addition of the substrate OAS (Figure 23A). These data indicate a faster kinetic of OASS in H_2S degradation. Based on our studies showing that exogenous H_2S stimulates *Mtb* respiration [153], we hypothesized that H_2S produced by *Mtb* will be degraded by exogenously added OASS and OAS, leading to a reduction in OCR. Indeed, Figure 23B shows that injecting this purified enzyme in the presence of its substrate (OAS) and *Mtb*-generated H_2S does not lead to an increase in OCR, since the *Mtb*-generated H_2S is degraded by OASS. However, it is also possible that intracellular H_2S may be consumed by *Mtb* CysK1 using OAS as substrate (Figure 23C) [195]. Regardless, our data suggests that Rv3684 uses Cys as a source for sulfur to produce H_2S, which modulates *Mtb* respiration.

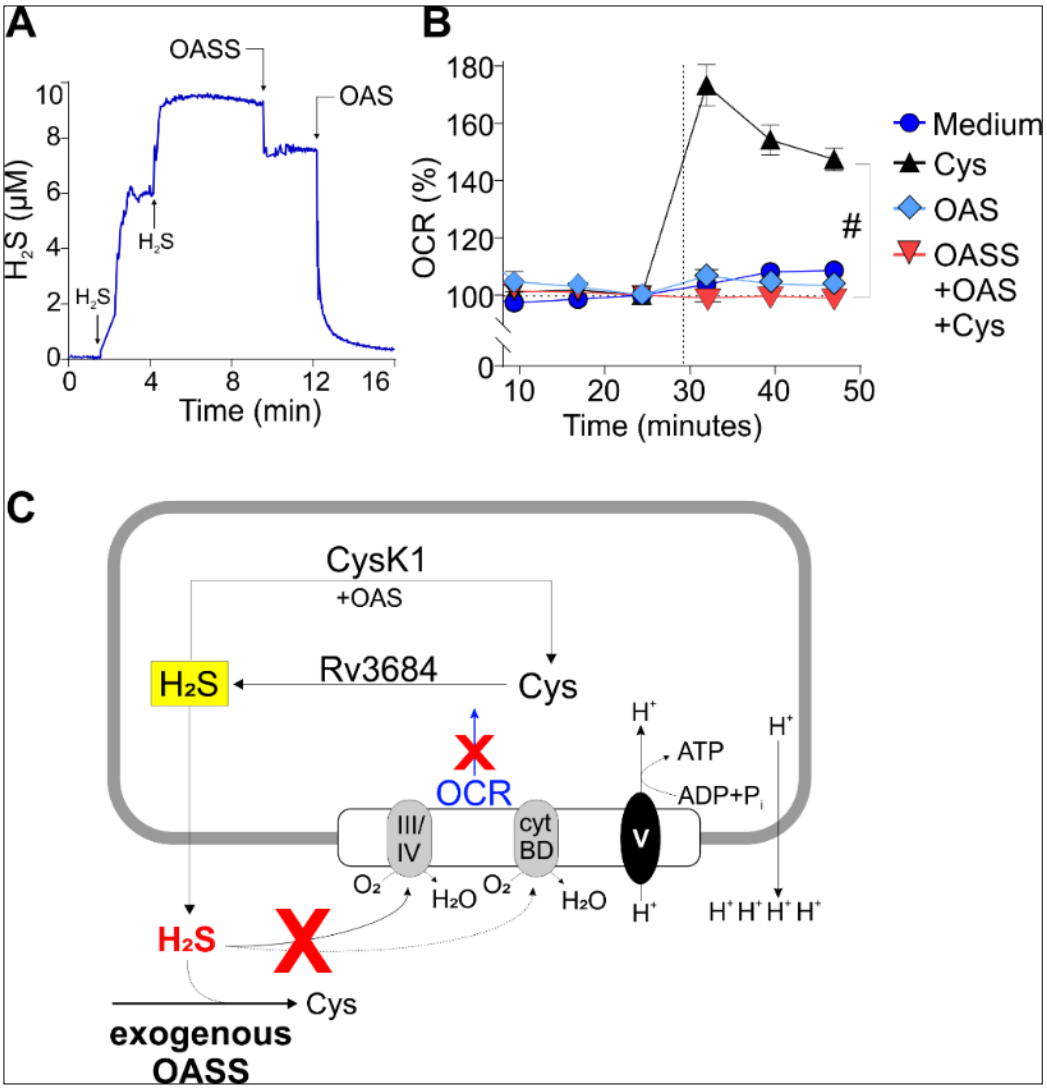

Figure 23: (A) Enzymatic activity of OASS confirmed via H_2S microsensor (Unisense, A/S) based assay. Addition of NaHS increases the H_2S level and addition of OASS (causes a small decrease in H_2S), whereas a rapid decrease in H_2S was observed after the addition of the substrate OAS, indicative of H_2S degradation. (B) %OCR of *Mtb* after injecting Cys, or O-acetyl-L-serine (OAS), or Cys with OAS and O-acetylserine sulfhydrylase (OASS). (C) schematic showing the possible role of H_2S on OXPHOS and the effect of H_2S consumption in reactions catalyzed by extracellular OASS and possibly by *Mtb* CysK1. Data shown is representative of 2 independent experiments, showing mean ±SEM from 6-8 wells. All *P* values are relative to untreated or wt controls. Statistical analysis was performed using GraphPad Prism 7.02. One-way ANOVA with Dunnett's multiple comparisons test was used for statistical significance; #$P < 0.0001$.

3.6 Endogenous generated H_2S modulates sulfur metabolism

Cysteine's chemical instability enables its rapid oxidization by molecular oxygen to cystine (the disulfide form of Cys; Cys_{ox}) and hydrogen peroxide [191]. This rapid oxidization triggers oxidative stress via the Fenton reaction [196, 197] and is detrimental to the cell. The toxic effect of excessive levels of cysteine were confirmed by our growth assays of *Mtb* in Cys containing media (Figure 18). To mitigate this toxic effect within the cytoplasm, our data has established that the detoxification of Cys is primarily performed by *rv3684*, which we designated as *cds1*, a cysteine desulfhydrase and that Rv3684's cysteine desulfhydrase enzymatic products are H_2S and pyruvate (Figure 15B). We next

`

hypothesized that H_2S regulates cellular sulfur metabolism. To test this hypothesis, we performed independent carbon tracing experiments using [U-$^{13}C_6$]-glucose (7H9 medium) and [U-$^{13}C_3$]-Cys (100 µM in 7H9 medium) and examined metabolite abundance and the carbon isotopologue distribution (CID) of targeted sulfur metabolites in wild-type *Mtb*, *Mtb*Δ*rv3684* and *Mtb*Δ*rv3684comp* cells.

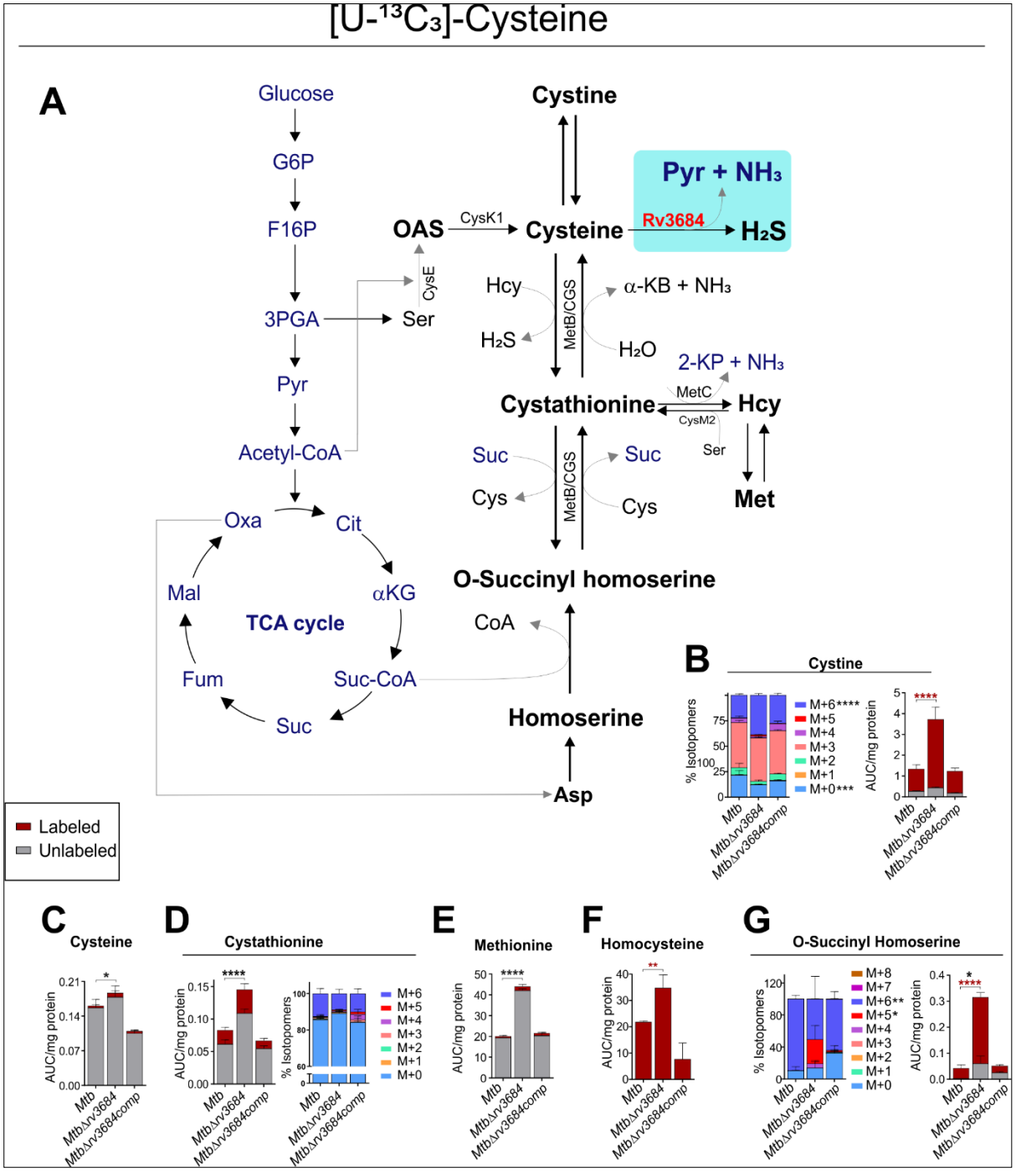

Figure 24: *Mtb* H_2S regulates sulfur metabolism. Results of carbon tracing experiments using [U-$^{13}C_3$]-Cys are presented. (A) Schematic showing how the central metabolism pathway links to sulfur metabolism via the reverse transulfuration pathway. An overall accumulation of the sulfur metabolites ((B) - (G)) was observed in *Mtb*Δ*rv3684*. Data shown is representative of 2 independent experiments, showing mean ±SEM from 3-5 samples. All *P* values are relative to untreated or wt controls. Statistical analysis was performed using GraphPad Prism 7.02. Two-way ANOVA with Dunnett's multiple comparisons test was used for statistical significance; $*P < 0.05$, $**P < 0.01$, $****P < 0.0001$.

`

In Figure 24A, we provide a schematic demonstrating how the central metabolic pathway and its metabolites link to sulfur metabolism via the reverse transulfuration pathway. For [U-$^{13}C_3$]-Cys labelling experiments, we observed an overall accumulation of the sulfur metabolites Cys_{ox} (Figure 24B), cysteine (Figure 24C), cystathionine (Figure 24D), methionine (Figure 24E), homocysteine (Figure 24F) and O-succinyl homoserine (Figure 24G) in *Mtb*Δ*rv3684* cells. The most likely explanation for this accumulation in *Mtb*Δ*rv3684* cells is because of the lack of Rv3684-mediated release of H_2S which dissipates sulfur atoms. The resultant lack of sulfur atom dissipation generates backpressure and metabolite accumulation. This explanation is further supported by the significant build-up of [U-$^{13}C_3$]-Cys labeled Cys_{ox} and increased CID of M+6 Cys_{ox} species (Figure 24B). Since, *Mtb*Δ*rv3684* cells lack cysteine desulfhydrase activity via Rv3684, most of the exogenously added [U-$^{13}C_3$]-Cys is rapidly oxidized to Cys_{ox} [191], shown by the increased flux of M+6 Cys_{ox} species (Figure 24B). Cys_{ox} accumulates in *Mtb*Δ*rv3684* cells due to the impairment of the cells ability to recycle sulfur atoms through Rv3684-mediated H_2S production. Reduced labelling of Cys (Figure 24C) suggests that most carbons for this amino acid originate from glucose or glycerol for *de novo* synthesis of Cys, leading to a small, but significant increase in unlabelled Cys in *Mtb*Δ*rv3684* cells. Also, the significant decrease in CID of M+6 species in the cystathionine metabolite pool is indicative of reduced flux of [U-$^{13}C_3$]-Cys carbons leading to the subsequent build-up in *Mtb*Δ*rv3684* cells.

Similarly, for [U-$^{13}C_6$]-glucose labelling experiments, (Figure 25) and using the same schematic (Figure 25A), we observed an overall accumulation of the sulfur metabolites Cys_{ox} (Figure 25B), cysteine (Figure 25C), methionine (Figure 25D), cystathionine (Figure 25E), O-succinyl homoserine (Figure 25F) and homoserine (Figure 25G) in *Mtb*Δ*rv3684* cells. The same explanation made for [U-$^{13}C_3$]-Cys above for the accumulation of these metabolites also applies for [U-$^{13}C_6$]-glucose labelling experiments. Notably, increased levels of homoserine were observed in *Mtb*Δ*rv3684* cells cultured in [U-^{13}C]-glucose medium. Similarly, we observed reduced labelling of Cys (Figure 25C), suggesting again that the majority of carbons for Cys synthesis originate from glucose or glycerol. Since [U-$^{13}C_3$]-Cys can be metabolized, comparing [U-$^{13}C_3$]-Cys and [U-$^{13}C_6$]-glucose labelling experiments should be avoided and each experiment should be interpreted independently within the proper context.

In summary, our data suggest that the cysteine desulfhydrase activity of Rv3684 maintains homeostatic levels of sulfur metabolites through the production of H_2S, allowing recycling of sulfur atoms back to Cys/Cys_{ox}. Lack of Rv3684 triggers metabolic dysregulation of key sulfur metabolites as is shown by the corresponding build-up of sulfur intermediates such as cystathionine, O-succinyl homoserine, homoserine and methionine, and reduced flux. Hence, Rv3684-generated H_2S functions as a gaseous sink to maintain sulfur homeostasis.

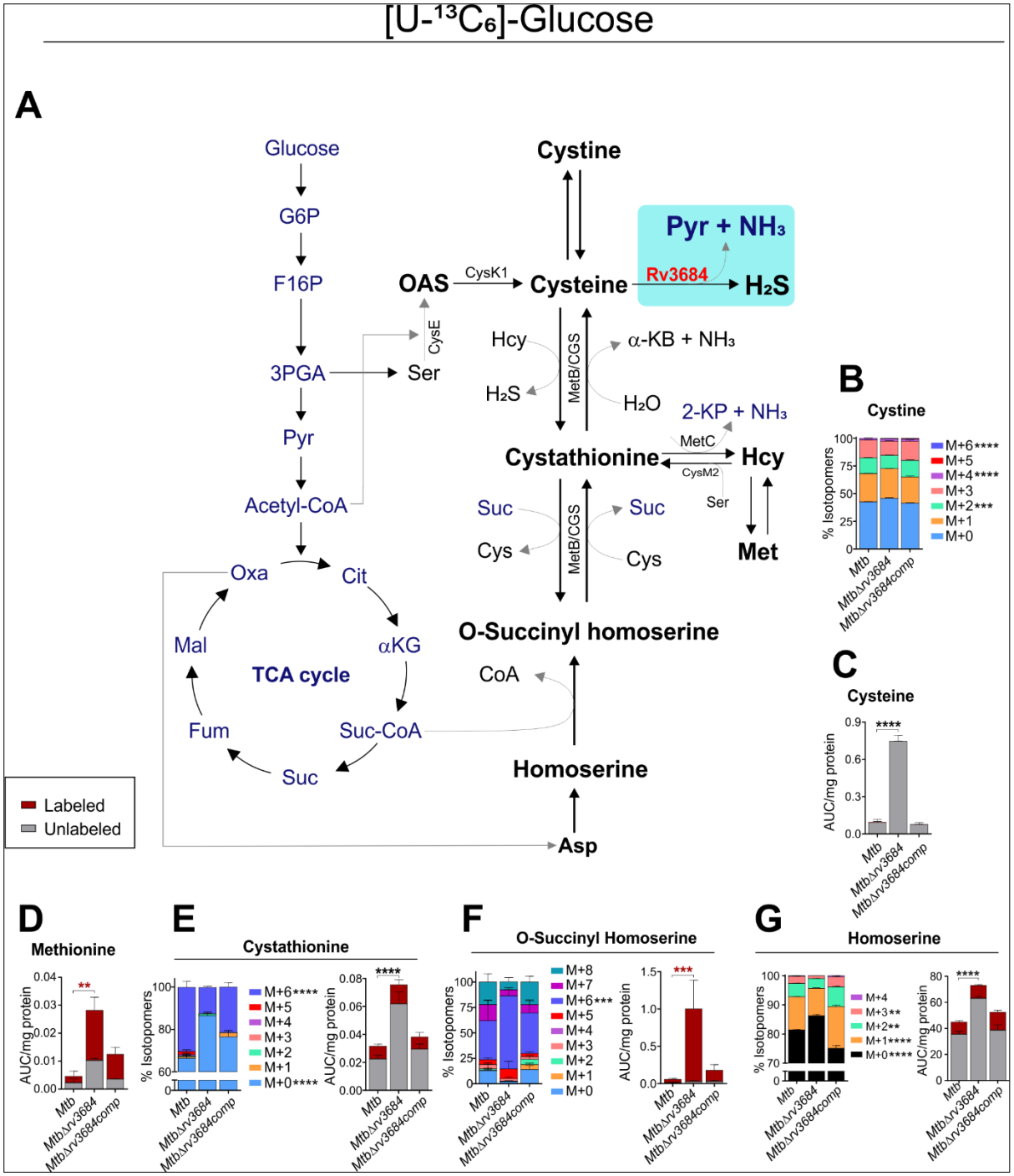

Figure 25: *Mtb* H_2S regulates sulfur metabolism. Results of carbon tracing experiments using [U-$^{13}C_6$]-glucose are presented. (A) Schematic showing how the central metabolism pathway and links to sulfur metabolism via the reverse transulfuration pathway. An overall accumulation of the sulfur metabolites ((B) - (G)) was observed in *MtbΔrv3684*. Data shown is representative of 2 independent experiments, showing mean ±SEM from 3-5 samples. All *P* values are relative to untreated or wt controls. Statistical analysis was performed using GraphPad Prism 7.02. Two-way ANOVA with Dunnett's multiple comparisons test was used for statistical significance; $^{**}P < 0.01$, $^{***}P < 0.001$, $^{****}P < 0.0001$.

`

3.7 Endogenous generated H_2S modulates central metabolism

Our extensive literature search has revealed that only two [198, 199] metabolomics studies specifically focus on sulfur metabolism in bacteria. Both studies showed that different sulfur fuel sources affect glycolysis, the TCA cycle, amino acid levels, and redox couples such as glutathione and mycothiol (MSH). Since we have shown that H_2S modulates growth (Figure 18) and respiration (Figure 21B), which is tightly linked to metabolism, we tested the hypothesis that Rv3684-generated H_2S modulates *Mtb* central metabolism. To test this hypothesis, we cultured wild-type *Mtb*, *Mtb*Δ*rv3684* cells and *Mtb*Δ*rv3684comp* in 7H9 medium containing [U-$^{13}C_3$]-Cys, and examined central metabolism metabolites (Figure 26A) in glycolysis, the pentose phosphate pathway (PPP), TCA cycle, and most of the central metabolism-associated amino acids (Figure 27A).

A notable observation was the significant increase of most glycolytic metabolites (Figure 26B and C), several PPP metabolites (erythrose, ribulose, ribulose-5-phosphate), TCA intermediates, and amino acids (Figure 27B and C) in *Mtb*Δ*rv3684* cells. This strongly suggests that H_2S modulates central metabolism. This was not entirely unanticipated since endogenous (Figure 21B) and exogenous H_2S regulates respiration in *Mtb* [153]. In addition, H_2S directly targets enzymes in the glycolytic pathway through S-sulfhydration [200] to modulate their activity, and has previously been shown to suppress glycolysis during macrophage infection with *Mtb* [154]. The overall reduced labelling of metabolites is consistent with the fact that metabolites in central metabolism obtain their carbons mainly from glucose and not Cys. However, Fructose-1,6-bisphosphate (F1,6BP) and phosphoenolpyruvate (PEP) were substantially labelled (~50%) in all three strains. These metabolites are the products and substrates of the first and last rate limiting step for glycolysis, respectively. These data point to phosphofructokinase (Pfk1) and pyruvate kinase (PykA) as important rate limiting flux control points for the metabolism of Cys carbons into central metabolism.

In summary, our targeted metabolomics data demonstrate that Rv3684-generated H_2S suppresses central metabolism, which is evident by increased levels in glycolytic and TCA cycle metabolites, and amino acids in *Mtb*Δ*rv3684* cells. Also, our data suggest that reduced levels of H_2S in *Mtb*Δ*rv3684* cells, which decreases respiration (OXPHOS) (Figure 21A), triggers a compensatory glycolytic response to maintain bioenergetic homeostasis. Hence, H_2S functions as a gaseous modulator of OXPHOS and glycolysis

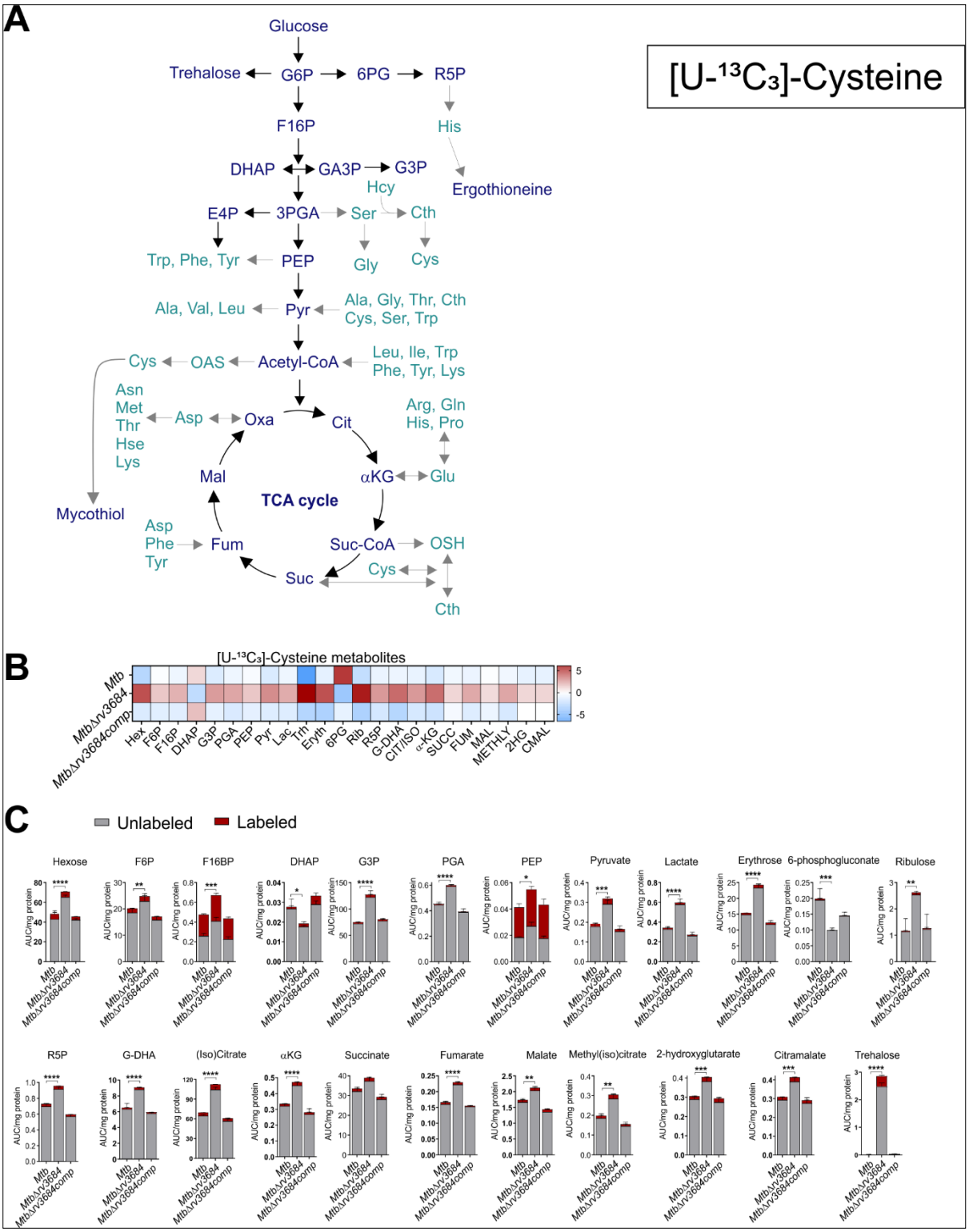

Figure 26: *Mtb* H_2S regulates central metabolism. Results of carbon tracing experiments using [U-$^{13}C_3$]-Cys are presented. (A) Schematic showing the main metabolites which are part of the *Mtb's* central metabolism. (B) shows a heatmap of the upregulation of the metabolites in *Mtb*Δ*rv3684*. (C) show an overall accumulation of the central metabolism metabolites in *Mtb*Δ*rv3684*. Data shown is representative of 2 independent experiments, showing mean ±SEM from 3-5 samples. All *P* values are relative to untreated or wt controls. Statistical analysis was performed using GraphPad Prism 7.02. Two-way ANOVA with Dunnett's multiple comparisons test was used for statistical significance; **P* < 0.05, ***P* < 0.01, ****P* < 0.001, *****P* < 0.0001.

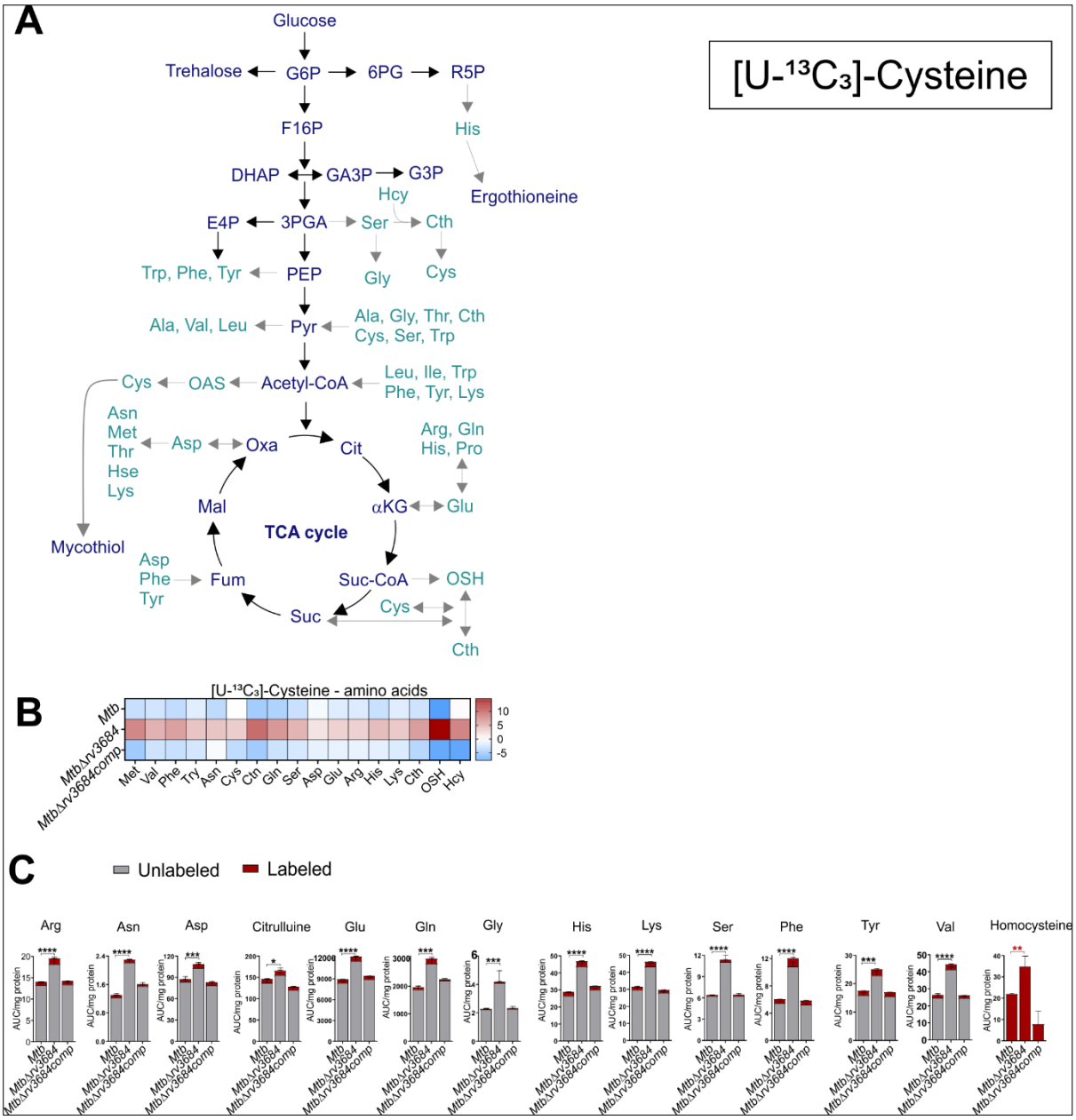

Figure 27: *Mtb* H_2S regulates central metabolism. Results of carbon tracing experiments using [U-$^{13}C_3$]-Cys are presented. (A) Schematic showing the various amino acids within the central metabolism machinery of *Mtb*. (B) shows a heatmap of the upregulation of the amnio acids in *Mtb*Δ*rv3684*. (C) show an overall accumulation of the amino acids in *Mtb*Δ*rv3684*. Data shown is representative of 2 independent experiments, showing mean ±SEM from 3-5 samples. All *P* values are relative to untreated or wt controls. Statistical analysis was performed using GraphPad Prism 7.02. Two-way ANOVA with Dunnett's multiple comparisons test was used for statistical significance; **P* < 0.05, ***P* < 0.01, ****P* < 0.001, *****P* < 0.0001.

`

3.8 Endogenous H_2S in *Mtb* regulates intracellular redox balance

Several studies have reported a role for H_2S in the modulation of redox homeostasis [61, 156, 201, 202]. In *E. coli*, endogenously produced H_2S maintains redox homeostasis by rendering *E. coli* resistant to oxidative stress [124]. Hence, we tested the hypothesis that H_2S produced by Rv3684 modulates *Mtb* redox homeostasis. To test this hypothesis, we used an established flow cytometry technique to quantify reactive oxygen intermediates (ROI) [153], as well as metabolomics to measure the abundance and flux of the two major redox couples ergothioneine (Ergo) and mycothiol (MSH). Since catalase (linked to the detoxification of the oxidant H_2O_2) is present in standard 7H9 liquid media, we examined *Mtb* cells cultured in the presence and absence of catalase. In medium containing catalase, we observed ~43% more ROI-positive *Mtb*Δ*rv3684* bacilli compared to wt *Mtb* and *Mtb*Δ*rv3684comp* (Figure 28A), suggesting that Rv3684-generated H_2S in wt *Mtb* may function as an antioxidant, as reported elsewhere [203]. In the absence of catalase, the percentage of ROI-positive cells increased by 4-5-fold in all strains. Of note, ~25% fewer *Mtb*Δ*rv3684* bacilli were ROI-positive compared to wt *Mtb* or *Mtb*Δ*rv3684comp* cells, suggesting that H_2S functions as a pro-oxidant under these conditions.

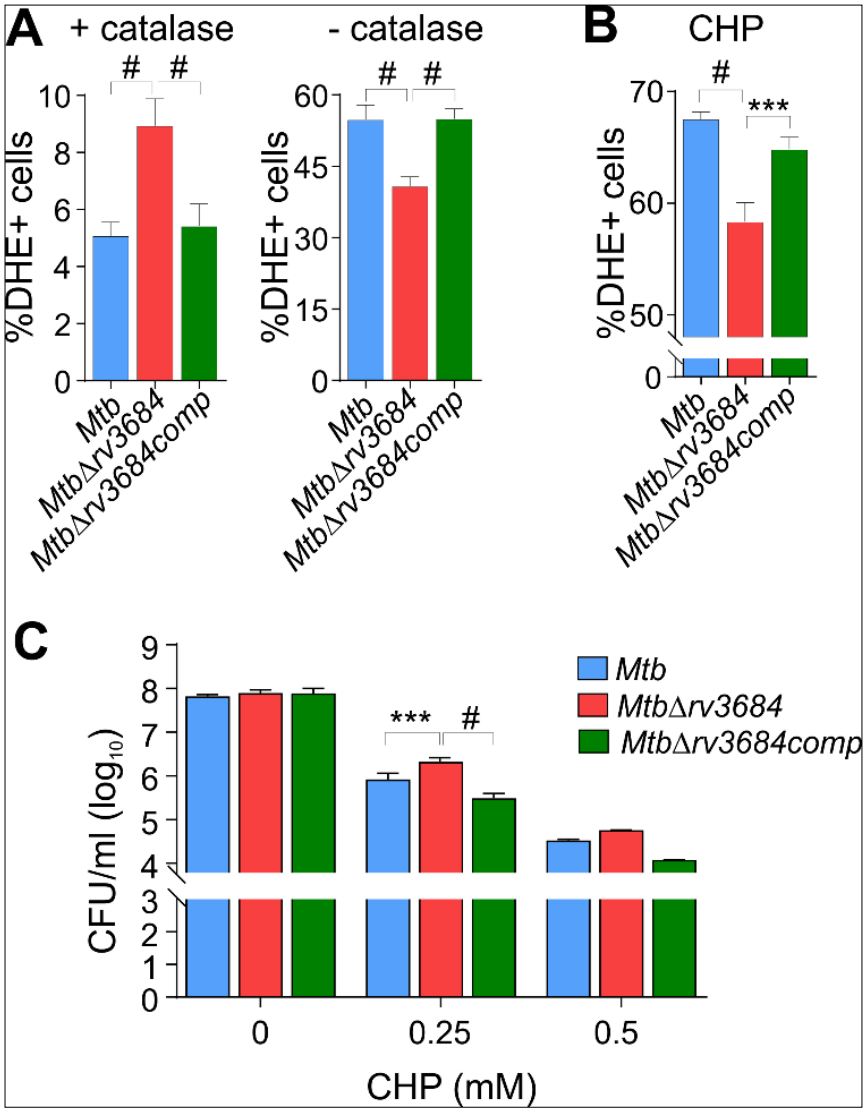

`

Figure 28: Endogenous H_2S in *Mtb* exacerbate the effect of oxidative stress. (A) Measurement of reactive oxygen species (ROS) using dihydroethidium (DHE) stain in bacilli with and without catalase, and (B) after treatment with 0.25 mM cumene hydroperoxide (CHP) for 16 h. (C) CFU-based survival of bacilli after treatment with 0.25 mM CHP. Data shown is representative of 2 independent experiments, showing mean ±SD from 3-5 samples. All *P* values are relative to untreated or wt controls. Statistical analysis was performed using GraphPad Prism 7.02. One-way (for (A) and (B)) and Two-way (for (C)) ANOVA with Dunnett's multiple comparisons test was used for statistical significance; ***$P < 0.001$, #$P < 0.0001$.

To further examine the role of H_2S in *Mtb* redox homeostasis, we exposed *Mtb* to the oxidant cumene hydroperoxide (CHP) without catalase and monitored ROI production and cell viability. In the presence of 0.25 mM CHP, *Mtb*Δ*rv3684* had significantly fewer ROI-positive cells (Figure 28B) with increased survival (Figure 28C) compared to wt *Mtb* and *Mtb* Δ*rv3684comp* cells. Since Cys is a sulfur precursor of MSH and Ergo, we performed carbon tracing experiments using [U-$^{13}C_6$]-glucose (7H9 medium) and [U-$^{13}C_3$]-Cys (100 µM in 7H9 medium) to examine their abundance and CID in *Mtb*Δ*rv3684* cells (Figure 29). Using [U-$^{13}C_6$]-glucose in 7H9 medium (Figure 29B), we observed that Ergo and MSH levels were reduced in *Mtb*Δ*rv3684* cells. The increase in the CID of M+1, M+2, M+3 species for Ergo, and M+1 and M+2 species for MSH, but not in the fully labelled species of the respective metabolites suggest reduced flux of carbons in response to the failure to recycle H_2S back to Cys in *Mtb*Δ*rv3684* cells. Our data in Figure 29B seem to support our observations made in Figure 29A, that lack of Rv3684-generated H_2S promotes oxidative stress, *i.e.* Rv3684-generated H_2S in wt *Mtb* functions as an antioxidant. Interestingly, we did not observe the reduction of Ergo and MSH levels that was previously observed using [U-$^{13}C_3$]-Cys (Figure 29C). There was no significant difference between wt *Mtb* and *Mtb*Δ*rv3684* cells. Our data in Figure 29B demonstrates that H_2S is necessary for maintaining homeostatic levels of MSH and Ergo, and therefore redox balance.

Collectively, these data (Figure 28 and 29) show that H_2S can function either as a pro-oxidant or antioxidant, depending on the environmental conditions. Further, the survival data indicate that reduced homeostatic levels of H_2S promote survival during oxidative stress in the absence of catalase. Hence, under oxidative stress, endogenously produced H_2S in *Mtb* functions as a pro-oxidant.

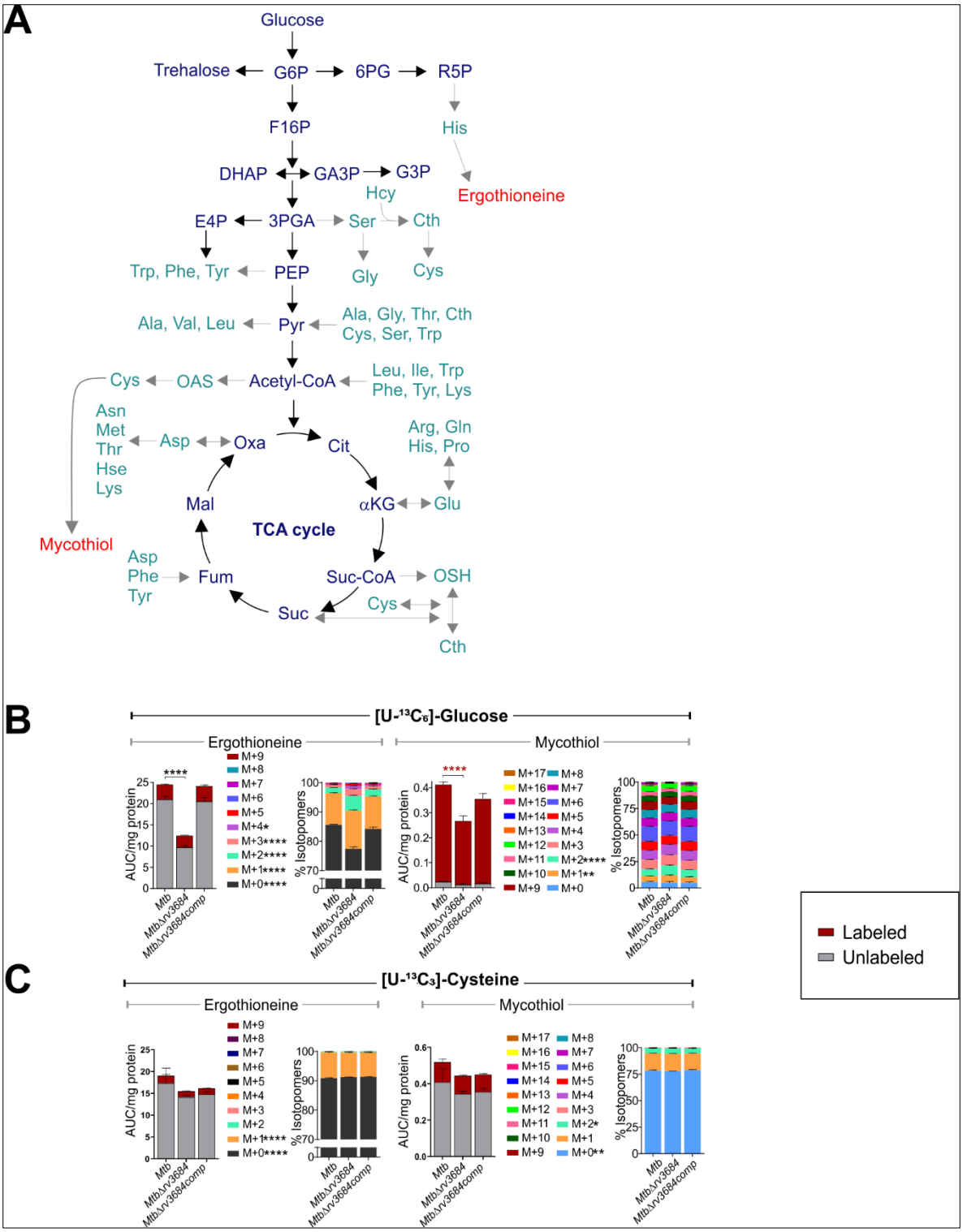

Figure 29: H_2S affects redox homeostasis. Results of carbon tracing experiments using [U-$^{13}C_6$]-glucose showing he effect of H_2S on intracellular redox balance. (A) Schematic showing the various amino acids, mycothiol (MSH) and ergothionine (Ergo) within the central metabolism machinery of *Mtb*. Examination of MSH and Ergo; their abundance and carbon isotopologue distribution (CID) is shown using [U-$^{13}C_6$]-glucose in (B) and [U-$^{13}C_3$]-cysteine in (C). Ergo and MSH levels were reduced in *Mtb*Δ*rv3684* cells. Data shown is representative of 2 independent experiments, showing mean ±SEM from 3-5 samples. All *P* values are relative to untreated or wt controls. Statistical analysis was performed using GraphPad Prism 7.02. Two-way ANOVA with Dunnett's multiple comparisons test was used for statistical significance; ****$P < 0.0001$.

`

3.9 Endogenously produced H_2S by *Mtb* increases *Mtb*'s susceptibility to clofazimine (CFZ) and rifampicin (RIF)

Exogenous H_2S has been implicated in the alteration of antibiotic susceptibility in several bacterial pathogens other than mycobacteria [124, 125, 204, 205]. Demonstrating a role for H_2S in anti-TB drug susceptibility will have significant clinical implications. Hence, even though our data demonstrate that Rv3684 is not the only H_2S producing enzyme in *Mtb*, here we posit that Rv3684-generated H_2S is involved in susceptibility to the anti-TB drug clofazimine (CFZ), a drug involved in ROI-mediated killing [177]. Exposure to CFZ at 60x MIC for 24 hours led to lower ROI-positive *MtbΔrv3684* cells (~30% fewer) compared to wt *Mtb* and *MtbΔrv3684comp* cells (Figure 30A), suggesting that H_2S may promote susceptibility to CFZ. Indeed, this was supported by CFU-based assays, which revealed increased survival of *MtbΔrv3684* cells compared to wt *Mtb* when exposed to CFZ for 8 days (Figure 30B). We do note that there is a small difference in survival between the strains, this could be explained by the fact that H_2S production was reduced, but not eliminated, in *MtbΔrv3684* cells (Figure 17B),. When treated with CFZ, a big difference might not be observed unless most, if not all *Mtb's* endogenously generated H_2S is eliminated. Studies using multiple gene (H_2S producing) knockouts associated with H_2S prodcution will likely be necessary to convincingly demonstrate the CFZ phenotype. Overall, our CFZ-exposure data further indicate that endogenous H_2S increases ROI in wt *Mtb* that contributes to CFZ susceptibility.

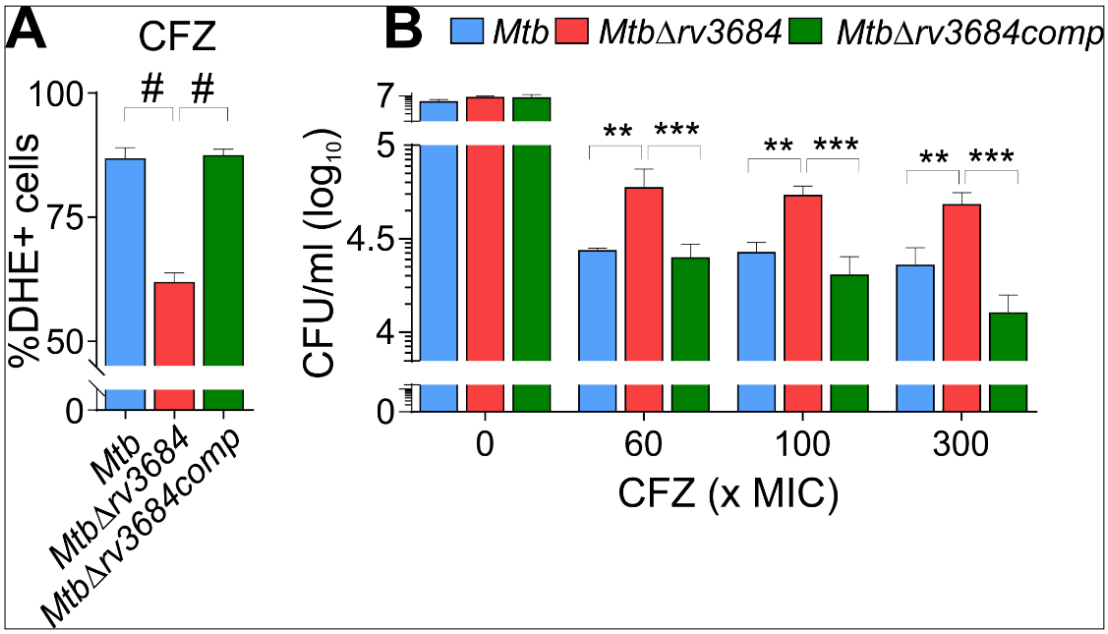

Figure 30: Endogenous H_2S increases *Mtb*'s susceptibility to CFZ. (A) Bacilli were treated with clofazimine (CFZ) at 60x MIC and observed for ROS after 24 h of treatment and (B) CFU-based survival after 8 days of treatment. Data shown is representative of 2 independent experiments, showing mean ±SD from 3-5 samples. All *P* values are relative to untreated or wt controls. Statistical analysis was performed using GraphPad Prism 7.02. One-way (for (A)) and Two-way (for (B)) ANOVA with Tukey's multiple comparisons test was used for statistical significance; $^{**}P < 0.01$, $^{***}P < 0.001$, $\#P < 0.0001$.

`

Previous seminal studies have shown that exogenous addition of H_2S to a range of bacterial pathogens modulate antibiotic susceptibility [125, 202]. Similarly, to determine whether exogenous H_2S plays a role in anti-TB drug susceptibility, CFZ-treated *Mtb* cells were exposed to H_2S via the addition of NaHS. Our data suggest that exogenous addition of H_2S reduces survival of CFZ-treated *Mtb* cells (Figure 31A and B). Likewise, rifampicin-treated, and isoniazid-treated *Mtb* cells were also exposed to H_2S via the addition of NaHS (Figure 31C). H_2S significantly increased *Mtb*'s susceptibility to rifampicin but not isoniazid after 5 days of incubation with 50 µM NaHS. In summary, these data show that H_2S increases *Mtb* susceptibility to CFZ and RIF, potentially through its function as a pro-oxidant.

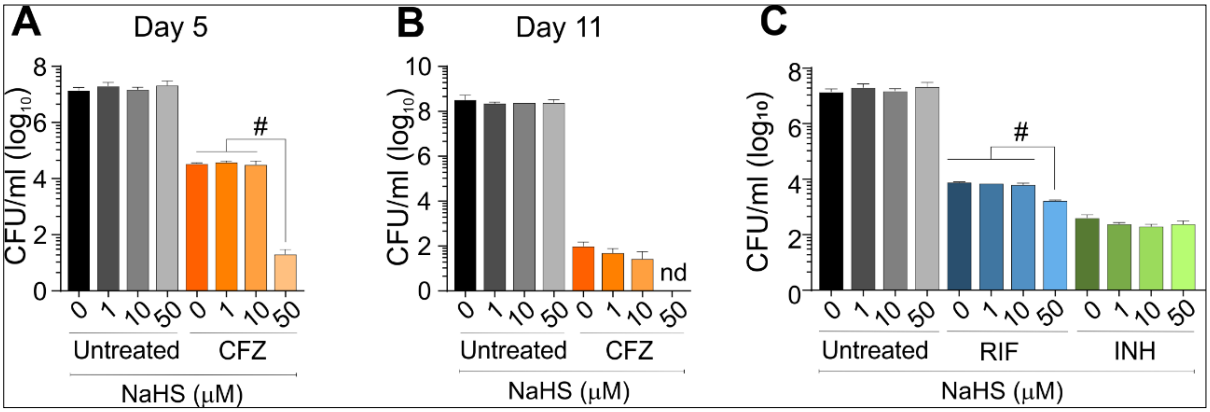

Figure 31: Exogenous H_2S increases *Mtb*'s susceptibility to CFZ. (A) CFU of *Mtb* after different amount of NaHS (H_2S donor) with or without 60x MIC of CFZ treatment for 5 days and (B) 11 days. (C) CFU of *Mtb* after different amounts of NaHS (H_2S donor) with or without RIF and INH treatment for 5 days. Data shown is representative of 2 independent experiments, showing mean ±SD from 3-5 samples. All P values are relative to untreated or wt controls. Statistical analysis was performed using GraphPad Prism 7.02. One-way ANOVA with Dunnett's multiple comparisons test was used for statistical significance; $\#P < 0.0001$.

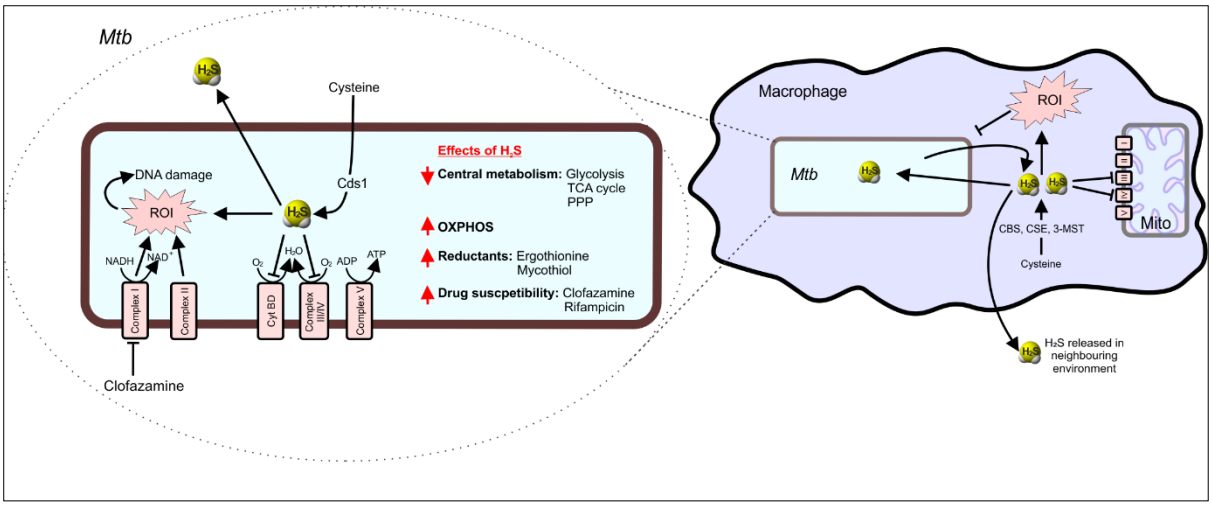

Figure 32: Proposed mechanism for H_2S in *Mtb* disease. Both *Mtb* and the host contribute to supraphysiological levels of H_2S at the site of infection. As a response to *Mtb* infection, the host increases H_2S production in the macrophages (via CBS, CSE and 3MST). The host-generated H_2S is sensed by *Mtb* to stimulate respiration and energy metabolism, thereby increasing bacterial growth and accelerating disease. In addition, excess toxic levels of Cys are degraded by *Mtb* Cds1 (i.e. Rv3684) into volatile H_2S. This endogenously produced H_2S can also lead to increase in ROI in both *Mtb* and host cells leading to DNA damage. Partial H_2S released in the surrounding environment could be essentially detected in the surrounding environment.

`

CHAPTER 4: GENERAL DISCUSSION AND CONCLUSIONS

Some of the general discussion points and conclusions arrived at in this study and presented in this thesis have been synthesized into a manuscript and submitted to Nature Communications for peer-review. Attached in the appendix section is proof of submission of the draft manuscript which was submitted at the time of writing this thesis.

This study demonstrates that *Mtb* produces H_2S, revealing previously unrecognized mechanisms whereby endogenous H_2S modulates *Mtb* bioenergetics, central metabolism, oxidative stress, and anti-TB drug susceptibility. An intriguing finding was that H_2S modulates both respiration (OXPHOS) and glycolysis. These findings are significant as they reveal new mechanisms in *Mtb* physiology. Our findings raise new questions on how *Mtb*-generated and host-generated H_2S triggered by *Mtb* infection, could modulate host immunity [154]. Also, the ability of H_2S to modulate anti-TB drug susceptibility has substantial implications for understanding how sulfur substrates *in vivo* contribute to TB disease. Since H_2S has been previously overlooked during routine culturing of *Mtb*, we anticipate our findings to have broad practical impact in the TB field.

Endogenous H_2S is predominantly produced by reductases, reducing sulfur-containing compounds [139], and orthologs of mammalian H_2S generating enzymes. However, only CBS and CSE, but not 3-MST are found in *Mtb* [125, 206]. To provide evidence that *Mtb* endogenously produces H_2S, we used several experimental approaches. Firstly, we used three methods to measure H_2S production in the headspace and culture supernatant of cultures. Secondly, of the probable *Mtb* enzymes involved in catabolism of sulfur amino acid for H_2S biosynthesis and metabolism, we conclusively demonstrated that *Mtb* produces H_2S via Rv3684. On the other hand, our genetic knockout of *Mtb rv3684* (Figure 17B) and other data (Table 2) indicate that more than one enzyme contributes to H_2S production in *Mtb*. The identified gene, *rv3684*, and the corresponding enzyme Rv3684, have revealed that *Mtb* has a powerful cysteine desulfhydrase activity. Also, analysis of reaction mixture using purified Rv3684 with cysteine as a substrate identified pyruvate as a major product. The formation of H_2S, pyruvate, and presumably NH_3, from the reaction mixture suggests that Rv3684 is catalytically homologous to mammalian and bacterial CSE, which is able to convert cysteine into H_2S, pyruvate and ammonia [186]. However, CSE has been implicated in endogenous H_2S generating activity in other bacteria [125], but not mycobacteria. In *Mtb,* the enzyme Rv1079, has been shown to possess both CSE and cystathionine-γ-synthase (CGS) activity [207]. In addition to the bifunctionality of this CSE/CGS enzyme, Rv1079 was shown to lack cysteine desulfhydrase activity, with the authors postulating a separate,

`

uncharacterised enzyme to perform that role [207]. It is our view that Rv3684 is responsible for cysteine desulfhydrase activity in *Mtb*, a reaction usually catalysed by CSE in mammals and bacteria. The findings in this study is consistent with that of Wheeler PR*, et al.,* (2005), where an unidentified enzyme with cysteine desulfhydrase activity was not inhibited by PAG and formed pyruvate as one of its products [207]. In this study, we have named the *Mtb rv3684* gene, to *cds1* and the enzyme Rv3684 to Cds1. We are of the opinion that we have ascribed a function to an un-annotated gene encoding a cysteine desulfhydrase enzyme (Cds1) that can diminish excess toxic Cys. High levels of cysteine have been shown to inhibit growth [208]. Our findings also reveal growth inhibition (Figure 18), and indicate that cysteine induces ROI production, leading to intracellular oxidative stress. It has been previously reported that the Cys triggered intracellular oxidative stress feeds the Fenton reaction to generate free radicals, leading to DNA damage in *E. coli* [196] and *Mtb* [209]. Our findings provide new insights into the mechanisms on how *Mtb* detoxifies Cys, since disruption of *cds1* in *Mtb* impaired its ability to dissipate Cys. Overall, our findings demonstrate how *Mtb* and recombinant strains of *Msm* are able to utilize *cds1* to mediate the Cys-induced intracellular oxidative stress by dissipating excess Cys into H_2S, which is then released from the cell and then recycled.

An important finding in this study is that clinical MDR *Mtb* strains are the most prolific producers of H_2S compared to laboratory strains and clinical DS strains of *Mtb*, whereas non-pathogenic slow- and fast-growing mycobacterial strains (*e.g.*, *Msm*) produce barely any H_2S. The variation in H_2S production among clinical strains is most likely due to SNPs or genomic rearrangements that contribute to strain-specific differential gene regulation. Since H_2S can be a potent inhibitor of respiration [149, 210], it is tempting to speculate that excessive H_2S is a contributing factor to the slow growth of many of these strains. Our genetic and biochemical evidence that *Mtb* produces H_2S has revealed this gas's possible role in the phenotypic variations observed amongst mycobacterial strains. Also, since H_2S is widely used as a diagnostic test for bacteria, these findings also suggest that there is potential for the development of innovative H_2S based diagnostics for *Mtb*, for example, using H_2S as a diagnostic biomarker in the exhaled breath of TB patients.

Mtb is an obligate aerobe, requiring an electron transport chain (ETC) for energy production via oxidative phosphorylation (OXPHOS) [211]. H_2S has been shown to have an impact on physiology, particularly respiration [153]. In mammals, H_2S has been implicated in reversibly inhibiting cytochrome c oxidase (Complex IV) at high concentrations, conversely, stimulating mitochondrial respiration at low concentrations [148-151]. Our study has shown that a disruption of *cds1* in *Mtb* impairs the basal respiration level by ~40% compared to wt *Mtb*. In addition, we have shown that endogenous H_2S produced in *Mtb* is essential to maintain aerobic respiration, whereas reduction of *Mtb*-derived H_2S lowers oxygen consumption thereby modulating the bioenergetic state of *Mtb*.

`

Another important finding in our study is how Cds1-generated H_2S suppresses glycolysis in *Mtb*. This was demonstrated by the increased levels of many of the glycolytic metabolites and amino acids in *Δcds1* cells. This is not surprising, since OXPHOS and central metabolism are linked [212]. Since our study conclusively demonstrates that H_2S is the effector molecule that affects *Mtb* respiration (OXPHOS) and not Cys, we put forward two possible mechanisms to explain how H_2S could modulate the balance between OXPHOS and glycolysis. A previous study postulated that *Mtb* activates a compensatory response in which glycolysis is induced to meet the demand for ATP through substrate level phosphorylation when OXPHOS is inhibited by the anti-TB drug bedaquiline [177]. Similarly, our first proposal is that, since there are low concentrations of H_2S in Δ*cds1* cells to stimulate respiration, ATP depletion (though not measured) is expected as previously reported in other bacterial studies [213, 214]. Since ATP depletion has occurred, our finding suggests that *Δcds1* cells trigger a compensatory glycolytic response, through substrate level phosphorylation to meet the bioenergetic demands for ATP. Our second proposal, is based on the studies that have shown H_2S to affect enzymes in the glycolytic pathway through S-sulfhydration [200] to modulate their activity. Also, recent studies have also shown that H_2S suppresses glycolysis in macrophages upon *Mtb* infection [154].

In addition, another interesting finding in our study is how Cds1-mediatated H_2S affects redox homeostasis. This is not surprising since several studies have reported a role for H_2S in the modulation of redox homeostasis [61, 156, 201, 202]. Redox balance, respiration (OXPHOS) and central metabolism are also linked [212]. Our study revealed an unusual effect of H_2S on oxidative stress in *Mtb*. In addition to demonstrating that H_2S deficient *Mtb* (*Mtb*Δ*cds1* cells) respire at lower basal levels compared to wt *Mtb*, our findings showed these cells to have reduced ROI production. Our data show that the presence of catalase in the growth media influences ROI production, and that H_2S can function as a pro-oxidant or reductant depending on the environmental conditions. In this regard, careful consideration should be given to experimental design and subsequent conclusions. Since CHP exerts oxidative stress by creating ROI [215], whereas CFZ's mode of action is associated with ROI mediated killing [216]; our findings demonstrate that H_2S exacerbates oxidative stress in the presence of these drugs. We also demonstrate that H_2S deficient *Mtb* (*Mtb*Δ*cds1* cells) had significantly less ROI when treated with CHP and CFZ. As expected, this reduction in ROI in *Mtb*Δ*cds1* cells confers resistance to CHP, and CFZ treatment. In *E.coli*, 3MST derived endogenous H_2S has been shown to protect cells against H_2O_2-mediated toxicity by directly sequestrating Fe^{2+} [124]. In addition, genetic manipulation of H_2S-producing genes in several bacterial pathogens rendered bacteria susceptible to numerous antibiotics [125]. However, we observed that Cds1-derived H_2S increases cells' susceptibility to CHP and CFZ. This difference in phenotypic behaviour may be explained by the difference in the species, for example, *Mtb* being an obligate aerobe, whereas *E. coli* is a facultative anaerobe, as well as the difference in the modes of action of antibiotics used by Shatalin *et. al* (2011). In support of this, we observed enhanced killing of *Mtb* by CFZ after the addition of exogenous H_2S. Since CFZ targets

`

NADH dehydrogenase (NDH-2) [177, 216] and H_2S stimulates respiration and increases ROI generation [209], one plausible explanation for the enhanced killing of CFZ is that during treatment, there is simultaneous disruption of electron flow in the ETC and increased generation of ROI leading to impaired *Mtb* survival. Whereas previous studies have shown that Cys increases *Mtb* respiration and susceptibility to INH, observed by the enhanced killing of *Mtb* persisters by INH and RIF [209], our study suggests that H_2S could be the effector molecule in that model. However, it should be recognized that exogenous Cys also generates H_2O_2 to trigger the Fenton reaction, which leads to continuous OH● formation that damages DNA. This may exacerbate the effect of INH, particularly in closed vessels where H_2O_2 accumulates [191]. In this study, H_2S in combination with RIF also increased *Mtb* killing, likely because RIF also induces oxidative stress [217], but this effect was less pronounced. These findings have important therapeutic implications as it suggests that sulfur sources *in vivo* could influence anti-TB drug efficacy. However, the role of H_2S in *Mtb* virulence is yet to be established. We propose that enhanced pharmacological inhibition of respiratory complexes coupled with *Mtb* derived H_2S may facilitate rapid bacterial killing.

Since this study has demonstrated that endogenously generated H_2S affects *Mtb* bioenergetics, redox homeostasis, and anti-TB drug susceptibility, we propose a complex mechanism for the role of H_2S in *Mtb* disease (Figure 32). Our findings add to our understanding of the role of H_2S in *Mtb* physiology and pathogenesis since we now know that both *Mtb* and the host contribute supraphysiological levels of H_2S at the site of infection. As a response to *Mtb* infection, the host increases H_2S production in the macrophages (via CBS, CSE and 3MST) leading to increased bacillary burden, increased inflammation, and reduced survival [153]. Host-generated H_2S is sensed by *Mtb*, stimulating respiration and energy metabolism, thereby increasing bacterial growth and accelerating disease [153]. During infection, H_2S produced by both the macrophage and *Mtb* may suppress central metabolism and stimulate or inhibit respiration to exacerbate disease. In the presence of excess toxic levels of Cys, Cds1 manages to degrade that excess Cys into H_2S. H_2S then leads to increased ROI levels, thereby increasing intracellular oxidative stress in both macrophages and *Mtb* cells, leading to DNA damage [209]. In this model, since both *Mtb* and the macrophage produce H_2S, we suggest that the resultant H_2S produced by these cells may be released in the surrounding environment, providing a potential pool of H_2S through which new TB diagnostics can exploit.

Overall, since H_2S is a previously overlooked molecule in Mtb experiments, our findings represent an important advance in *Mtb* physiology and may broadly impact the TB field. Our findings present a paradigm for how *Mtb*-derived H_2S metabolism affects *Mtb* bioenergetics, redox homeostasis, and anti-TB drug susceptibility. Once these mechanisms are known, we anticipate that targeted pharmacological manipulation will result in novel approaches to TB treatment whereas the phenotypic variation in clinical strains could lead to the development of new TB diagnostics assay based on H_2S production.

`

CHAPTER 5: FUTURE WORK

A recent study by Rahman *et al*. (2020) showed that *Mtb* infection of the host triggers supraphysiological levels of host-generated H_2S that suppresses central metabolism in infected macrophages and exacerbates disease by down regulating the adaptive immune response and promoting innate immunity [154]. This study implicated host H_2S in host immunometabolic mechanisms and TB pathogenesis. Considering this study has shown that *Mtb* endogenously produces H_2S, future studies are needed to investigate the role of *Mtb*-derived H_2S on host energy metabolism and immune response upon *Mtb* infection of host. We posit two hypotheses. The first hypothesis is that upon *Mtb* infection, *Mtb* generated H_2S exacerbates disease by suppressing the host's central metabolism and hampering an adequate immune response to control infection. To test this hypothesis, mice will be infected with both the wt and mutant *Mtb* and the immune response will be monitored. We expect the wt to trigger excessive inflammation at the site of infection in comparison to the infection with the mutant. Controlling or reducing excessive inflammation in TB patients is an area of concern for most pharmacological intervention developers.

The second hypothesis is that *Mtb* generated H_2S is essential for virulence. To test this hypothesis, complete elimination of *Mtb* produced H_2S would be necessary. To achieve this, we propose two methods. The first, is to identify other H_2S producing enzymes using different substrates and co-factors and ultimately disrupt those genes to eliminate *Mtb*'s ability to endogenously produce H_2S. This approach could be challenging and if unsuccessful, an alternative method involves inserting a sulfide quinone oxidoreductase (SQR) gene into *Mtb*. SQR is a key enzyme for maintaining sulfide homeostasis and is known to oxidise H_2S to funnel electrons into the electron transport chain. We are of the view that SQR could potentially eliminate *Mtb*-generated H_2S under diverse environmental conditions. Testing this hypothesis would be in alignment with our proposal in Figure 32 since we posited that the large number of H_2S-producing *Mtb* cells in the infected human lung could increase the local H_2S concentration to target host immune cells by reversibly binding Complex IV to inhibit the binding of O_2 leading to the suppression of the host's immune cell's central metabolism. We are of the view that H_2S deficient *Mtb* cells would aid in testing both hypotheses.

On the other hand, while testing the above hypotheses, one could also test the hypothesis that *Mtb* generated H_2S is necessary for *Mtb* to survive drug treatment. Since our study showed that MDR clinical strains produced more H_2S than drug susceptible strains and considering H_2S is toxic, and is an important signalling molecule, we are of the view that H_2S plays a role in *Mtb* drug resistance. To test this hypothesis, one could also make use of SQR or an H_2S degrading enzyme like OASS to eliminate the H_2S produced by MDR *Mtb* strains and perform drug susceptibility assays. To the best of our knowledge, examining a role for H_2S as a key driver of *Mtb* drug resistance has not yet been considered.

`

Therefore, successful completion of this study would provide new knowledge of how *Mtb* H_2S influences drug resistance and lead to the development of novel therapeutic intervention strategies.

Overall, it is likely that the successful completion of these future studies on the synergy of the H_2S produced by both the host and *Mtb* will establish new paradigms in *Mtb* physiology, pathogenesis, and host immunometabolism.

]

`

CHAPTER 6: THESIS APPENDICES

7.1 Appendix A: *Mtb* clinical strains additional information

Drug & PID → ↓	**TKK-01-0001**	**TKK-01-0027**	**TKK-01-0035**	**TKK-01-0047**
INH (0.2µg/ml)	R	S	R	S
INH (1µg/ml)	R	S	R	S
RIF (1µg/ml)	R	S	R	S
ETH (7.5µg/ml)	R	S	R	S
STR (2 µg/ml)	R	S	R	S
OFLOX (2 µg/ml)	S	S	S	S
KAN (6µg/ml)	S	S	S	S
CFZ (0.125µg/ml)	S	S	S	R
CFZ (0.5µg/ml)	S	S	S	S
CFZ (1µg/ml)	S	S	S	S
CAPREO (5µg/ml)	S	S	S	S
CAPREO (10µg/ml)	S	S	S	S
ETHION (5µg/ml)	R	S	S	S
ETHION (10µg/ml)	R	S	S	S
STRAIN LINEAGE	KZN LAM4	Beijing	KZN LAM4	Unknown
COMMENT	MDR	Drug susceptible	MDR	Drug susceptible

Abbreviations:

- R = Resistant
- S = Susceptible
- INH = Isoniazid
- RIF= Rifampicin
- ETH = Ethambutol
- STR = Streptomycin
- OFLOX = Ofloxacin
- KAN = Kanamycin
- CFZ = Clofazamine
- CAPREO = Capreomycin
- ETHION = Ethionamide
- MDR – Multidrug resistant

`

7.2 Appendix B: Purification of Rv3684 protocol

1. Transform the pET15b:Rv3684 construct in BL21(DE3) cells.
2. Select the single colony the next day and use it to set the secondary culture.
3. Inoculate secondary culture using overnight grown BL21::pET15b:Rv3684 cells in 500ml media till OD_{600} is between 0.5 - 0.6 at 37°C.
4. Induce the cells at OD_{600} of 0.5-0.6 with 0.4 mM of IPTG and grow overnight at 18°C.
5. Centrifuge the cells the next day and store at -80°C.
6. Resuspend the pellet in 30 ml of 50 mM sodium phosphate buffer pH 7.9, add lysozyme to a final concentration of 0.5 mg/ml and then keep on ice for 30 min.
7. Sonicate the samples for 10 min with 20 sec ON and 40 sec OFF cycle (make sure the probe tip is always properly dipped in cell suspension).
8. Centrifuge the sonicated sample for 30 mins at high speed.
9. Take the supernatant and use it for binding step with prewashed IMAC Ni charged resins.
10. Keep for binding till 30 mins at 4°C in the presence of 20 mM Imidazole.
11. Add the binding mix to the column and allow beads to settle and let the reminder supernatant to flow through.
12. Wash the beads with 20 ml of buffer, 20 ml 1.2 M NaCl buffer, 20 ml of 20 mM Imidazole, and finally elute the protein with 2 ml of 150 mM elution buffer.
13. Dialyse the protein sample against 50 mM sodium phosphate buffer containing 150 mM NaCl, 5% glycerol.
14. Run the SDS-PAGE gel to check the purity of the protein.

`

7.3 Appendix C: Proof of manuscript submission

manuscripttrackingsystem — nature communications

tracking system home | author instructions | reviewer instructions | help | logout | journal home

Detailed Status Information

Manuscript #	NCOMMS-20-45815-T
Current Revision #	0
Submission Date	18th November 20
Current Stage	Manuscript under consideration
Title	*Mycobacterium tuberculosis* H_2S functions as a sink to modulate central metabolism, bioenergetics, and drug susceptibility
Manuscript Type	Article
Corresponding Author	Prof. Adrie Steyn (asteyn@uab.edu) (University of Alabama at Birmingham)
Contributing Authors	Mr. Tafara Kunota , Dr. Md. Rahman , Mr. Barry Truebody , Dr. Jared Mackenzie , Dr. Dirk Lamprecht , Dr. Vikram Saini , John Adamson , Dr. Ritesh Sevalkar , Prof. Jack Lancaster Jr. , Prof. Michael Berney , Dr. Joel Glasgow
Authorship	Yes
Abstract	H_2S is a potent gasotransmitter in eukaryotes and bacteria. Host-derived H_2S was shown to profoundly alter *M. tuberculosis (Mtb)* energy metabolism and growth. However, compelling evidence for endogenous production of H_2S and its role in *Mtb* physiology is lacking. We show that multi-drug-resistant and drug-susceptible clinical *Mtb* strains produce H_2S, whereas H_2S production in non-pathogenic *M. smegmatis* is barely detectable. We identified Rv3684 (Cds1) as an H_2S-producing enzyme in *Mtb* and show that *cds1* disruption reduces, but does not eliminate H_2S production, suggesting the involvement of multiple genes in H_2S production. We identified endogenous H_2S to be an effector molecule that maintains bioenergetic homeostasis by regulating respiration. Importantly, H_2S plays a key role in central metabolism by modulating the balance between oxidative phosphorylation and glycolysis, and functions as a sink to recycle sulfur atoms back to cysteine to maintain sulfur homeostasis. Lastly, *Mtb*-generated H_2S regulates redox homeostasis and susceptibility to the anti-TB drugs clofazimine and rifampicin. These findings reveal previously unknown facets of *Mtb* physiology and have implications for routine laboratory culturing, understanding drug susceptibility, and improved diagnostics.
Subject Terms	Biological sciences/Microbiology/Pathogens Health sciences/Pathogenesis/Infection
Show Author Information	Allow Reviewers to see Author information.
Research Square author dashboard	I understand that my manuscript and associated personal data will be shared with Research Square for the delivery of the author dashboard.
In Review	No, my co-authors and I would not like to benefit from *In Review*
Competing interests policy	There is **NO** Competing Interest.
Applicable Funding Source	No Applicable Funding

`

REFERENCES

1. Dye, C., et al., *Consensus statement. Global burden of tuberculosis: estimated incidence, prevalence, and mortality by country. WHO Global Surveillance and Monitoring Project.* Jama, 1999. **282**(7): p. 677-86.

2. WorldHealthOrganization. *Global tuberculosis report 2019. Geneva: World Health Organization; 2019*

2019 [cited 2020 24 February 2020].

3. Orgeur, M. and R. Brosch, *Evolution of virulence in the Mycobacterium tuberculosis complex.* Curr Opin Microbiol, 2018. **41**: p. 68-75.

4. Delogu, G., M. Sali, and G. Fadda, *The biology of mycobacterium tuberculosis infection.* Mediterranean journal of hematology and infectious diseases, 2013. **5**(1): p. e2013070-e2013070.

5. de Jong, B.C., M. Antonio, and S. Gagneux, *Mycobacterium africanum--review of an important cause of human tuberculosis in West Africa.* PLoS neglected tropical diseases, 2010. **4**(9): p. e744-e744.

6. Daniel, T.M., *The history of tuberculosis.* Respir Med, 2006. **100**(11): p. 1862-70.

7. Hershkovitz, I., et al., *Detection and molecular characterization of 9,000-year-old Mycobacterium tuberculosis from a Neolithic settlement in the Eastern Mediterranean.* PLoS One, 2008. **3**(10): p. e3426.

8. Nerlich, A.G., et al., *Molecular evidence for tuberculosis in an ancient Egyptian mummy.* Lancet, 1997. **350**(9088): p. 1404.

9. Ducati, R.G., et al., *The resumption of consumption -- a review on tuberculosis.* Mem Inst Oswaldo Cruz, 2006. **101**(7): p. 697-714.

`

10. Bloom, B.R. and C.J. Murray, *Tuberculosis: commentary on a reemergent killer.* Science, 1992. **257**(5073): p. 1055-64.

11. Shiloh, M.U., *Mechanisms of mycobacterial transmission: how does Mycobacterium tuberculosis enter and escape from the human host.* Future Microbiol, 2016. **11**: p. 1503-1506.

12. Bates, J.H. and W.W. Stead, *The history of tuberculosis as a global epidemic.* Med Clin North Am, 1993. **77**(6): p. 1205-17.

13. Cole, S.T., et al., *Deciphering the biology of Mycobacterium tuberculosis from the complete genome sequence.* Nature, 1998. **393**(6685): p. 537-44.

14. Churchyard, G.J., et al., *Tuberculosis control in South Africa: successes, challenges and recommendations.* S Afr Med J, 2014. **104**(3 Suppl 1): p. 244-8.

15. Bateman, C., *The protracted TB struggle - SA ups the intensity.* S Afr Med J, 2010. **100**(4): p. 207-9.

16. Gandhi, N.R., et al., *Extensively drug-resistant tuberculosis as a cause of death in patients co-infected with tuberculosis and HIV in a rural area of South Africa.* Lancet, 2006. **368**(9547): p. 1575-80.

17. Lin, P.L. and J.L. Flynn, *Understanding latent tuberculosis: a moving target.* J Immunol, 2010. **185**(1): p. 15-22.

18. Timmermans, W.M.C., et al., *Immunopathogenesis of granulomas in chronic autoinflammatory diseases.* Clinical & translational immunology, 2016. **5**(12): p. e118-e118.

19. Bussi, C. and M.G. Gutierrez, *Mycobacterium tuberculosis infection of host cells in space and time.* FEMS Microbiol Rev, 2019. **43**(4): p. 341-361.

20. Lerner, T.R., S. Borel, and M.G. Gutierrez, *The innate immune response in human tuberculosis.* Cell Microbiol, 2015. **17**(9): p. 1277-85.

`

21. Eum, S.-Y., et al., *Neutrophils are the predominant infected phagocytic cells in the airways of patients with active pulmonary TB.* Chest, 2010. **137**(1): p. 122-128.

22. Clemens, D.L., B.-Y. Lee, and M.A. Horwitz, *The Mycobacterium tuberculosis phagosome in human macrophages is isolated from the host cell cytoplasm.* Infection and immunity, 2002. **70**(10): p. 5800-5807.

23. Deretic, V., *Autophagy in tuberculosis.* Cold Spring Harbor perspectives in medicine, 2014. **4**(11): p. a018481-a018481.

24. Simeone, R., et al., *Cytosolic access of Mycobacterium tuberculosis: critical impact of phagosomal acidification control and demonstration of occurrence in vivo.* PLoS pathogens, 2015. **11**(2): p. e1004650-e1004650.

25. Lugton, I., *Mucosa-associated lymphoid tissues as sites for uptake, carriage and excretion of tubercle bacilli and other pathogenic mycobacteria.* Immunol Cell Biol, 1999. **77**(4): p. 364-72.

26. Cooper, A.M., *Cell-mediated immune responses in tuberculosis.* Annual review of immunology, 2009. **27**: p. 393-422.

27. de Martino, M., et al., *Immune Response to Mycobacterium tuberculosis: A Narrative Review.* Frontiers in pediatrics, 2019. **7**: p. 350-350.

28. Choreño-Parra, J.A., et al., *Thinking Outside the Box: Innate- and B Cell-Memory Responses as Novel Protective Mechanisms Against Tuberculosis.* Frontiers in Immunology, 2020. **11**(226).

29. Cai, J., et al., *Factors associated with patient and provider delays for tuberculosis diagnosis and treatment in Asia: a systematic review and meta-analysis.* PloS one, 2015. **10**(3): p. e0120088-e0120088.

`

30. Sreeramareddy, C.T., et al., *Time delays in diagnosis of pulmonary tuberculosis: a systematic review of literature.* BMC Infectious Diseases, 2009. **9**(1): p. 91.

31. Ryu, Y.J., *Diagnosis of pulmonary tuberculosis: recent advances and diagnostic algorithms.* Tuberculosis and respiratory diseases, 2015. **78**(2): p. 64-71.

32. Perkins, M.D. and J. Cunningham, *Facing the crisis: improving the diagnosis of tuberculosis in the HIV era.* Journal of Infectious Diseases, 2007. **196**(Supplement 1): p. S15-S27.

33. Davis, J.L., et al., *Diagnostic accuracy of same-day microscopy versus standard microscopy for pulmonary tuberculosis: a systematic review and meta-analysis.* Lancet Infect Dis, 2013. **13**(2): p. 147-54.

34. Pai, N.P. and M. Pai, *Point-of-care diagnostics for HIV and tuberculosis: landscape, pipeline, and unmet needs.* Discovery medicine, 2012. **13**(68): p. 35-45.

35. Marais, B.J., et al., *Use of Light-Emitting Diode Fluorescence Microscopy to Detect Acid-Fast Bacilli in Sputum.* Clinical Infectious Diseases, 2008. **47**(2): p. 203-207.

36. Achkar, J.M., et al., *Adjunctive Tests for Diagnosis of Tuberculosis: Serology, ELISPOT for Site-Specific Lymphocytes, Urinary Lipoarabinomannan, String Test, and Fine Needle Aspiration.* The Journal of Infectious Diseases, 2011. **204**(suppl_4): p. S1130-S1141.

37. Steingart, K.R., et al., *Serological tests for the diagnosis of active tuberculosis: relevance for India.* The Indian journal of medical research, 2012. **135**(5): p. 695-702.

38. Lalvani, A., *Diagnosing Tuberculosis Infection in the 21st Century: New Tools To Tackle an Old Enemy.* Chest, 2007. **131**(6): p. 1898-1906.

39. Nachega, J.B. and G. Maartens, *Chapter 51 - Clinical aspects of tuberculosis in HIV-infected adults*, in *Tuberculosis*, H.S. Schaaf, et al., Editors. 2009, W.B. Saunders: Edinburgh. p. 524-531.

`

40. Rezai, M.S., et al., *Estimating the prevalence of Positive Tuberculin Skin Test Reactions in General Population and High-risk Groups: A Meta-analysis.* International journal of preventive medicine, 2017. **8**: p. 97-97.

41. Iskandar, A., et al., *The Diagnostic Value of Urine Lipoarabinomannan (LAM) Antigen in Childhood Tuberculosis.* Journal of clinical and diagnostic research : JCDR, 2017. **11**(3): p. EC32-EC35.

42. Qin, L., et al., *Identification and evaluation of a new nucleic acid amplification test target for specific detection of Mycobacterium tuberculosis.* Clin Chem Lab Med, 2010. **48**(10): p. 1501-5.

43. Lawn, S.D., et al., *Advances in tuberculosis diagnostics: the Xpert MTB/RIF assay and future prospects for a point-of-care test.* The Lancet infectious diseases, 2013. **13**(4): p. 349-361.

44. Ardizzoni, E., et al., *Implementing the Xpert® MTB/RIF Diagnostic Test for Tuberculosis and Rifampicin Resistance: Outcomes and Lessons Learned in 18 Countries.* PloS one, 2015. **10**(12): p. e0144656-e0144656.

45. Lawn, S.D. and M.P. Nicol, *Xpert® MTB/RIF assay: development, evaluation and implementation of a new rapid molecular diagnostic for tuberculosis and rifampicin resistance.* Future microbiology, 2011. **6**(9): p. 1067-1082.

46. Sulis, G., et al., *Recent developments in the diagnosis and management of tuberculosis.* npj Primary Care Respiratory Medicine, 2016. **26**(1): p. 16078.

47. Bassett, I.V., et al., *Test and Treat TB: a pilot trial of GeneXpert MTB/RIF screening on a mobile HIV testing unit in South Africa.* BMC Infectious Diseases, 2019. **19**(1): p. 110.

48. Ojha, A.K., et al., *Growth of Mycobacterium tuberculosis biofilms containing free mycolic acids and harbouring drug-tolerant bacteria.* Mol Microbiol, 2008. **69**(1): p. 164-74.

`

49. Nahid, P., et al., *Treatment of Drug-Resistant Tuberculosis. An Official ATS/CDC/ERS/IDSA Clinical Practice Guideline.* Am J Respir Crit Care Med, 2019. **200**(10): p. e93-e142.

50. Dooley, K.E., E.L. Nuermberger, and A.H. Diacon, *Pipeline of drugs for related diseases: tuberculosis.* Curr Opin HIV AIDS, 2013. **8**(6): p. 579-85.

51. Sotgiu, G., et al., *Tuberculosis treatment and drug regimens.* Cold Spring Harbor perspectives in medicine, 2015. **5**(5): p. a017822-a017822.

52. Chhabra, N., et al., *Pharmacotherapy for multidrug resistant tuberculosis.* Journal of pharmacology & pharmacotherapeutics, 2012. **3**(2): p. 98-104.

53. NIH, *Tuberculosis Drugs and Mechanisms of Action.* 2016.

54. Dooley, K.E., et al., *World Health Organization group 5 drugs for the treatment of drug-resistant tuberculosis: unclear efficacy or untapped potential?* The Journal of infectious diseases, 2013. **207**(9): p. 1352-1358.

55. Shah, N.S., et al., *Worldwide emergence of extensively drug-resistant tuberculosis.* Emerging infectious diseases, 2007. **13**(3): p. 380-387.

56. CDC, *Treatment for TB Disease.* 2017.

57. Shah, N.S., et al., *Increasing drug resistance in extensively drug-resistant tuberculosis, South Africa.* Emerg Infect Dis, 2011. **17**(3): p. 510-3.

58. WorldHealthOrganization, *WHO consolidated guidelines on drug-resistant tuberculosis treatment. Geneva: World Health Organization; 2019.* 2019.

59. Sharma, S.K. and K. Dheda, *What is new in the WHO consolidated guidelines on drug-resistant tuberculosis treatment?* The Indian journal of medical research, 2019. **149**(3): p. 309-312.

60. Wang, R., *Hydrogen sulfide: the third gasotransmitter in biology and medicine.* Antioxid Redox Signal, 2010. **12**(9): p. 1061-4.

`

61. Kimura, Y., Y. Goto, and H. Kimura, *Hydrogen sulfide increases glutathione production and suppresses oxidative stress in mitochondria.* Antioxid Redox Signal, 2010. **12**(1): p. 1-13.

62. Gadalla, M.M. and S.H. Snyder, *Hydrogen sulfide as a gasotransmitter.* J Neurochem, 2010. **113**(1): p. 14-26.

63. Polhemus, D.J. and D.J. Lefer, *Emergence of hydrogen sulfide as an endogenous gaseous signaling molecule in cardiovascular disease.* Circ Res, 2014. **114**(4): p. 730-7.

64. Wareham, L.K., H.M. Southam, and R.K. Poole, *Do nitric oxide, carbon monoxide and hydrogen sulfide really qualify as 'gasotransmitters' in bacteria?* Biochem Soc Trans, 2018. **46**(5): p. 1107-1118.

65. Mustafa, A.K., M.M. Gadalla, and S.H. Snyder, *Signaling by gasotransmitters.* Sci Signal, 2009. **2**(68): p. re2.

66. Jamaati, H., et al., *Nitric Oxide in the Pathogenesis and Treatment of Tuberculosis.* Frontiers in microbiology, 2017. **8**: p. 2008-2008.

67. Zacharia, V.M. and M.U. Shiloh, *Effect of carbon monoxide on Mycobacterium tuberculosis pathogenesis.* Medical gas research, 2012. **2**(1): p. 30-30.

68. Shiloh, M.U., P. Manzanillo, and J.S. Cox, *Mycobacterium tuberculosis senses host-derived carbon monoxide during macrophage infection.* Cell Host Microbe, 2008. **3**(5): p. 323-30.

69. Koshland, D., *The molecule of the year.* Science, 1992. **258**(5090): p. 1861-1861.

70. Bryan, N.S. and J. Loscalzo, *Nitrite and nitrate in human health and disease*. 2011: Springer.

71. Blaise, G.A., et al., *Nitric oxide, cell signaling and cell death.* Toxicology, 2005. **208**(2): p. 177-192.

72. Wink, D.A., et al., *Nitric oxide and redox mechanisms in the immune response.* Journal of Leukocyte Biology, 2011. **89**(6): p. 873-891.

`

73. Chinta, K.C., et al., *The emerging role of gasotransmitters in the pathogenesis of tuberculosis.* Nitric Oxide, 2016. **59**: p. 28-41.

74. Hill, B.G., et al., *What Part of NO Don't You Understand? Some Answers to the Cardinal Questions in Nitric Oxide Biology.* Journal of Biological Chemistry, 2010. **285**(26): p. 19699-19704.

75. Nathan, C. and Q.W. Xie, *Nitric oxide synthases: roles, tolls, and controls.* Cell, 1994. **78**(6): p. 915-8.

76. Weaver, J., et al., *A comparative study of neuronal and inducible nitric oxide synthases: generation of nitric oxide, superoxide, and hydrogen peroxide.* Biochim Biophys Acta, 2005. **1726**(3): p. 302-8.

77. Schön, T., et al., *Local production of nitric oxide in patients with tuberculosis.* Int J Tuberc Lung Dis, 2004. **8**(9): p. 1134-7.

78. Choi, H.S., et al., *Analysis of nitric oxide synthase and nitrotyrosine expression in human pulmonary tuberculosis.* Am J Respir Crit Care Med, 2002. **166**(2): p. 178-86.

79. Pieters, J., *Mycobacterium tuberculosis and the macrophage: maintaining a balance.* Cell Host Microbe, 2008. **3**(6): p. 399-407.

80. Chao, M.C. and E.J. Rubin, *Letting sleeping dos lie: does dormancy play a role in tuberculosis?* Annu Rev Microbiol, 2010. **64**: p. 293-311.

81. Nathan, C., *Inducible nitric oxide synthase in the tuberculous human lung.* Am J Respir Crit Care Med, 2002. **166**(2): p. 130-1.

82. Nathan, C., *Role of iNOS in human host defense.* Science, 2006. **312**(5782): p. 1874-5; author reply 1874-5.

`

83. MacMicking, J., Q.W. Xie, and C. Nathan, *Nitric oxide and macrophage function.* Annu Rev Immunol, 1997. **15**: p. 323-50.

84. Davis, A.S., et al., *Mechanism of inducible nitric oxide synthase exclusion from mycobacterial phagosomes.* PLoS Pathog, 2007. **3**(12): p. e186.

85. Voskuil, M.I., et al., *Inhibition of respiration by nitric oxide induces a Mycobacterium tuberculosis dormancy program.* The Journal of experimental medicine, 2003. **198**(5): p. 705-713.

86. Kumar, A., et al., *Mycobacterium tuberculosis DosS is a redox sensor and DosT is a hypoxia sensor.* Proc Natl Acad Sci U S A, 2007. **104**(28): p. 11568-73.

87. Sivaramakrishnan, S. and P.R.O. de Montellano, *The DosS-DosT/DosR Mycobacterial Sensor System.* Biosensors, 2013. **3**(3): p. 259-282.

88. Wilson, J.L., et al., *Antibacterial effects of carbon monoxide.* Curr Pharm Biotechnol, 2012. **13**(6): p. 760-8.

89. Davidge, K.S., et al., *Carbon monoxide-releasing antibacterial molecules target respiration and global transcriptional regulators.* J Biol Chem, 2009. **284**(7): p. 4516-24.

90. Wu, L. and R. Wang, *Carbon Monoxide: Endogenous Production, Physiological Functions, and Pharmacological Applications.* Pharmacological Reviews, 2005. **57**(4): p. 585-630.

91. Dennery, P.A., *Signaling function of heme oxygenase proteins.* Antioxidants & redox signaling, 2014. **20**(11): p. 1743-1753.

92. Nobre, L.S., et al., *Antimicrobial action of carbon monoxide-releasing compounds.* Antimicrob Agents Chemother, 2007. **51**(12): p. 4303-7.

93. Murray, T.S., et al., *The Carbon Monoxide Releasing Molecule CORM-2 Attenuates Pseudomonas aeruginosa Biofilm Formation.* PLOS ONE, 2012. **7**(4): p. e35499.

`

94. Chung, S.W., et al., *Heme oxygenase-1-derived carbon monoxide enhances the host defense response to microbial sepsis in mice.* J Clin Invest, 2008. **118**(1): p. 239-47.

95. Chin, B.Y. and L.E. Otterbein, *Carbon monoxide is a poison... to microbes! CO as a bactericidal molecule.* Curr Opin Pharmacol, 2009. **9**(4): p. 490-500.

96. Kumar, A., et al., *Heme oxygenase-1-derived carbon monoxide induces the Mycobacterium tuberculosis dormancy regulon.* J Biol Chem, 2008. **283**(26): p. 18032-9.

97. Chung, S.W., S.R. Hall, and M.A. Perrella, *Role of haem oxygenase-1 in microbial host defence.* Cell Microbiol, 2009. **11**(2): p. 199-207.

98. Chinta, K.C., et al., *Microanatomic Distribution of Myeloid Heme Oxygenase-1 Protects against Free Radical-Mediated Immunopathology in Human Tuberculosis.* Cell Rep, 2018. **25**(7): p. 1938-1952.e5.

99. Zhao, Y., T.D. Biggs, and M. Xian, *Hydrogen sulfide (H2S) releasing agents: chemistry and biological applications.* Chemical communications (Cambridge, England), 2014. **50**(80): p. 11788-11805.

100. Lloyd, D., *Hydrogen sulfide: clandestine microbial messenger?* Trends Microbiol, 2006. **14**(10): p. 456-62.

101. Szabó, C., *Hydrogen sulphide and its therapeutic potential.* Nat Rev Drug Discov, 2007. **6**(11): p. 917-35.

102. Szabo, C., *A timeline of hydrogen sulfide (H2S) research: From environmental toxin to biological mediator.* Biochem Pharmacol, 2017.

103. Abe, K. and H. Kimura, *The possible role of hydrogen sulfide as an endogenous neuromodulator.* The Journal of Neuroscience, 1996. **16**(3): p. 1066-1071.

104. Furne, J., A. Saeed, and M.D. Levitt, *Whole tissue hydrogen sulfide concentrations are orders of magnitude lower than presently accepted values.* American Journal of Physiology-Regulatory, Integrative and Comparative Physiology, 2008. **295**(5): p. R1479-R1485.

105. Yang, G., et al., *H2S as a physiologic vasorelaxant: hypertension in mice with deletion of cystathionine gamma-lyase.* Science, 2008. **322**(5901): p. 587-90.

106. Whiteman, M., et al., *The effect of hydrogen sulfide donors on lipopolysaccharide-induced formation of inflammatory mediators in macrophages.* Antioxid Redox Signal, 2010. **12**(10): p. 1147-54.

107. Whiteman, M. and P.G. Winyard, *Hydrogen sulfide and inflammation: the good, the bad, the ugly and the promising.* Expert Rev Clin Pharmacol, 2011. **4**(1): p. 13-32.

108. Wedmann, R., et al., *Working with "H2S": facts and apparent artifacts.* Nitric Oxide, 2014. **41**: p. 85-96.

109. Calvert, J.W., W.A. Coetzee, and D.J. Lefer, *Novel Insights Into Hydrogen Sulfide–Mediated Cytoprotection.* Antioxidants & Redox Signaling, 2009. **12**(10): p. 1203-1217.

110. Blackstone, E., M. Morrison, and M.B. Roth, *H2S induces a suspended animation–like state in mice.* Science, 2005. **308**(5721): p. 518-518.

111. Kimura, H., N. Shibuya, and Y. Kimura, *Hydrogen sulfide is a signaling molecule and a cytoprotectant.* Antioxid Redox Signal, 2012. **17**(1): p. 45-57.

112. Li, Q. and J.R. Lancaster, Jr., *Chemical foundations of hydrogen sulfide biology.* Nitric Oxide, 2013. **35**: p. 21-34.

113. Panthi, S., et al., *Physiological Importance of Hydrogen Sulfide: Emerging Potent Neuroprotector and Neuromodulator.* Oxidative Medicine and Cellular Longevity, 2016. **2016**: p. 9049782.

114. Cao, X., et al., *A Review of Hydrogen Sulfide Synthesis, Metabolism, and Measurement: Is Modulation of Hydrogen Sulfide a Novel Therapeutic for Cancer?* Antioxidants & redox signaling, 2019. **31**(1): p. 1-38.

115. Hughes, M.N., M.N. Centelles, and K.P. Moore, *Making and working with hydrogen sulfide: The chemistry and generation of hydrogen sulfide in vitro and its measurement in vivo: a review.* Free Radic Biol Med, 2009. **47**(10): p. 1346-53.

116. Flannigan, K.L., K.D. McCoy, and J.L. Wallace, *Eukaryotic and prokaryotic contributions to colonic hydrogen sulfide synthesis.* American Journal of Physiology-Gastrointestinal and Liver Physiology, 2011. **301**(1): p. G188-G193.

117. Tomasova, L., P. Konopelski, and M. Ufnal, *Gut Bacteria and Hydrogen Sulfide: The New Old Players in Circulatory System Homeostasis.* Molecules, 2016. **21**(11).

118. Sawa, T., et al., *Reactive Cysteine Persulphides: Occurrence, Biosynthesis, Antioxidant Activity, Methodologies, and Bacterial Persulphide Signalling.* Adv Microb Physiol, 2018. **72**: p. 1-28.

119. Kumagai, H., et al., *Crystallization and properties of cysteine desulfhydrase from Aerobacter aerogenes.* FEBS Lett, 1975. **52**(2): p. 304-7.

120. Awano, N., et al., *Identification and functional analysis of Escherichia coli cysteine desulfhydrases.* Appl Environ Microbiol, 2005. **71**(7): p. 4149-52.

121. Nagahara, N., et al., *Tissue and subcellular distribution of mercaptopyruvate sulfurtransferase in the rat: confocal laser fluorescence and immunoelectron microscopic studies combined with biochemical analysis.* Histochem Cell Biol, 1998. **110**(3): p. 243-50.

122. Shibuya, N., et al., *3-Mercaptopyruvate sulfurtransferase produces hydrogen sulfide and bound sulfane sulfur in the brain.* Antioxid Redox Signal, 2009. **11**(4): p. 703-14.

123. Vandiver, M. and S.H. Snyder, *Hydrogen sulfide: a gasotransmitter of clinical relevance.* J Mol Med (Berl), 2012. **90**(3): p. 255-63.

124. Mironov, A., et al., *Mechanism of H2S-mediated protection against oxidative stress in Escherichia coli.* Proc Natl Acad Sci U S A, 2017. **114**(23): p. 6022-6027.

125. Shatalin, K., et al., *H2S: a universal defense against antibiotics in bacteria.* Science, 2011. **334**(6058): p. 986-990.

126. Clarke, P.H., *Hydrogen Sulphide Production by Bacteria.* Microbiology, 1953. **8**(3): p. 397-407.

127. Basic, A., et al., *Estimation of bacterial hydrogen sulfide production in vitro.* Journal of Oral Microbiology, 2015. **7**(1): p. 28166.

128. Yoshida, A., et al., *Hydrogen sulfide production from cysteine and homocysteine by periodontal and oral bacteria.* J Periodontol, 2009. **80**(11): p. 1845-51.

129. Jarosz, A.P., T. Yep, and B. Mutus, *Microplate-based colorimetric detection of free hydrogen sulfide.* Anal Chem, 2013. **85**(7): p. 3638-43.

130. Basic, A., et al., *The proteins of Fusobacterium spp. involved in hydrogen sulfide production from L-cysteine.* BMC Microbiology, 2017. **17**(1): p. 61.

131. Singh, S., et al., *Relative contributions of cystathionine β-synthase and γ-cystathionase to H2S biogenesis via alternative trans-sulfuration reactions.* Journal of Biological Chemistry, 2009. **284**(33): p. 22457-22466.

132. Shibuya, N., et al., *A novel pathway for the production of hydrogen sulfide from D-cysteine in mammalian cells.* Nature Communications, 2013. **4**(1): p. 1366.

`

133. Chen, X., K.H. Jhee, and W.D. Kruger, *Production of the neuromodulator H2S by cystathionine beta-synthase via the condensation of cysteine and homocysteine.* J Biol Chem, 2004. **279**(50): p. 52082-6.

134. Kabil, O., et al., *The quantitative significance of the transsulfuration enzymes for H2S production in murine tissues.* Antioxid Redox Signal, 2011. **15**(2): p. 363-72.

135. Kimura, H., *Production and physiological effects of hydrogen sulfide.* Antioxidants & redox signaling, 2014. **20**(5): p. 783-793.

136. Kabil, O. and R. Banerjee, *Enzymology of H2S biogenesis, decay and signaling.* Antioxid Redox Signal, 2014. **20**(5): p. 770-82.

137. Kolluru, G.K., et al., *Hydrogen sulfide chemical biology: pathophysiological roles and detection.* Nitric oxide, 2013. **35**: p. 5-20.

138. Searcy, D.G. and S.H. Lee, *Sulfur reduction by human erythrocytes.* J Exp Zool, 1998. **282**(3): p. 310-22.

139. Schnell, R., et al., *Siroheme- and [Fe4-S4]-dependent NirA from Mycobacterium tuberculosis is a sulfite reductase with a covalent Cys-Tyr bond in the active site.* J Biol Chem, 2005. **280**(29): p. 27319-28.

140. Koj, A., J. Frendo, and Z. Janik, *[35S]thiosulphate oxidation by rat liver mitochondria in the presence of glutathione.* Biochem J, 1967. **103**(3): p. 791-5.

141. Olson, K.R., E.R. DeLeon, and F. Liu, *Controversies and conundrums in hydrogen sulfide biology.* Nitric Oxide, 2014. **41**: p. 11-26.

142. Zheng, Y., et al., *Hydrogen sulfide prodrugs-a review.* Acta Pharm Sin B, 2015. **5**(5): p. 367-77.

143. Li, L., et al., *Characterization of a Novel, Water-Soluble Hydrogen Sulfide–Releasing Molecule (GYY4137).* Circulation, 2008. **117**(18): p. 2351-2360.

144. Lee, Z.W., et al., *The slow-releasing hydrogen sulfide donor, GYY4137, exhibits novel anti-cancer effects in vitro and in vivo.* PLoS One, 2011. **6**(6): p. e21077.

145. Forbes, B.A., D.F. Sahm, and A. Weissfeld, *Diagnostic Microbiology, Mosby, St.* Louis, MO, 1998.

146. Olson, K.R., *A practical look at the chemistry and biology of hydrogen sulfide.* Antioxidants & redox signaling, 2012. **17**(1): p. 32-44.

147. Jeroschewski, P., C. Steuckart, and M. Kühl, *An Amperometric Microsensor for the Determination of H2S in Aquatic Environments.* Analytical Chemistry, 1996. **68**(24): p. 4351-4357.

148. Hill, B.C., et al., *Interactions of sulphide and other ligands with cytochrome c oxidase. An electron-paramagnetic-resonance study.* Biochem J, 1984. **224**(2): p. 591-600.

149. Szabo, C., et al., *Regulation of mitochondrial bioenergetic function by hydrogen sulfide. Part I. Biochemical and physiological mechanisms.* Br J Pharmacol, 2014. **171**(8): p. 2099-122.

150. Goubern, M., et al., *Sulfide, the first inorganic substrate for human cells.* FASEB J, 2007. **21**(8): p. 1699-706.

151. Kabil, O. and R. Banerjee, *Redox biochemistry of hydrogen sulfide.* Journal of Biological Chemistry, 2010. **285**(29): p. 21903-21907.

152. Pal, V.K., P. Bandyopadhyay, and A. Singh, *Hydrogen sulfide in physiology and pathogenesis of bacteria and viruses.* IUBMB Life, 2018. **70**(5): p. 393-410.

153. Saini, V., et al., *Hydrogen sulfide stimulates Mycobacterium tuberculosis respiration, growth and pathogenesis.* Nature Communications, 2020. **11**(1): p. 557.

154. Rahman, M.A., et al., *Hydrogen sulfide dysregulates the immune response by suppressing central carbon metabolism to promote tuberculosis.* Proc Natl Acad Sci U S A, 2020. **117**(12): p. 6663-6674.

155. Román-Morales, E., et al., *Structural determinants for the formation of sulfhemeprotein complexes.* Biochemical and biophysical research communications, 2010. **400**(4): p. 489-492.

156. Predmore, B.L., D.J. Lefer, and G. Gojon, *Hydrogen sulfide in biochemistry and medicine.* Antioxidants & redox signaling, 2012. **17**(1): p. 119-140.

157. Carballal, S., et al., *Reactivity of hydrogen sulfide with peroxynitrite and other oxidants of biological interest.* Free Radic Biol Med, 2011. **50**(1): p. 196-205.

158. Nagy, P. and C.C. Winterbourn, *Rapid reaction of hydrogen sulfide with the neutrophil oxidant hypochlorous acid to generate polysulfides.* Chem Res Toxicol, 2010. **23**(10): p. 1541-3.

159. Stasko, A., et al., *Electron transfer: a primary step in the reactions of sodium hydrosulphide, an H2S/HS(-) donor.* Free Radic Res, 2009. **43**(6): p. 581-93.

160. Peng, H., et al., *Hydrogen Sulfide and Reactive Sulfur Species Impact Proteome S-Sulfhydration and Global Virulence Regulation in Staphylococcus aureus.* ACS Infect Dis, 2017. **3**(10): p. 744-755.

161. Iciek, M., et al., *S-sulfhydration as a cellular redox regulation.* Bioscience reports, 2015. **36**(2): p. e00304.

162. Yang, J., et al., *Non-enzymatic hydrogen sulfide production from cysteine in blood is catalyzed by iron and vitamin B6.* Commun Biol, 2019. **2**: p. 194.

163. Berney, M., et al., *An obligately aerobic soil bacterium activates fermentative hydrogen production to survive reductive stress during hypoxia.* Proceedings of the National Academy of Sciences, 2014. **111**(31): p. 11479-11484.

164. Mishra, R., et al., *Targeting redox heterogeneity to counteract drug tolerance in replicating Mycobacterium tuberculosis.* Sci Transl Med, 2019. **11**(518).

165. Parish, T., et al., *Production of mutants in amino acid biosynthesis genes of Mycobacterium tuberculosis by homologous recombination.* Microbiology, 1999. **145 (Pt 12)**: p. 3497-3503.

166. Schnell, R., D. Sriram, and G. Schneider, *Pyridoxal-phosphate dependent mycobacterial cysteine synthases: Structure, mechanism and potential as drug targets.* Biochim Biophys Acta, 2015. **1854**(9): p. 1175-83.

167. Singhal, A., et al., *Regulation of homocysteine metabolism by Mycobacterium tuberculosis S-adenosylhomocysteine hydrolase.* Sci Rep, 2013. **3**: p. 2264.

168. Hatzios, S.K. and C.R. Bertozzi, *The regulation of sulfur metabolism in Mycobacterium tuberculosis.* PLoS Pathog, 2011. **7**(7): p. e1002036.

169. Yin, J., et al., *Expression, purification and preliminary crystallographic analysis of O-acetylhomoserine sulfhydrylase from Mycobacterium tuberculosis.* Acta Crystallogr Sect F Struct Biol Cryst Commun, 2011. **67**(Pt 8): p. 959-63.

170. McDonough, P.L., S.J. Shin, and D.H. Lein, *Diagnostic and public health dilemma of lactose-fermenting Salmonella enterica serotype Typhimurium in cattle in the Northeastern United States.* J Clin Microbiol, 2000. **38**(3): p. 1221-6.

171. Huhtanen, C.N., J. Naghski, and E.S. Dellamonica, *Microfermentation series for identification of single colonies of Enterobacteriaceae.* Appl Microbiol, 1972. **24**(4): p. 618-27.

172. Duerden, B.I., *Pigment production by Bacteroides species with reference to sub-classification.* J Med Microbiol, 1975. **8**(1): p. 113-25.

173. Ederer, G.M., et al., *Motility-indole-lysine-sulfide medium.* J Clin Microbiol, 1975. **2**(3): p. 266-7.

174. Oberhofer, T.R., et al., *Evaluation of the oxi/ferm tube system with selected Gram-negative bacteria.* J Clin Microbiol, 1977. **6**(6): p. 559-66.

175. Kodaka, H., et al., *Improvement of mannitol lysine crystal violet brilliant green agar for the selective isolation of H2S-positive Salmonella.* J Food Prot, 2000. **63**(12): p. 1643-7.

176. Hine, C. and J.R. Mitchell, *Endpoint or Kinetic Measurement of Hydrogen Sulfide Production Capacity in Tissue Extracts.* Bio-protocol, 2017. **7**(13): p. e2382.

177. Lamprecht, D.A., et al., *Turning the respiratory flexibility of Mycobacterium tuberculosis against itself.* Nat Commun, 2016. **7**: p. 12393.

178. Bardarov, S., et al., *Specialized transduction: an efficient method for generating marked and unmarked targeted gene disruptions in Mycobacterium tuberculosis, M. bovis BCG and M. smegmatis.* Microbiology, 2002. **148**(10): p. 3007-3017.

179. Forte, E., et al., *The Terminal Oxidase Cytochrome bd Promotes Sulfide-resistant Bacterial Respiration and Growth.* Sci Rep, 2016. **6**: p. 23788.

180. Raggio, R., et al., *Silk Fibroin Porous Scaffolds Loaded with a Slow-Releasing Hydrogen Sulfide Agent (GYY4137) for Applications of Tissue Engineering.* ACS Biomaterials Science & Engineering, 2018. **4**(8): p. 2956-2966.

181. Liu, H., et al., *Sulfate reducing bacterial community and in situ activity in mature fine tailings analyzed by real time qPCR and microsensor.* J Environ Sci (China), 2016. **44**: p. 141-147.

182. Chen, W., et al., *Bacteria-derived hydrogen sulfide promotes IL-8 production from epithelial cells.* Biochemical and biophysical research communications, 2010. **391**(1): p. 645-650.

183. Barrett, E.L. and M.A. Clark, *Tetrathionate reduction and production of hydrogen sulfide from thiosulfate.* Microbiol Rev, 1987. **51**(2): p. 192-205.

184. Zhang, Y. and J.H. Weiner, *A simple semi-quantitative in vivo method using H(2)S detection to monitor sulfide metabolizing enzymes.* Biotechniques, 2014. **57**(4): p. 208-10.

185. Claesson, R., et al., *Production of volatile sulfur compounds by various Fusobacterium species.* Oral microbiology and immunology, 1990. **5**(3): p. 137-142.

186. Singh, S. and R. Banerjee, *PLP-dependent H(2)S biogenesis.* Biochim Biophys Acta, 2011. **1814**(11): p. 1518-27.

187. Jacobs, W.R., Jr., *Gene Transfer in Mycobacterium tuberculosis: Shuttle Phasmids to Enlightenment.* Microbiology spectrum, 2014. **2**(2): p. 10.1128/microbiolspec.MGM2-0037-2013.

188. Hatfull, G.F., *Molecular Genetics of Mycobacteriophages.* Microbiology spectrum, 2014. **2**(2): p. 1-36.

189. Junqueira-Kipnis, A.P., et al., *Prime–Boost with Mycobacterium smegmatis Recombinant Vaccine Improves Protection in Mice Infected with Mycobacterium tuberculosis.* PLOS ONE, 2013. **8**(11): p. e78639.

190. Tseng, C.-C., D.C. Chang, and K.-C. Chang *Development of a Biocontrol Method Applying Bacteriophage-Containing Aerosol against Mycobacterium tuberculosis Using the Bacteriophage BTCU-1 and M. smegmatis as Models*. Microorganisms, 2019. **7**, DOI: 10.3390/microorganisms7080237.

191. Korshunov, S., K.R.C. Imlay, and J.A. Imlay, *Cystine import is a valuable but risky process whose hazards Escherichia coli minimizes by inducing a cysteine exporter.* Mol Microbiol, 2020. **113**(1): p. 22-39.

192. Saini V, et al., *Hydrogen sulfide stimulates Mycobacterium tuberculosis respiration, growth and pathogenesis.* Nature Communications, 2020. **11**(1): p. 557.

193. Beteck, R.M., et al., *Accessible and distinct decoquinate derivatives active against Mycobacterium tuberculosis and apicomplexan parasites.* Communications Chemistry, 2018. **1**(1): p. 62.

194. Foo, C.S., et al., *Arylvinylpiperazine Amides, a New Class of Potent Inhibitors Targeting QcrB of Mycobacterium tuberculosis.* MBio, 2018. **9**(5).

195. Schnell, R., et al., *Structural insights into catalysis and inhibition of O-acetylserine sulfhydrylase from Mycobacterium tuberculosis. Crystal structures of the enzyme alpha-aminoacrylate intermediate and an enzyme-inhibitor complex.* J Biol Chem, 2007. **282**(32): p. 23473-81.

196. Park, S. and J.A. Imlay, *High levels of intracellular cysteine promote oxidative DNA damage by driving the fenton reaction.* Journal of bacteriology, 2003. **185**(6): p. 1942-1950.

197. Vilchèze, C., et al., *Enhanced respiration prevents drug tolerance and drug resistance in Mycobacterium tuberculosis.* Proceedings of the National Academy of Sciences, 2017: p. 201704376.

198. Weissgerber, T., et al., *Metabolomic profiling of the purple sulfur bacterium Allochromatium vinosum during growth on different reduced sulfur compounds and malate.* Metabolomics, 2014. **10**(6): p. 1094-1112.

199. Forquin, M.-P., et al., *Global regulation of the response to sulfur availability in the cheese-related bacterium Brevibacterium aurantiacum.* Applied and environmental microbiology, 2011. **77**(4): p. 1449-1459.

200. Mustafa, A.K., et al., *H2S signals through protein S-sulfhydration.* Sci Signal, 2009. **2**(96): p. ra72.

201. Xie, Z.-Z., Y. Liu, and J.-S. Bian, *Hydrogen Sulfide and Cellular Redox Homeostasis.* Oxidative Medicine and Cellular Longevity, 2016. **2016**: p. 6043038.

`

202. Shukla, P., et al., *"On demand" redox buffering by H2S contributes to antibiotic resistance revealed by a bacteria-specific H2S donor.* Chemical Science, 2017. **8**(7): p. 4967-4972.

203. Kimura, Y. and H. Kimura, *Hydrogen sulfide protects neurons from oxidative stress.* The FASEB journal, 2004. **18**(10): p. 1165-1167.

204. Weikum, J., et al., *Sulfide Protects Staphylococcus aureus from Aminoglycoside Antibiotics but Cannot Be Regarded as a General Defense Mechanism against Antibiotics.* Antimicrobial agents and chemotherapy, 2018. **62**(10): p. e00602-18.

205. Álvarez, R., et al., *Participation of S. Typhimurium cysJIH Operon in the H(2)S-mediated Ciprofloxacin Resistance in Presence of Sulfate as Sulfur Source.* Antibiotics, 2015. **4**(3): p. 321-328.

206. Wu, G., et al., *Endogenous generation of hydrogen sulfide and its regulation in Shewanella oneidensis.* Frontiers in Microbiology, 2015. **6**(374).

207. Wheeler, P.R., et al., *Functional demonstration of reverse transsulfuration in the Mycobacterium tuberculosis complex reveals that methionine is the preferred sulfur source for pathogenic Mycobacteria.* J Biol Chem, 2005. **280**(9): p. 8069-78.

208. Kari, C., et al., *Mechanism of the growth inhibitory effect of cysteine on Escherichia coli.* Microbiology, 1971. **68**(3): p. 349-356.

209. Vilcheze, C., et al., *Enhanced respiration prevents drug tolerance and drug resistance in Mycobacterium tuberculosis.* Proc Natl Acad Sci U S A, 2017. **114**(17): p. 4495-4500.

210. Modis, K., et al., *Regulation of mitochondrial bioenergetic function by hydrogen sulfide. Part II. Pathophysiological and therapeutic aspects.* Br J Pharmacol, 2014. **171**(8): p. 2123-46.

211. Cook, G.M., et al., *Oxidative Phosphorylation as a Target Space for Tuberculosis: Success, Caution, and Future Directions.* Microbiol Spectr, 2017. **5**(3).

`

212. Saini, V., et al., *Ergothioneine Maintains Redox and Bioenergetic Homeostasis Essential for Drug Susceptibility and Virulence of Mycobacterium tuberculosis.* Cell reports, 2016. **14**(3): p. 572-585.

213. Vestergaard, M., et al., *Inhibition of the ATP Synthase Eliminates the Intrinsic Resistance of Staphylococcus aureus towards Polymyxins.* mBio, 2017. **8**(5): p. e01114-17.

214. Yu, W.-B., Q. Pan, and B.-C. Ye, *Glucose-Induced Cyclic Lipopeptides Resistance in Bacteria via ATP Maintenance through Enhanced Glycolysis.* iScience, 2019. **21**: p. 135-144.

215. Deavall, D.G., et al., *Drug-Induced Oxidative Stress and Toxicity.* Journal of Toxicology, 2012. **2012**: p. 645460.

216. Yano, T., et al., *Reduction of clofazimine by mycobacterial type 2 NADH:quinone oxidoreductase: a pathway for the generation of bactericidal levels of reactive oxygen species.* J Biol Chem, 2011. **286**(12): p. 10276-87.

217. Piccaro, G., et al., *Rifampin induces hydroxyl radical formation in Mycobacterium tuberculosis.* Antimicrobial agents and chemotherapy, 2014. **58**(12): p. 7527-7533.